Modelling the transmission of Buruli ulcer in fluctuating environments

by

Belthasara Assan

Thesis presented in partial fulfilment of the requirements for the degree of Master of Science in Mathematics in the Faculty of Science at Stellenbosch University

Department of Mathematical Sciences,
University of Stellenbosch,
Private Bag X1, Matieland 7602, South Africa.

Supervisor: Prof. Farai Nyabadza & Co-Supervisor: Prof. Cang Hui

December 2015

Declaration

By submitting this thesis electronically, I declare that the entirety of the work contained therein is my own, original work, that I am the sole author thereof (save to the extent explicitly otherwise stated), that reproduction and publication thereof by Stellenbosch University will not infringe any third party rights and that I have not previously in its entirety or in part submitted it for obtaining any qualification.

December 2015

Abstract

Modelling the transmission of Buruli ulcer in fluctuating environments

Belthasara Assan

Department of Mathematical Sciences,
University of Stellenbosch,
Private Bag X1, Matieland 7602, South Africa.

Thesis: MSc

December 2015

Buruli ulcer is a disease caused by *Mycobacterium ulcerans*. The transmission dynamics of this disease largely depends on environmental changes. In this thesis a deterministic model for the transmission of Buruli ulcer in fluctuating environments is proposed. The model incorporates periodicity in the disease transmission pathways and the *Mycobacterium ulcerans* density, that are thought to vary seasonally. Two reproduction numbers, time-averaged reproduction number $[R_0]$ and the basic reproduction number R_0, are determined and compared. The time-averaged reproduction number obtained shows that Buruli ulcer epidemic is driven by the dynamics of the environments. It shows inaccuracy in predicting the number of infections. Numerical simulations confirmed that if $R_0 > 1$ the infection is sustained seasonally. The model outcome suggests that environmental fluctuation should be taken into consideration in designing policies aimed at Buruli ulcer control and management. In addition to the deterministic model, a systems dynamic model for the transmission of Buruli ulcer by using *STELLA* is also proposed with and without periodicity in the disease transmission pathways and the *Mycobacterium ulcerans* density. The model simulations confirm that when $R_0 < 1$ and $R_0 > 1$ the solutions

converge to the disease free and endemic equilibrium respectively. A very good synergy was obtained between the deterministic model and *STELLA* model. The *STELLA* model however, provided flexibility through its ability to accommodate more social dynamics without adding mathematical intractability. The model provides useful insights in the dynamics of Buruli ulcer and has significant implication to the management of disease.

Uittreksel

Modellering van die oordrag van Buruli ulkus in wisselende omgewings

Belthasara Assan

Departement Wiskundige Wetenskappe,
Universiteit van Stellenbosch,
Privaatsak X1, Matieland 7602, Suid Afrika.

Tesis: MSc

Desember 2015

Buruli ulkus is 'n siekte wat veroorsaak word deur *Mycobacterium ulcerans*. Die oordrag dinamika van hierdie siekte hang grootliks van omgewingsveranderinge af. In hierdie tesis word 'n deterministiese model vir die oordrag van Buruli ulkus in wisselende omgewings voorgestel. Die model inkorporeer periodisiteit in die siekte oordrag paaie en die *Mycobacterium ulcerans* digtheid, wat seisoenaal wissel.

Twee reproduksie syfers, tyd-gemiddelde reproduksie syfer $[R_0]$ en die basiese reproduksie syfer R_0, word bepaal en vergelyk. Die tyd-gemiddelde reproduksie syfer wat verkry word toon dat die Buruli ulkus epidemie deur die dinamika van die omgewing gedryf word. Dit toon 'n mate van onakkuraatheid in die voorspelling van die aantal infeksies. Numeriese simulasie bevestig dat, as $R_0 > 1$, dan word die infeksie seisoenaal opgedoen. Die uitkomste van die model stel voor dat fluksuasies in die omgewing in ag geneem moet word in die ontwerp van beleide gemik op Buruli ulkus beheer en bestuur.

Bykomend tot die deterministiese model, word 'n stelsel dinamika model vir die oordrag van Buruli ulkus wat STELLA gebruik ook voorgestel met en sonder periodisiteit in die siekte oordrag paaie en die *Mycobacterium*

ulcerans digtheid. Die model simulasies bevestig dat as $R_0 < 1$ en $R_0 > 1$, die oplossings na die siekte-vry en endemiese ewewigte, onderskeidelik, konvergeer.

'n Baie goeie sinergie was verkry tussen die deterministiese model en die STELLA model. Die STELLA model verskaf egter buigsaamheid deur sy vermoë om meer sosiale dinamika, sonder om wiskundige onregeerbaarheid by te voeg, te akkomodeer. Die model verskaf nuttige insigte in die dinamika van BU en het beduidende implikasie tot die bestuur van die siekte.

Acknowledgements

" Not to us, Lord, not to us but to your name be the glory, because of your love and faithfulness! " Psalm, 115 : 1. My greatest thanks goes to my Lord and Saviour Jesus Christ who is my strength, rock, fortress, deliverer, God, shield, stronghold and the horn of my salvation.

I would like to extent my profound gratitude to my supervisor Prof. Farai Nyabadza and my co-supervisor Prof. Cang Hui for their patience and guidance throughout the entire research period. My special thanks goes to Dr. Pietro Landi for useful discussions and consultations through the entire project.

My appreciation goes to National Research foundation (NRF; grants 81825 and 76912) and the African Institute for Mathematical Sciences (AIMS) for providing financial support for this project.

My appreciation also goes to ASSAN family, especially to my parent Mr & Mrs ASSAN and my sister Melchoira ASSAN for their constant encouragement and prayers.

" How great are God's riches! How deep are his wisdom and knowledge!... For all things were created by him, and all things exist through him and for him. To God be the glory for ever! Amen."
Romans, 11 : 33*a*/36

Dedications

This thesis is dedicated to " who is and who was and who is to come, the Almighty. Amen" Revelation, 1 : 8*b and to all friends of New Covenant Gospel for your unceasing prayers and encouragement for me. My love to you all.*

Publications

This following publications are extracts from this thesis. They are appended at the end of the thesis.

- Modelling the transmission of Buruli ulcer in fluctuating environments. Submitted to the Journal of Biological Dynamics (Manuscript under Review).
- A *STELLA* model for Buruli ulcer transmission with periodicity. To be submitted to the Journal of Biological Dynamics (Manuscript under compilation).

Contents

List of Figures

List of Tables

Chapter 1

Introduction

1.1 Buruli ulcer

Buruli ulcer (**BU**) is a neglected tropical disease caused by *Mycobacterium ulcerans* [1, 14, 35]. BU is the third most common mycobacterial disease which belongs to the same group with tuberculosis and leprosy [37] but BU has received less attention than these diseases. In most cases the disease occurs in children between the ages of 4 and 15 years. It however, affects all ages and sexes. The infection in most instances presents painless lumps under the skin [17]. Infection leads to extensive destruction of skin and soft tissue with the formation of large ulcers usually on the legs or arms. Patients who are not treated early often suffer long-term functional disability such as restriction of joint movement as well as the obvious cosmetic problem, scarring, contractual deformities and amputations [6, 35]. Early diagnosis and treatment are vital in preventing such disabilities. In West Africa, gender distribution of the disease also varies, males with 52% and females 48% [39]. About 37.8% of the recorded cases require surgery while 48% of those affected are children under 15 years [39]. It is a poorly understood disease that has emerged dramatically since the 1980s. It is driven by speedy environmental changes coupled together with deforestation, eutrophication, construction of dams, irrigation, farming, mining, and habitat fragmentations [24, 35, 45, 52, 53]. These factors affect the survival of the pathogens in the environments and its transmissions. Epidemiological studies show that this mycobacteriosis is mainly found and also endemic near wetlands and slow-moving rivers. *Mycobacterium ulcerans*

survive best under low oxygen tensions, such as in the mud or the bottom of swamps [47].

1.2 Ecology and epidemiology

Fundamental aspects of the ecology and epidemiology of *Mycobacterium ulcerans*, including its environmental distribution, niche, host range, and mode of transmission and infection, are poorly understood [29]. The likely mode of transmission of BU is driven by two processes: firstly, it occurs through direct contact with *Mycobacterium ulcerans* in the environments when the skin is broken (e.g. a cut) [39, 48, 58] and secondly, Portaels et al. [47] hypothesised that some water-filtering organisms such as fish and mollusks concentrate the *Mycobacterium ulcerans* present in water or mud and release the *Mycobacterium ulcerans* into the environments. It is then ingested by water-dwelling predators such as beetles and water bugs. These insect may end up transmitting the disease by biting humans [2, 14, 33, 47]. The likely mode of transmission among human population however, occurs through contact with the environments and not human-to-human transmission.

1.3 Treatment

BU treatment is by surgery and skin grafting or antibiotics. It is documented that antibiotics kill *Mycobacterium ulcerans* bacilli, arrest the disease, and promote healing without relapse or reduce the extent of surgical excision [14, 15]. In an environment where resources are limited and services are lean, such as in rural areas and endemic countries, often lack adequate surgical capacity, and prolonged hospitalization stretches the limited bed capacity of health centres, further reducing the number of patients who can be admitted for treatment. In addition, the cost of surgical treatment is far beyond the means of those most severely affected [6, 27].

1.4 Motivation

Environmental forcing, such as floods, rainfall, dry seasons, temperatures and other climatic factors, is often seasonal and could significantly af-

fects BU disease dynamics. Diseases such as cholera, whooping cough, malaria, influenza, dengue and many more exhibit periodic fluctuations [5, 13, 21, 26, 28, 30, 31]. A series of epidemiological studies show seasonal variations in the appearance of BU cases. The number of cases increases during dry periods or after inundations [16, 41]. These conditions are probably favourable for the development of *Mycobacterium ulcerans*, because of the density of possible vectors in areas that are frequently visited by humans. For example if we consider Ghana where BU is endemic, this country experience a typical tropical climate. Where in December to February is Harmattan (dry and dusty weather), March is the hottest month, through April to June they experience major rainfall, July to October there is small rains and in the month of November there is mild and dry weather [49]. Such field observations underline the limitation of all current BU models and imply that mathematical insights into BU seasonality has largely lagged behind. It is thus important for mathematical BU studies to incorporate these seasonal factors to gain deeper quantitative understanding of the short and long-term evolution of BU.
Following [14], we propose a BU model by incorporating periodicity in the environments, with the aim of determining how periodic changes in the environments affect the transmission dynamics of BU. That is the incidence and the rate of change for the *Mycobacterium ulcerans* density are subject to periodicity. Following [55], we analysed the basic reproduction number, R_0, for this BU model and establish that R_0 is a sharp threshold for BU dynamics in fluctuating environments: when $R_0 < 1$, the disease free equilibrium (DFE) is globally asymptotically stable, and the disease completely dies out; when $R_0 > 1$, the system admits a positive periodic solution, and the disease is uniformly persistent. The method of analysis for extinction and persistence results for periodic epidemic systems is inspired by the research done in [10, 11, 32, 42, 46, 61]

1.5 Objectives

The main objective of this thesis is to model the dynamics of BU in fluctuating environments. We first model the transmission of BU in fluctuating environments, secondly we use a systems dynamic to model the transmission of BU using *STELLA*.

Specific objectives include:

1. Incorporating periodicity in the model in [14]. This is motivated by including periodicity in the environments and the disease transmission pathways.

2. Carrying out the mathematical analysis of BU model in both the non fluctuating and fluctuating environments to compare the results.

3 Carrying out the numerical analysis of the model.

4 Use *STELLA* to model BU with the object of incorporating aspects that usually makes standard system differential equations intractable.

1.6 Mathematical preliminaries

1.6.1 Dynamical system

Dynamical systems are referred to as any phenomena which changes with time. They are therefore usually, represented by

(a) discrete-time mathematical models, in the form of difference equations. For example,

$$x_{t+1} = f(x_t), \quad t = 0, 1, 2, ...n$$

if information about the physical system is known only at a finite number of time values,

(b) a continuous-time mathematical models, in the form of differential equations. For example,

$$\frac{dx}{dt} = f(x, t), \quad t \in [0, T]$$

if information about the phenomenon is known at every time value on the interval $[0, T]$.

We consider a dynamical system given by a system of first-order differential equations of the form

$$\frac{d\mathbf{x}}{dt} = \mathbf{f(x)} \tag{1.6.1}$$

where $\mathbf{x} = (x_1, x_2, \cdots, x_n)^T$,
$\mathbf{f(x)} = (f_1(x_1, x_2, \cdots, x_n),\ f_2(x_1, x_2, \cdots, x_n),\ \cdots,\ f_n(x_1, x_2, \cdots, x_n))^T$
and $\mathbf{f}$ does not depend explicitly on t.

Definition 1.6.2 (Equilibrium Point)**.** A point $\mathbf{x}^* \in \mathbb{R}^n$ is called an *equilibrium point* of (1.6.1) if

$$f(x^*) = 0.$$

Equilibrium points of dynamical systems represent *constant solutions* of the system and therefore give an indication of the long-term behaviour of the system [3].

1.6.3 Reproduction number

The basic reproduction number, denoted R_0, is the expected number of secondary cases produced, in a completely susceptible population, by a typical infective individual. If $R_0 < 1$, then on average, an infected individual produces less than one new infected individual over the course of its infectious period, and the infection cannot grow. Conversely, if $R_0 > 1$, then each infected individual produces, on average, more than one new infection, and the disease can invade the population [4, 20].
The concept of reproduction number is fundamental to the study of epidemiology of infectious diseases. It is useful in predicting factors and parameters that enhance the growth of an epidemic or those that help reduce or stop the growth of the epidemic. Its value is very useful in prevention strategies and management plans in disease epidemics [18]. In this project we calculated the time-averaged reproduction number and the basic reproduction number (spectral radius using the evolution operator). For comparison, we will also calculate time-averaged reproduction number, denoted by $[R_0]$, for our model. For any continuous periodic function $h(t)$ with period ω, we may define its average as

$$[h] = \frac{1}{\omega}\int_0^{\omega} h(t)dt.$$

Keeping this notation, we define the time-averaged matrices of $F(t)$ and $V(t)$ where

$$F(t) = \left(\frac{\partial \mathcal{F}_i(t, x^0(t))}{\partial x_j}\right)_{1\leq i,j\leq m}, \tag{1.6.2}$$

$\mathcal{F}_i$ represent the new infections and

$$V(t) = \left(\frac{\partial \mathcal{V}_i(t, x^0(t))}{\partial x_j} \right)_{1 \leq i,j \leq m} \tag{1.6.3}$$

where $\mathcal{V}_i$ is the transfers of infections from one compartment to another and x^0 is the disease free equilibrium state. The time-averaged reproduction number is defined as the spectral radius of the time-averaged next generation matrix $[F][V]^{-1}$, given by

$$[R_0] = \rho([F][V]^{-1}).$$

Furthermore, we donote R_0 to be the basic reproduction number for our non-autonomous systems, it is defined as the spectral radius of the next infection operator in [8, 9]. The next infection operator L is given as

$$(L\phi)(t) = \int_0^\infty Y(t, t-s)F(t-s)\phi(t-s)ds \tag{1.6.4}$$

where $Y(t,s)$, $t \geq s$, is the evolution operator of the linear ω-periodic system $\frac{dy}{dt} = -V(t)y$ and $\phi(t)$, the initial distribution of infectious individuals, is ω-periodic and non-negative. The basic reproduction number is then defined as the spectral radius of the next infection operator,

$$R_0 = \rho(L).$$

1.7 System dynamics

System dynamics (SD) is a methodology and mathematical modelling technique for framing, understanding and discussing complex issues and problems. Originally developed in the 1950s to help corporate managers improve their understanding of industrial processes, system dynamics is currently being used throughout the public and private sector for policy analysis and design [43].

STELLA, which is the Structural Thinking Experimental Learning Labratory with Animation, software can be found from [50]. It is a user-friendly and commercial software package for building a dynamic modelling system. It uses an iconographic interface to facilitate construction of dynamic systems models. It includes a procedural programming language that are created as a result of manipulating the icons. The key features in *STELLA* consist of the following four tools:

- Stocks, which are the state variables for accumulation. They collect whatever flows into and out of them.
- Flows, which are the exchange variables and which control the arrival or the exchanges of information between the state variables.
- Converters, which are the auxiliary variables. These variables can be represented by constant values or by values depending on other variables and functions of various categories.
- Connectors, which connect among modelling features, variables and elements.

Figure 1.1 show how a stock, flow, connector and converter look like. Connector is the one connecting the flow and converter together.

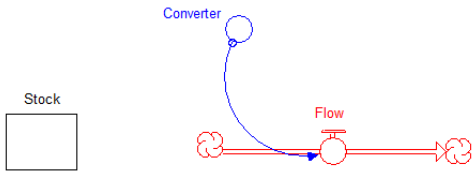

Figure 1.1: An example of a stock, flow, converter and connector

1.7.1 Systems preliminary

In this preliminary, we use the population model as an example to explain some of the terms used in SD. A population model with two flows is shown in Figure 1.2. A single stock represents the size of the population. Births and deaths are the only flows, there is no migration. The flows are represented by double lines which depict the flow of material in and out of the stock. For mathematical modelling in this case, the material is people, also flows represent any material that acquire an increase in a stock. We use the stocks to represent the present state of the system and flows to represent the actions that change the state over time. It will take some time for the flows to have their effect on the stocks, so the stocks tend to change more slowly over time. Stocks accumulate the effect of the flows, and they will

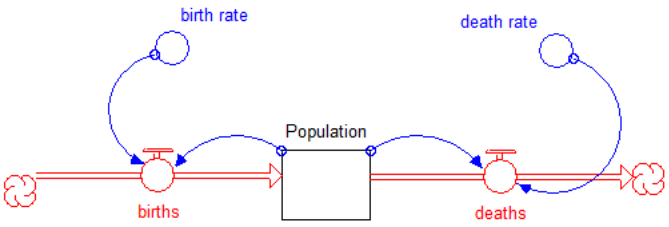

Figure 1.2: Population model with one stock.

remain at their current position if there are no flows acting on them. The only way a stock may be changed is by the action of the flows. In the case of Figure 1.2, the only way the population may change is by the action of births or deaths.

1.8 Feedback thinking

Conceptually, the feedback concept is at the heart of the system dynamics approach. Diagrams of loops of information feedback and circular causality are tools for conceptualizing the structure of a complex system and for communicating model-based insights. Intuitively, a feedback loop exists when information resulting from some action travels through a system and eventually returns in some form to its point of origin, potentially influencing future action. If the tendency in the loop is to reinforce the initial action, the loop is called a positive or reinforcing feedback loop. If also the tendency is to oppose the initial action, the loop is called a negative or balancing feedback loop. The sign of the loop is called its polarity. Balancing loops can be variously characterized as goal-seeking, equilibrating, or stabilizing processes. They can sometimes generate oscillations, as when a pendulum seeking its equilibrium goal gathers momentum and overshoots it. Reinforcing loops are sources of growth or accelerating collapse; they are disequilibrating and destabilizing. Combined, reinforcing and balancing circular causal feedback processes can generate all manner of dynamic patterns. Below are causal loop diagrams, they can't be simulated but are

very useful for high level feedback loop simple modelling [51, 57]. In Fig-

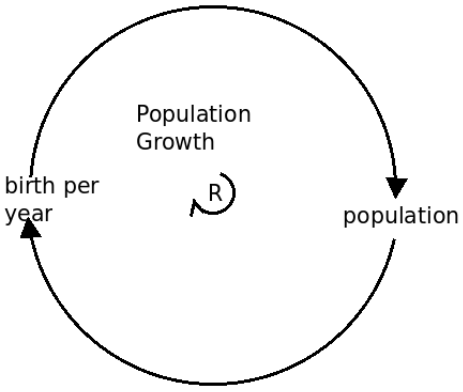

Figure 1.3: An example of a reinforcing loop is population growth.

ure 4.1, as population goes up, so does births per year, and so does future population. The loop goes round and round, growing exponentially until the loop hits its limits, which are not shown.

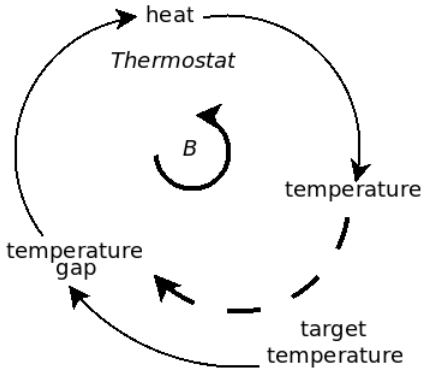

Figure 1.4: An example of a balancing loop is a thermostat

In a balancing loop the gap equals the target minus the actual state (see Figure 1.4). The higher the target the greater the temperature gap. The greater the gap the more heat that flows into the system which increases the temperature. As this goes up, the temperature gap goes down. It keeps going down until the gap is zero, at that point the system has reached the target [40, 51, 57].

1.8.1 Modelling and simulation

Mathematically, the basic structure of a formal system dynamics computer simulation model is a system of coupled, nonlinear, first-order differential (or integral) equations,

$$\frac{d}{dt}\mathbf{x}(t) = \mathbf{f}(\mathbf{x}, p)$$

where $\mathbf{x}$ is a vector of levels (stocks or state variables), p is a set of parameters, and $\mathbf{f}$ is a nonlinear vector-valued function. Simulation of such systems is easily accomplished by partitioning simulated time into discrete intervals of length dt and stepping the system through time one dt at a time. Each state variable is computed from its previous value and its net rate of change $x'(t) : x(t) = x(t - dt) + dt \times x'(t - dt)$.
Simulation modelling is the other method to describe the feedback loops that cause the problem.

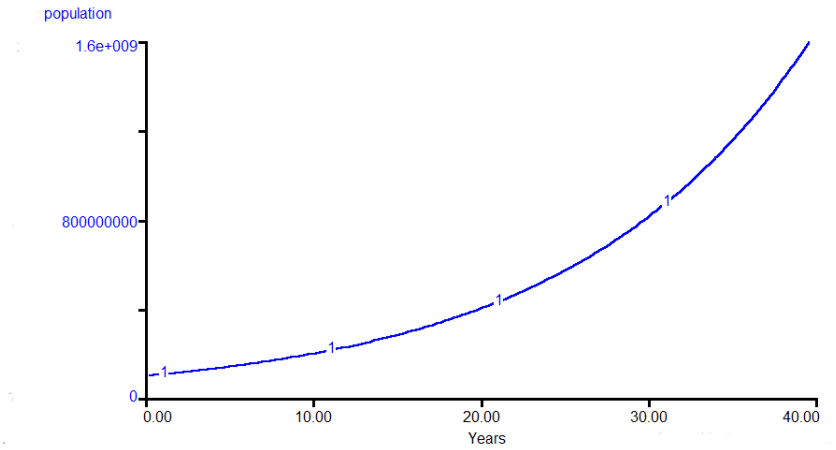

Figure 1.5: Exponential growth in population.

Figure 1.5 shows a simulation results of the *STELLA* model 1.2. The graph shows that in every decade the population size is increased by 200 million.

1.9 Project outline

The research project is organized into five chapters. In Chapter 1, we give an introduction on the transmission of BU in fluctuating environments. In Chapter 2 we provide literature reviews on mathematical models of BU, models with seasonality and *STELLA* models respectively. We now give the compartmental diagram for BU in fluctuating environments and we derive the dynamical system from the compartmental diagram in Chapter 3. In this Chapter, the model analysis and the underlying assumptions are established, followed by the global stability analysis of the disease extinction and we establish the existence and uniform persistence of an endemic periodic solution. Furthermore, numerical results on the behaviour of the periodic model are presented and analysed in Chapter 3. In Chapter 4 we introduce a system dynamic model for the transmission of BU in both fluctuating and non fluctuating environments using *STELLA*. The project is concluded in Chapter 5 with relevant discussions, recommendations and the retrieved papers are attached.

Chapter 2

Literature review

In order to develop a model for the transmission of BU in fluctuating environments using both deterministic and *STELLA* model, two processes are involved; firstly to capture the two potential routes of transmission and the appropriate mathematical tools employed in order to obtain logical qualitative and quantitative predictive results. In this chapter we reviewed some previous work studied using mathematical models, models with seasonality and *STELLA* models as a basis for our work.

2.1 Mathematical models of BU

Few mathematical models have been designed to study the dynamics of BU in order to understand the transmission dynamics of the disease, effective control measures and also to determine adequate prevention [2, 14]. Aidoo and Osei [2], proposed a mathematical model of the SIR type to explain the transmission of BU. They claimed that the *Mycobacterium ulcerans* is postulated to depend on the arsenic environments and water bugs biting frequency. In particular, it is stated that the higher the rate of ingestion of *Mycobacterium ulcerans* by water bugs, the higher the rate of its infectiousness.
In their model they proposed that BU is a micro parasitic disease in which host parasite interaction basically occurs within isolated communities. Again it was assumed humans who develop BU become immune to any further attack and this assumption led them to the SIR model. Below is the figure used to demonstrates possible interrelationships between these variables.

Table 2.1: Model variables and parameters

Parameters	meaning
m	Density of water bugs (number of water bugs per human host)
a	Bite frequency (biting rate of humans by a single water bug)
a_1	Rate of ingestion of *Mycobacterium ulcerans* by water bugs
b	Proportion of infected bites on humans that produce infection
α	Relative concentration of arsenic in water
μ	Mortality rate of water bugs
x	Proportion of humans infected by *Mycobacterium ulcerans*
y	Proportion of water bugs infected by *Mycobacterium ulcerans*
r	Death rate of humans

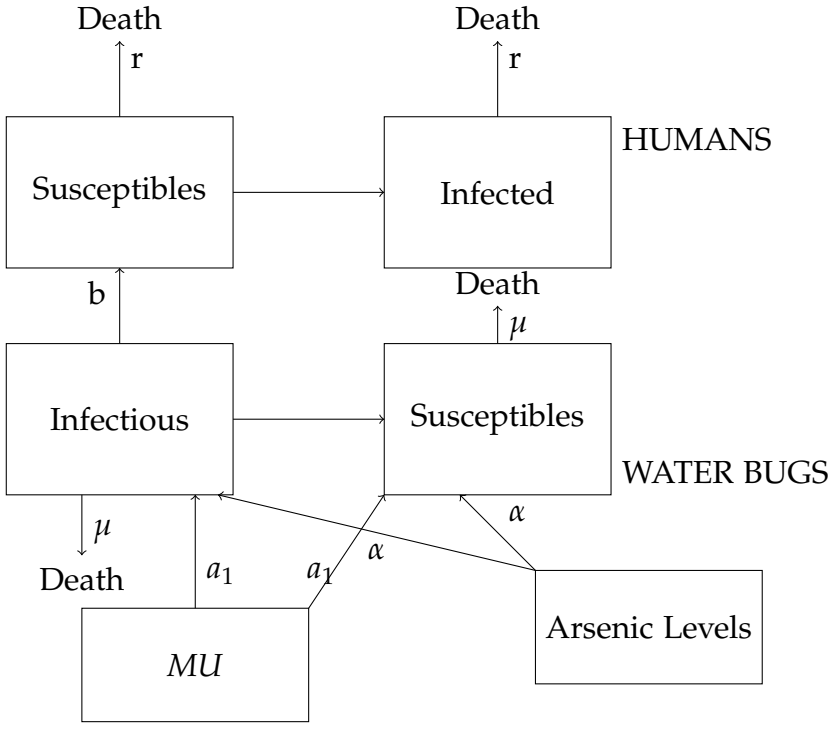

Figure 2.1: Schematic representation showing interrelations between the compartmented sections of human and water bug populations and the role of arsenic concentration in the epidemiology of BU.

The model equations describing the proportion of humans infected by *Mycobacterium ulcerans* and the corresponding proportion of water bugs are

given by

$$\frac{dx}{dt} = maby(1-x) - rx, \tag{2.1.1}$$

$$\frac{dy}{dt} = a_1 x(1-y) - (\mu - \alpha)y. \tag{2.1.2}$$

Their study showed a nonlinear relationship between the basic reproductive number R_0 and the prevalence of infection of both infected water bugs and infected humans. Moreover, a small increase in the reproductive number lead to a large change in both the prevalence levels of humans and water bugs. They also deducted from their graph that, higher levels of R_0 will lead to increases in cases of BU for $R_0 > 1$. Thus, if BU is not controlled it will continue to spread in regions with conducive conditions.

Bonyah, Dontwi and Nyabadza [14], developed a theoretical model for the transmission dynamics of Buruli ulcer with saturated treatment. This paper captured the two modes of transmission: firstly, the one that occurs through direct contact with *Mycobacterium ulcerans* in the environment and secondly, the one that occurs through biting by water bugs. They also incorporated saturated treatment in their model. Their aim was to model theoretically, the possible impact of the challenges associated with the treatment and management of BU such as; delays in accessing treatment, limited resources, and few medical facilities to deal with the highly complex treatment of the ulcer. They also endeavoured to holistically include the main forms of transmission of the disease in humans. This made their model richer than the few attempts made by some authors. The model is analysed by determining the steady states and carrying out model analysis in terms of the basic reproduction number R_T. Their analysis was done through the submodels. The model presented in this paper has a unique challenge in which the infection in one submodel takes place at the steady state of the other submodel. Bonyah and Nyabadza [14], concluded that the BU epidemic is highly influenced by the shedding of *Mycobacterium ulcerans* into the environment.

One limitation of these models, however, is that most of them assumed that the model parameters are constant in time, meaning that the disease contact rate, recovery rate, pathogen growth rate, etc., all take fixed values independent of time.

2.2 Models with seasonality

For a compartmental epidemiological model based on an autonomous system, the basic reproduction number is determined by the spectral radius of the next-generation matrix (which is independent of time) [18]. The definition of the basic reproduction number of a general non-autonomous system, however, still remains an open question [42]. Bacaër and Guernaoui [9], introduced R_0 for periodic epidemic models (including ODE and PDE systems) as the spectral radius of an integral operator. Related work for some periodic ODE systems was also discussed in [7]. Furthermore, Wang and Zhao [55], extended the framework done by Driessche and Watmough [18], to include epidemiological models in periodic environments. They introduced the next infection operator L by

$$(L\phi)(t) = \int_0^\infty Y(t, t-s)F(t-s)\phi(t-s)ds \tag{2.2.1}$$

where $Y(t,s), t \geq s$, is the evolution operator of the linear ω-periodic system $\frac{dy}{dt} = -V(t)y$ and $\phi(t)$, the initial distribution of infectious individuals, is ω-periodic and non-negative. The basic reproduction number is then defined as the spectral radius of the next infection operator,

$$R_0 = \rho(L).$$

In addition Bacaër [7], assert other methods for computing R_0. The basic reproduction number R_0 can be numerically calculated by solving the equation $f(R) = 1$, where $f(R)$ is the dominant Floquet multiplier of

$$\frac{dw}{dt} = \left(-V(t) + \frac{F(t)}{\lambda}\right) w, \quad t \in \mathbb{R} \tag{2.2.2}$$

with parameter $\lambda \in (0, \infty)$.

Liua, Zhaob and Zhoua [32], model tuberculosis (TB) with seasonality, using similar methods above. They developed a mathematical TB model with seasonality to study the possible seasonal variation in pulmonary TB in the mainland of China. Their simple TB model incorporates periodic coefficients based on the possible fact that there is a seasonal trend in new TB cases. They divided their population into four classes: the susceptible class, the latent/exposed class, the infectious class, and the treated/recovered

class. In this paper, they introduce the fast and slow progression based on the real situation of tuberculosis disease. The model has the compartmental structure of the classical SEIR epidemic model. The basic reproduction ratio R_0 is defined, and the disease free equilibrium is found to be globally asymptotically stable and the disease eventually disappears if $R_0 < 1$, and there exists at least one positive periodic solution and the disease is uniformly persistent if $R_0 > 1$. Numerical simulations indicate that there may be a unique positive periodic solution which is globally asymptotically stable if $R_0 > 1$. Their simulation results was in good accordance with the seasonal variation of the reported cases of active TB in China.

Furthermore, in the paper modelling cholera in periodic environment by Posny and Wang [42], their objective was to propose a general cholera model in a periodic environment by including seasonal variations in the environment and the disease transmission pathways. In particular, the incidence (or force of infection) and the rate of change for the pathogen concentration are subject to periodicity. Using the next infection operator introduced by Wang and Zhao in [55], they derived and computed the basic reproduction number R_0, for their periodic cholera model and conducted analysis on the epidemic and endemic dynamics. They established that R_0 is a sharp threshold for cholera dynamics in periodic environment: when $R_0 < 1$, the disease free equilibrium (DFE) is globally asymptotically stable, and the disease completely dies out; when $R_0 > 1$, the system admits a positive periodic solution, and the disease is uniformly persistent. They also discussed the disease extinction and persistence of their periodic epidemic system. Several specific examples were presented in this paper to demonstrate the general cholera model. Numerical simulation results were used to validate the analytical prediction.

2.3 *STELLA* models

In 2009, Ying et al. [60] gave a model for atrazine fate in agriculture, this was developed using *STELLA*. The mechanisms and processes used in this modelling included atrazine runoff, leaching, volatilization, adsorption, degradation and uptake. Their model was calibrated using experimental data prior to its applications. They obtain a good agreement between the

model predictions and the field measurements. Their study suggested that the model, developed with *STELLA,* has great potentials as a modelling tool for effective investigations of atrazine dynamics in agriculture soil due to its simplicity yet being realistic.
Diamond, in 2009 [19], applied dynamic systems to model zombie invasion using *STELLA*. Zombie invasion scenario has been a common trope in American popular culture for decades. Diamond suggested that the outbreak begins with a mutant virus introduced into a small population of humans, the virus kills those it infects, and after a period of time, causes them to rise from the dead with an insatiable hunger for human flesh. As decaying mockeries of human life, those walking undead are insensible to cold, heat, fatigue or fear. His study claims that the zombies basic instinct is to feed upon the living. Diamond modified the work done by Munz et al. [36], by incorporating the following elements:

- A hybrid Lotka-Volterra/epidemiological model to simulate a multi-stage disease spread by predation, with a $1:1$ efficiency of conversion of prey to "infected prey."
- A persistent, rather than impulsive, zombie eradication mechanism which more closely resembles prey defence systems in the natural world.
- A "panic factor" coupled with the ratio of infection verses zombie elimination rate, plus the zombie feed rate which gives a rough approximate value for the general feel of which side is winning. The panic factor causes indirect human casualties (i.e. not directly caused by zombie infection or consumption).
- A "learning curve " which simulates adaptive human behavioral changes over time.
- A "zombie feed rate " term which simulates destruction, but not infection and conversion, of living humans.

He used four stocks and two conveyors, a conveyor is similar to a stock, but the primary output is controlled by a transit-time factor. We give the detailed *STELLA* model in Figure 2.2 ,

Table 2.2: Detailed description of *STELLA* model

S	susceptible humans
I	infected humans
Z	zombies
X	removed
$IFREE$	"free infected " infected humans not quarantined
Q	quarantined humans
$elim$	elimination
$quar$	quarantine
inf	infection
res	resurrect.

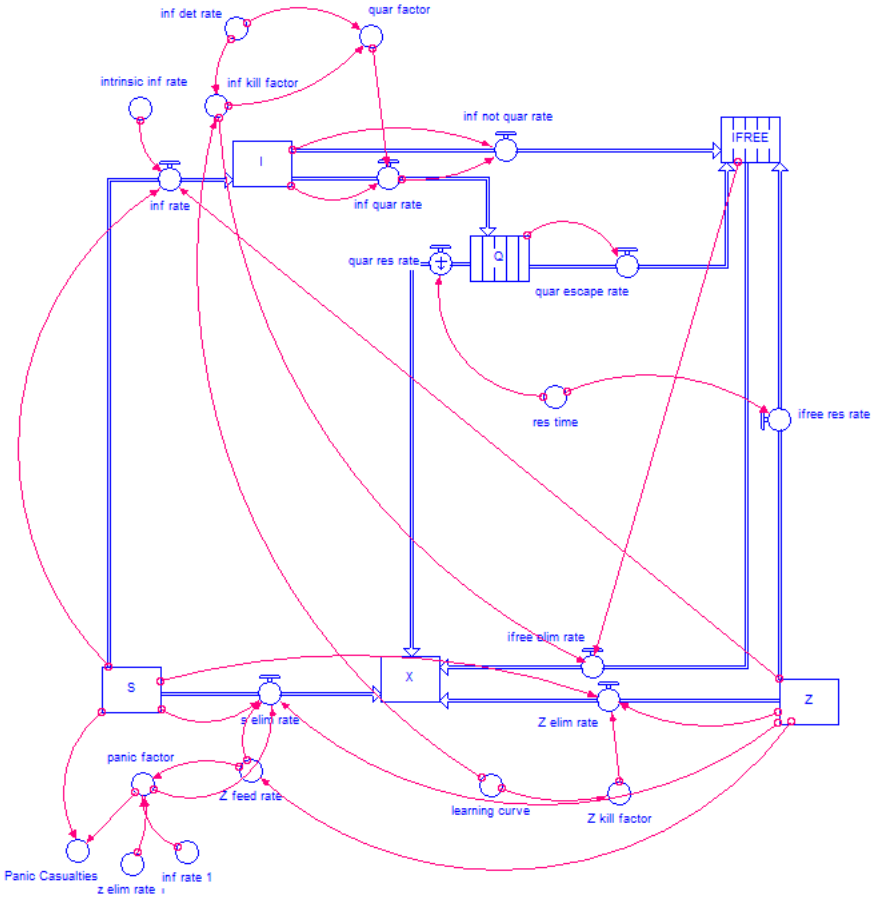

Figure 2.2: Complete *STELLA* model for zombie invasion

His study suggested that the zombie model itself is inherently unstable. A small change in the infection rate, or a small change in the intrinsic zombie kill factor can result in rapid population crash of either humans or zombies. Parameters were finely turned to demonstrate a long, draw-out contest between the living and undead.

2.4 Our project

It is against this background that we endeavour to model the dynamics of Buruli ulcer with a focus on the transmission of BU in fluctuating environments. We include seasonal variations in the disease transmission pathways and in the environments. In particular, the transmission rate and the rate of change for the bacteria density in the environment are subjected to periodicity. Using the next infection operator introduced by Wang and Zhao in [55], we derive and compute the basic reproduction number R_0, for BU model and conduct careful analysis on the disease extinction and persistence dynamics. Using parameters from literature on vector borne diseases and on assumptions about the disease we provide some simulations to show when BU disease goes to extinction and when it will persist. In addition, we use *STELLA* to model the transmission of BU with the object of incorporating aspects that usually makes standard system differential equations intractable.

Chapter 3

Model formulation of the transmission of BU in fluctuating environments

3.1 Introduction

In this chapter, we study the model of the transmission of BU in fluctuating environments, we formulate the model and derive the necessary dynamical system to describe the dynamics of the transmission of BU in fluctuating environments. We then establish the basic properties of the model by showing that the model is positively invariant, therefore, is epidemiologically and mathematically well posed. The steady states are determined and analysed using the two reproduction numbers; time-averaged reproduction number $[R_0]$ and the basic reproduction number R_0 for their stability. We also compare our two reproduction numbers to see which one shows accuracy or inaccuracy in predicting the number of infections by numerically varying our disease transmission parameters. We carry out numerical simulations on the behaviour of the model and conclude.

3.2 Model formulation

In the transmission of BU in fluctuating environments, the human population size N_H, comprises of susceptible individuals S_H, infectious individuals I_H, those under treatment T_H and the recovered R_H. Thus, the

population at any time t is,

$$N_H = S_H + I_H + T_H + R_H. \tag{3.2.1}$$

Similarly, the water bugs population size N_B, which also includes susceptible water bugs S_B and infectious water bugs I_B. Thus, the population at any time t is,

$$N_B = S_B + I_B. \tag{3.2.2}$$

The compartment M represents *Mycobacterium ulcerans* in the environments whose carrying capacity is K_M. The possible interrelations between humans, the water bugs and *Mycobacterium ulcerans* in the environment is represented in Figure 3.1.

We present below a compartmental diagram for the transmission of BU in fluctuating environments.

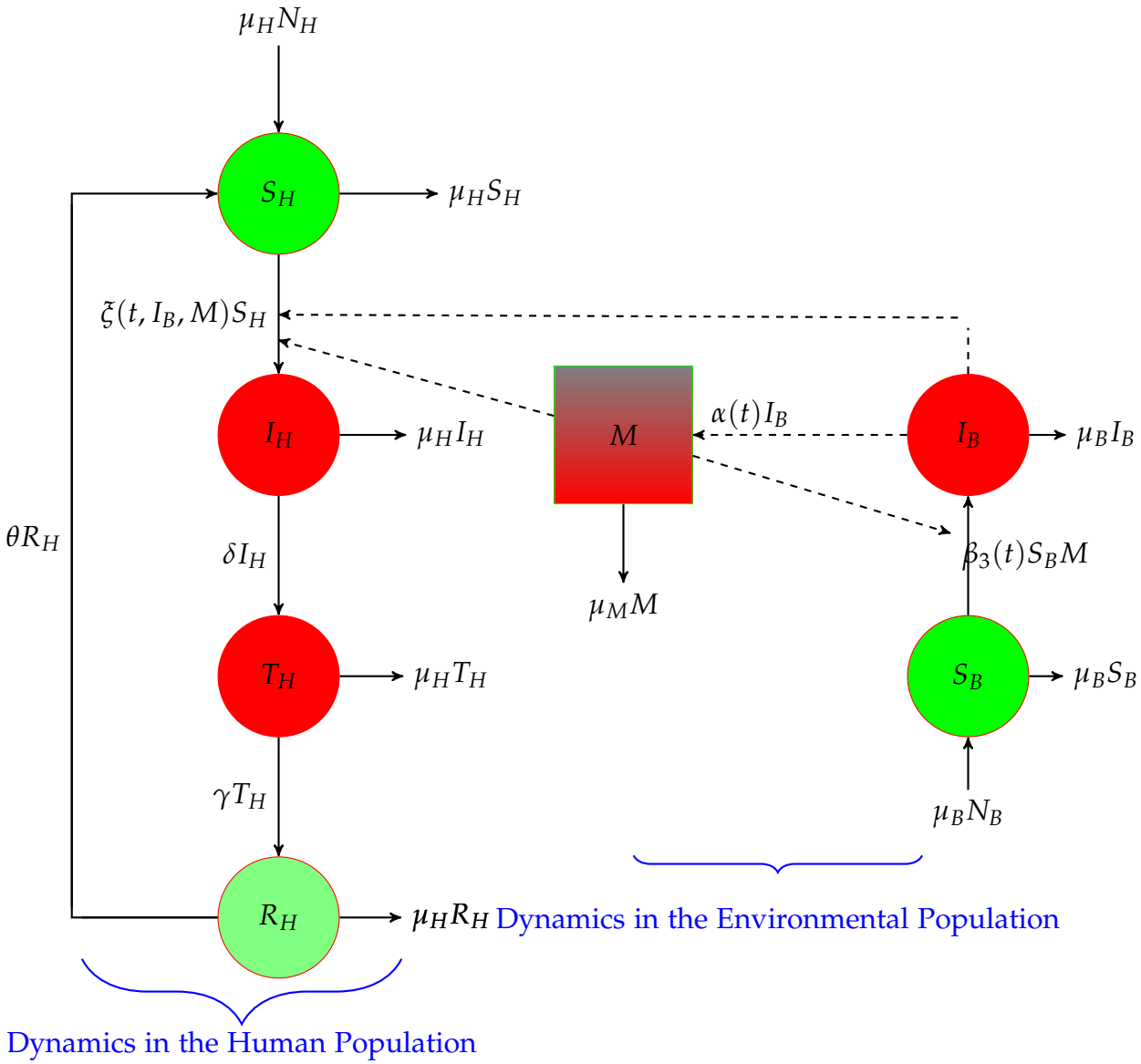

Figure 3.1: Compartmental diagram for the transmission of BU in fluctuating environments. We have in the human population susceptible human(S_H), infected humans(I_H), individuals in treatments(T_h) and the recovered humans(R_H). In the environmental population S_B is the susceptible water bugs, I_B is the infected water bugs and M is the *Mycobacterium ulcerans* in the environment. We have used the dashed lines with arrow head to indicates contact and solid lines with arrow head to indicates movement.

Table 3.1: Description of diagram variables and parameters

Variables	Interpretation
S_H	Susceptible humans
I_H	Infected humans
T_H	Treated humans
R_H	Recovered humans
S_B	Susceptible water bugs
I_B	Infected water bugs
M	*Mycobacterium ulcerans* in the environment
Parameters	**Interpretation**
δ	Treatment rate of infected humans
γ	Recovery rate of infected humans
K_M	Carrying capacity of the *Mycobacterium ulcerans*
θ	Lost of immunity by the recovered humans
β_1	Effective contact rates between susceptible humans with the water bugs
β_2	Effective contact rates between susceptible humans with the *Mycobacterium ulcerans*
β_3	The effective contact rate between the water bugs and the *Mycobacterium ulcerans*
ξ	The disease transmission rate for humans by infected water bugs and *Mycobacterium ulcerans*
μ_H	Natural mortality/birth rate for humans
μ_B	Natural mortality/birth rate for water bugs
μ_M	Natural mortality rate for *Mycobacterium ulcerans*
$\widetilde{\alpha}$	Rate of shedding of *Mycobacterium ulcerans* in the environments by the water bugs
N_H	Total number of human population
N_B	Total number of water bugs population

Table 3.1 gives the detailed description of all model variables and parameters used in our model formulation.

Equation (3.2.3) gives the dynamics of the susceptible population, the parameters $\mu_H N_H$, θR_H, $\mu_H S_H$ and $\xi(t, I_B, M)S_H$ respectively denote new population entering into the susceptible population, the rate at which recovered individuals loss their immunity and return return to the susceptible population again, the natural mortality rate and the disease transmission rate which changes periodically

$$\frac{dS_H}{dt} = \mu_H N_H + \theta R_H - \xi(t, I_B, M)S_H - \mu_H S_H \tag{3.2.3}$$

where

$$\xi(t, I_B, M) = \beta_1(t)\frac{I_B}{N_H} + \beta_2(t)\frac{M}{(K_{50} + M)}.$$

The seasonal parameters $\beta_1(t)$ and $\beta_2(t)$ are the effective contact rates of the susceptible humans with the water bugs and the density of *Mycobacterium ulcerans* in the environment, respectively. Here β_1 is the product of the biting frequency of the water bugs on humans, density of *Mycobacterium ulcerans* per human host, and the probability that a bite will result in an infection. Also β_2 is the product of density of *Mycobacterium ulcerans* per human host and the probability that a contact will result in an infection. The parameter K_{50} gives the density of *Mycobacterium ulcerans* in the environments that yields 50% chance of infection of with BU.

Considering equation (3.2.4), the infectious stage of BU the parameters represent the individuals who enter from the susceptible pool driven by the transmission rate $\xi(t, I_B, M)$, δI_H is the treatment rate and $\mu_H I_H$ is the natural mortality of infected humans respectively.

$$\frac{dI_H}{dt} = \xi(t, I_B, M)S_H - \mu_H I_H - \delta I_H. \tag{3.2.4}$$

The equation that models those undergoing treatment T_H, has parameters μ_H and γ denoting natural mortality and recovery rates respectively. The equation is given by,

$$\frac{dT_H}{dt} = \delta I_H - \mu_H T_H - \gamma T_H. \tag{3.2.5}$$

In the recovery state in equation (3.2.6), the dynamics is as follows: The parameters γ, μ_H and θ denote those who recover at a per capita rate, natural mortality and loss of immunity respectively. The rate of change of the recovered humans is given by

$$\frac{dR_H}{dt} = \gamma T_H - \mu_H R_H - \theta R_H. \tag{3.2.6}$$

In the susceptible water bugs, the dynamics is as follows: $\mu_B N_B$ being the recruitment rate, β_3 is the disease transmission rate of the water bugs by the *Mycobacterium ulcerans* and μ_B is the natural mortality of the water bugs.

$$\frac{dS_B}{dt} = \mu_B N_B - \mu_B S_B - \beta_3(t) S_B \frac{M}{K_M}. \tag{3.2.7}$$

The dynamics of the infected water bugs is given in equation (3.2.8), the parameter μ_B and β_3 model the natural mortality of the water bugs and the disease transmission rate from the environments.

$$\frac{dI_B}{dt} = \beta_3(t) S_B \frac{M}{K_M} - \mu_B I_B. \tag{3.2.8}$$

The dynamics of the *Mycobacterium ulcerans* in the environment are modelled by .

$$\frac{dM}{dt} = \alpha(t) I_B - \mu_M \frac{M}{K_M}. \tag{3.2.9}$$

The first term α denotes the shedding of *Mycobacterium ulcerans* by the infected water bugs into the environments and the term μ_M is the death rate of the *Mycobacterium ulcerans* in the environment.

3.3 Model equations

From the above compartmental model 3.1 the following dynamical systems are derived to describe the dynamics of the transmission of BU in fluctuating environments:

$$\left.\begin{aligned}
\frac{dS_H}{dt} &= \mu_H N_H + \theta R_H - \xi(t, I_B, M) S_H - \mu_H S_H, \\
\frac{dI_H}{dt} &= \xi(t, I_B, M) S_H - (\mu_H + \delta) I_H, \\
\frac{dT_H}{dt} &= \delta I_H - (\mu_H + \gamma) T_H, \\
\frac{dR_H}{dt} &= \gamma T_H - (\mu_H + \theta) R_H, \\
\frac{dS_B}{dt} &= \mu_B N_B - \mu_B S_B - \beta_3(t) S_B \frac{M}{K_M}, \\
\frac{dI_B}{dt} &= \beta_3(t) S_B \frac{M}{K_M} - \mu_B I_B, \\
\frac{dM}{dt} &= \alpha(t) I_B - \mu_M \frac{M}{K_M}
\end{aligned}\right\} \tag{3.3.1}$$

where

$$\xi(t, I_B, M) = \beta_1(t) \frac{I_B}{N_H} + \beta_2(t) \frac{M}{(K_{50} + M)}.$$

The incidence function $\xi(t, I_B, M)$ determines the rate at which new cases of BU are generated and $\alpha(t)$ the shedding rate of *Mycobacterium ulcerans* by the water bugs in the environments. The rates $\beta_1, \beta_2, \beta_3$ and α are periodic functions of time with a common period, $\omega = \frac{365}{4} = 91.25$ days. Periodic transmission is often assumed to be sinusoidal, such that

$$\beta_i(t) = \hat{\beta}_i \left[1 + \bar{\beta}_i \sin\left(\frac{2\pi t}{91.25}\right)\right] \quad \text{and} \quad \alpha(t) = \hat{\alpha} \left[1 + \bar{\alpha} \sin\left(\frac{2\pi t}{91.25}\right)\right],$$

where $i = 1, 2, 3$. $\hat{\beta}\bar{\beta}_i$ and $\hat{\alpha}\bar{\alpha}$ are the amplitude of the periodic oscillations in $\beta_i(t)$ and $\alpha(t)$. There is no periodic infections when $\bar{\beta}_i = \bar{\alpha} = 0$. Here $\hat{\beta}_i$ and $\hat{\alpha}$ is the baseline values or the time-average.

The following expressions transform (3.3.1) into a dimensionless system,

$$s_h = \frac{S_H}{N_H},\ i_h = \frac{I_H}{N_H}, \tau_h = \frac{T_H}{N_H}, r_h = \frac{R_H}{N_H},$$
$$s_b = \frac{S_B}{N_B},\ i_b = \frac{I_B}{N_B}, m = \frac{M}{K_M}, p = \frac{N_B}{N_H}.$$

since we have a constant population, $r_h = 1 - (s_h + i_h + \tau_h), s_b = 1 - i_b$ and the system becomes,

$$\left.\begin{aligned}
\frac{ds_h}{dt} &= (\mu_h + \theta)(1 - s_h) - \theta(i_h + \tau_h) - \widetilde{\xi}(t, i_b, m)s_h, \\
\frac{di_h}{dt} &= \widetilde{\xi}(t, i_b, m)s_h - \delta i_h - \mu_h i_h, \\
\frac{d\tau_h}{dt} &= \delta i_h - (\mu_h + \gamma)\tau_h, \\
\frac{di_b}{dt} &= \beta_3(t)(1 - i_b)m - \mu_b i_b, \\
\frac{dm}{dt} &= \widetilde{\alpha}(t)i_b - \mu_m m
\end{aligned}\right\} \tag{3.3.2}$$

where

$$\widetilde{\xi}(t, i_b, m) = \beta_1(t)p(N_B, N_H)i_b + \beta_2(t)\frac{m}{\widetilde{K} + m}, \quad \widetilde{\alpha}(t) = \frac{\alpha(t)N_B}{K_m}, \quad \widetilde{K} = \frac{K_{50}}{K_m},$$

because the total number of bites made by the water bugs must be equal the number of bites received by "humans ", $p(N_B, N_H)$ is a constant; see [14, 25]. Model equations 3.3.2 above represents the dynamics of BU transmission, we analyse the system 3.3.2 by considering some basic properties of the model.

3.3.1 Basic properties of the model

Here we study the basic results of solutions of system 3.3.1. This results are essential in the proofs of stability results and to ensure that our model is epidemiologically and mathematically well posed.

3.3.2 Positivity of the solutions

We need to ensure that the state variables remain non-negative and solutions of the system remain positive for all $t \geq 0$ given positive initial conditions, thus to establish the long term behaviour of the solutions. We have the following lemma.

Lemma 3.3.3. Given the initial conditions $s_h(0) \geq 0, i_h(0) \geq 0, \tau_h(0) \geq 0, i_b(0) \geq 0$, and $m(0) \geq 0$, then the solutions $(s_h(t), i_h(t), \tau_h(t), i_b(t), m(t))$ of the system (3.3.2) remain positive for all $t \geq 0$.

Proof. Suppose $\hat{t} = sup\{t > 0 : s_h(0) \geq 0, i_h(0) \geq 0, \tau_h(0) \geq 0, i_b(0) \geq 0, m(0) \geq 0\} \in [0, t]$, thus $\hat{t} \geq 0$. From the first equation we have,

$$\frac{ds_h}{dt} \geq -[(\mu_h + \theta) + \widetilde{\xi}(t, i_b, m)]s_h.$$

Simple integration yields,

$$s_h(t) \geq s_h(0) \exp^{-(\mu_h+\theta)t + \int_0^t \widetilde{\xi}(\tau, i_b, m)d\tau} \geq 0.$$

The solution $s_h(t)$ will thus always be positive even for a non constant force of infection $\widetilde{\xi}(t, i_b, m)$.
From the second equation we have,

$$\frac{di_h}{dt} \geq -[(\delta + \mu_h)i_h],$$

which result in

$$i_h(t) \geq i_h(0) \exp^{-(\delta+\mu_h)t} \geq 0.$$

From the third equation we have,

$$\frac{d\tau_h}{dt} \geq -[(\mu_h + \gamma)\tau_h].$$

Simple integration yields,

$$\tau_h(t) \geq \tau_h(0) \exp^{-(\mu_h+\gamma)t} \geq 0.$$

From the fourth equation we have,

$$\frac{di_b}{dt} \geq -[\mu_b i_b],$$

which result in

$$i_b(t) \geq i_b(0)\exp^{-\mu_b t} \geq 0.$$

Lastly,

$$\frac{dm}{dt} \geq -[\mu_m m].$$

Simple integration yields,

$$m(t) \geq m(0)\exp^{-\mu_m t} \geq 0.$$

Thus all the state variables are positive for any non-negative initial conditions. □

3.3.4 Invariant region

The biological feasible region for the system (3.3.2) is in $\mathbb{R}^5_+$ and is represented by the following invariant region:

$$\Omega = \left\{(s_h, i_h, \tau_h, i_h, m) \in \mathbb{R}^5_+ | 0 \leq s_h + i_h + \tau_h \leq 1, 0 \leq i_b \leq 1, 0 \leq m \leq m^*\right\}$$

where the basic properties of local existence, uniqueness, and continuity of solutions are valid for the Lipschitzian systems 3.3.2. The populations described in this model are assumed to be constant over the modelling time. We can easily establish the positive invariance of Ω. Given that,

$$\frac{dm}{dt} = \widetilde{\alpha}(t) i_b - \mu_m m \leq \widetilde{\alpha}(t) - \mu_m m, \tag{3.3.3}$$

we have $m \leq m^*$ where $m^* = \left\{\frac{\hat{\alpha}}{\mu_m} + \hat{\alpha}\bar{\alpha}\left[\frac{(91.25)^2\mu_m + (2\pi)^2\mu_m}{(91.25\mu)^2 + (2\pi)^2}\right]\sin\left(\frac{2\pi t}{91.25}\right)\right\}$. The solutions of systems 3.3.2 starting in Ω remain in Ω for all $t > 0$. The ω-limit sets of systems 3.3.2 are contained in Ω. It thus suffices to consider the dynamics of our system in Ω, where the model is epidemiologically and mathematically well posed.

3.3.5 Equilibrium points

From Definition 1.6.2 to obtain our steady state we set the right hand side of system 3.3.2 to zero. It is easy to see that system (3.3.2) has one disease free equilibrium in the non-negative feasible region $\mathbb{R}^5_+$; $E^0 = (s_h^0, i_h^0, \tau_h^0, i_b^0, m^0) = (1, 0, 0, 0, 0)$.

3.3.6 The basic reproduction number

The basic reproduction number, R_0, is defined as the expected number of secondary infections in a population of susceptible individuals arising from a single individual during the entire infectious period [18]. R_0 often serves as the threshold parameter that predicts whether an infection will spread or not. Using the standard next-generation matrix theory, we transform the system (3.3.2) into the following,

$$\begin{pmatrix} \frac{di_h}{dt} \\ \\ \frac{d\tau_h}{dt} \\ \\ \frac{di_b}{dt} \\ \\ \frac{dm}{dt} \end{pmatrix} = \begin{pmatrix} \widetilde{\xi}(t, i_b, m)s_h \\ \\ 0 \\ \\ \beta_3(1-i_b)m \\ \\ 0 \end{pmatrix} - \begin{pmatrix} (\delta+\mu_h)i_h \\ \\ -\delta i_h + (\mu_h+\gamma)\tau_h \\ \\ \mu_b i_b \\ \\ -\widetilde{\alpha} i_b + \mu_m m \end{pmatrix} = \mathcal{F} - \mathcal{V}$$

where $\mathcal{F}$ denotes the occurrence rate of new infections and $\mathcal{V}$ the rate of transfer of individuals into or out of each compartments [18]. The next generation matrix is given as $F(t)V(t)^{-1}$ where $F(t)$ and $V(t)$ are the Jacobian matrices given by

$$F(t) = D\mathcal{F}(E^0) = \begin{pmatrix} 0 & 0 & 0 & 0 \\ \\ 0 & 0 & 0 & 0 \\ \\ \beta_1(t)p & 0 & 0 & 0 \\ \\ \frac{\beta_2(t)}{K} & 0 & \beta_3(t) & 0 \end{pmatrix} \text{ and}$$

$$V(t) = D\mathcal{V}(E^0) = \begin{pmatrix} \delta+\mu_h & -\delta & 0 & 0 \\ \\ 0 & (\mu_h+\gamma) & 0 & 0 \\ \\ 0 & 0 & \mu_b & -\widetilde{\alpha}(t) \\ \\ 0 & 0 & 0 & \mu_m \end{pmatrix}.$$

For the time-averaged lets consider

$$[F] = \begin{pmatrix} 0 & 0 & 0 & 0 \\ 0 & 0 & 0 & 0 \\ \beta_1 p & 0 & 0 & 0 \\ \frac{\beta_2}{K} & 0 & \beta_3 & 0 \end{pmatrix},$$

$$[V] = \begin{pmatrix} \delta + \mu_h & -\delta & 0 & 0 \\ 0 & (\mu_h + \gamma) & 0 & 0 \\ 0 & 0 & \mu_b & -\tilde{\alpha} \\ 0 & 0 & 0 & \mu_m \end{pmatrix},$$

$$[V^{-1}] = \begin{pmatrix} \frac{1}{\delta+\mu_h} & \frac{\delta}{(\gamma+\mu_h)(\delta+\mu_h)} & 0 & 0 \\ 0 & \frac{1}{\delta+\mu_h} & 0 & 0 \\ 0 & 0 & \frac{1}{\mu_b} & \frac{\tilde{\alpha}}{\mu_b\mu_m} \\ 0 & 0 & 0 & \frac{1}{\mu_m} \end{pmatrix},$$

$$([F][V]^{-1}) = D[\mathcal{F}][\mathcal{V}]^{-1}(E^0) = \begin{pmatrix} 0 & 0 & 0 & 0 \\ 0 & 0 & 0 & 0 \\ \frac{\beta_1 p}{\delta+\mu_h} & \frac{\beta_1 p\delta}{(\gamma+\mu_h)(\delta+\mu_h)} & 0 & 0 \\ \frac{\beta_2}{(\delta+\mu_h)K} & \frac{\beta_2\delta}{(\gamma+\mu_h)(\delta+\mu_h)} & \frac{\beta_3}{\mu_b} & \frac{\beta_3\alpha}{\mu_b\mu_m} \end{pmatrix},$$

and where E^0 is the disease-free equilibrium of the model defined in system (3.3.2). The time-averaged basic reproduction number of the system

(3.3.2) is defined as the spectral radius of the time-averaged next generation matrix $[F][V]^{-1}$, and is given by

$$[R_0] = \rho([F][V]^{-1}) = \frac{\widehat{\beta_3 \widetilde{\alpha}}}{\mu_b \mu_m}. \tag{3.3.4}$$

We interpreted our $[R_0]$ to be the number of secondary cases of infected water bugs generated by the shedding rate of *Mycobacterium ulcerans* in the environments. The time-averaged basic reproduction number $[R_0]$ is independent of the parameters of human population but only dependent on the life spans of the water bugs and *Mycobacterium ulcerans* in the environments, shedding rate, and infection rate of the water bugs. From this we can conclude that the infection of BU is driven by the water bug population and the density of the *Mycobacterium ulcerans* in the environments making the human being victims of the BU epidemic. It has been noted, however, that $[R0]$ may overestimate or underestimate the infection risk for a non-autonomous epidemiological system see [61]. As such, it is enough to only consider the water bugs and *Mycobacterium ulcerans* compartments for the following analysis on the transmission of BU in fluctuating environments. Now we consider our environmental dynamics for the following analysis.

$$\left.\begin{aligned} \frac{ds_b}{dt} &= \mu_b - \mu_b s_b - \beta_3(t) s_b m, \\ \frac{di_b}{dt} &= \beta_3(t) s_b m - \mu_b i_b, \\ \frac{dm}{dt} &= \widetilde{\alpha}(t) i_b - \mu_m m. \end{aligned}\right\} \tag{3.3.5}$$

By setting $s_b = 1 - i_b$ we have,

$$\left.\begin{aligned} \frac{di_b}{dt} &= \beta_3(t)(1 - i_b) m - \mu_b i_b, \\ \frac{dm}{dt} &= \widetilde{\alpha}(t) i_b - \mu_m m. \end{aligned}\right\} \tag{3.3.6}$$

3.4 The basic reproduction number using the next infection operator L

Wang and Zhao [55], extended the framework done by Driessche and Watmough [18] to include epidemiological models in periodic environments.

To establish our basic reproduction number R_0, in periodic environment of the system 3.3.2, we restate and use the assumptions in [55].

3.4.1 Assumptions on the basic reproduction number R_0

We consider a heterogeneous population whose individuals can be grouped into n homogeneous compartments. Let $x = (x_1, \ldots, x_n)^T$, with each $x_i \geq 0$, be the state of individuals in each compartment. We assume that the compartments can be divided into two types: infected compartments, labelled by $i = 1, \ldots, m$ and uninfected compartments, labelled by $i = m+1, \ldots, n$. Define X_s to be the set of all disease free states:

$$X_s := \{x \geq 0 : x_i = 0, \forall i = 1, \ldots, m\}. \tag{3.4.1}$$

Let $\mathcal{F}_i(t,x)$ be the input rate of newly infected individuals in the ith compartment, $\mathcal{V}_i^+(t,x)$ be the input rate of individuals by other means (for example, births, immigrations) and $\mathcal{V}_i^-(t,x)$ be the rate of transfer of individuals out of compartment i (for example, deaths, recovery and emigrations). Thus, the disease transmission model is governed by a non-autonomous ordinary differential system:

$$\frac{dx_i}{dt} = \mathcal{F}_i(t,x) - \mathcal{V}(t,x) \triangleq f_i(t,x), \quad i = 1, \ldots, n \tag{3.4.2}$$

where $\mathcal{V}_i = \mathcal{V}_i^- - \mathcal{V}_i^+$. Following the setting of [18] for autonomous compartmental epidemic models, we make the following assumptions:

(1) For each $1 \leq i \leq n$, the functions $\mathcal{F}_i(t,x), \mathcal{V}_i^+(t,x)$ and $\mathcal{V}_i^-(t,x)$ are non-negative and continuous on $\mathbb{R} \times \mathbb{R}_+^n$ and continuously differential with respect to x.

(2) There is a real number $\omega > 0$ such that for each $1 \leq i \leq n$, the functions $\mathcal{F}_i(t,x), \mathcal{V}_i^+(t,x)$ and $\mathcal{V}_i^-(t,x)$ are $\omega-$periodic in t.

(3) If $x_i = 0$, then $\mathcal{V}_i^- = 0$. In particular, if $x \in X_s$, then $\mathcal{V}_i^- = 0$ for $i = 1, \ldots, m$.

(4) $\mathcal{F}_i = 0$ for $i > m$.

(5) If $x \in X_s$, then $\mathcal{F}_i(x) = \mathcal{V}_i^+(x) = 0$ for $i = 1, \ldots, m$.

Note that assumption (1) arises from the simple fact that each function denotes a directed non-negative transfer of individuals. Biologically, assumption (2) describes a periodic environment (e.g., due to seasonality); assumption (3) says if a compartment is empty, then there is no transfer of individuals out of the compartment; assumption (4) means that the incidence of infection for uninfected compartments is zero; and assumption (5) implies that the population will remain free of disease if it is free of disease at the beginning. We assume that the model (3.4.2) has a disease free periodic solution $x^0(t) = (0,\dots,0,x^0_{m+1}(t),\dots,x^0_n(t))^T$ with $x^0_i(t) > 0$, $m+1 \le i \le n$ for all t. Let $f = (f_1,\dots,f_n)^T$ and define an $(n-m)\times(n-m)$ matrix

$$M(t) := \left(\frac{\partial f_i(t,x^0(t))}{\partial x_j}\right)_{m+1\le i,j\le n}.$$

Let $\Phi_M(t)$ be the monodromy matrix of the linear $\omega-$periodic system $\frac{dz}{dt} = M(t)z$. We further assume that $x^0(t)$ is linearly asymptotically stable in the disease free subspace X_s, that is,

(6) $\rho(\Phi_M(\omega)) < 1$, where $\rho(\Phi_M(\omega))$ is the spectral radius of $\Phi_M(\omega)$.

By the arguments similar to those in [[18], Lemma 1,] it then follows that

$$D_x\mathcal{F}(t,x^0(t)) = \begin{pmatrix} F(t) & 0 \\ 0 & 0 \end{pmatrix} \text{ and } \quad D_x\mathcal{V}(t,x^0(t)) = \begin{pmatrix} V(t) & 0 \\ J(t) & -M(t) \end{pmatrix},$$

where $F(t)$ and $V(t)$ are two $m\times m$ matrices defined by

$$F(t) = \left(\frac{\partial \mathcal{F}_i(t,x^0(t))}{\partial x_j}\right)_{1\le i,j\le m}, \quad V(t) = \left(\frac{\partial \mathcal{V}_i(t,x^0(t))}{\partial x_j}\right)_{1\le i,j\le m}, \tag{3.4.3}$$

respectively, and $J(t)$ is an $(n-m)\times n$ matrix. Furthermore, $F(t)$ is non-negative, and $-V(t)$ is cooperative in the sense that the off-diagonal elements of $-V(t)$ are non-negative. Let $Y(t,s)$, $t \ge s$, be the evolution operator of the linear $\omega-$periodic system

$$\frac{dy}{dt} = -V(t)y. \tag{3.4.4}$$

That is, for each $s \in \mathbb{R}$, the $m\times m$ matrix $Y(t,s)$ satisfies

$$\frac{d}{dt}Y(t,s) = V(t)Y(t,s), \quad \forall t \ge s, \quad Y(s,s) = I$$

where I is $m \times m$ identity matrix. Thus, the monodromy matrix $\Phi_{-V}(t)$ of equation (3.4.4) equals $Y(t,0)$, $t \geq 0$. Note that the internal evolution of individuals in the infectious compartments due to deaths and movements among the compartments is dissipative and exponentially decays in many cases because of the loss of infective members from natural mortalities and disease-induced mortalities. Thus, we assume that

(7) $\rho(\Phi_{-V}(\omega)) < 1$.

Based on the assumptions above, we now analyse the reproduction ratios for the epidemic model (3.4.2). We assume that the population is near the disease free periodic state $x^0(t)$.
In view of the periodic environment, we assume that $\phi(s)$, $\omega-$periodic in s, is the initial distribution of infectious individuals. Then $F(s)\phi(s)$ is the distribution of new infections produced by the infected individuals who were introduced at time s. Given $t \geq s$, then $Y(t,s)F(s)\phi(s)$ gives the distribution of those infected individuals who were newly infected at time s and remain in the infected compartments at time t. It follows that

$$\lambda(t) := \int_{-\infty}^{t} Y(t,s)F(s)\phi(s)ds = \int_{0}^{\infty} Y(t,t-s)F(t-s)\phi(t-s)ds$$

is the distribution of accumulative new infections at time t produced by all those infected individuals $\phi(s)$ introduced at time previous to t.
Let C_ω be the ordered Banach space of all $\omega-$periodic functions from $\mathbb{R}$ to $\mathbb{R}^m$, which is equipped with the maximum norm $||.||$ and the positive cone $C_\omega^+ := \{\phi \in C_\omega : \phi(t) \geq 0, \forall t \in \mathbb{R}\}$. Then we can define a linear operator $L : C_\omega \to C_\omega$ by

$$(L\phi)(t) = \int_{0}^{\infty} Y(t,t-s)F(t-s)\phi(t-s)ds, \quad \forall t \in \mathbb{R}, \phi \in C_\omega. \tag{3.4.5}$$

Following [55], we call L the next infection operator, and define the spectral radius of L as the basic reproduction number

$$R_0 := \rho(L),$$

for the periodic epidemic model (3.4.2).

Using the assumptions above and from system 3.3.6, we define our new $F(t)$ and $V(t)$ to be,

$$F(t) = \begin{pmatrix} 0 & \beta_3(t) \\ 0 & 0 \end{pmatrix} \text{ and } \quad V(t) = \begin{pmatrix} \mu_b & 0 \\ -\widetilde{\alpha}(t) & \mu_m \end{pmatrix}.$$

$$-V(t) = \begin{pmatrix} -\mu_b & 0 \\ \widetilde{\alpha}(t) & -\mu_m \end{pmatrix},$$

From assumption (6) we solve the system of differential equations

$$\frac{dy}{dt} = -V(t)y,$$

as follows,

$$\begin{pmatrix} \frac{dy_1}{dt} & \frac{dy_2}{dt} \\ \frac{dy_3}{dt} & \frac{dy_4}{dt} \end{pmatrix} = \begin{pmatrix} -\mu_b & 0 \\ \widetilde{\alpha}(t) & -\mu_m \end{pmatrix} \begin{pmatrix} y_1 & y_2 \\ y_3 & y_4 \end{pmatrix}$$

We have

$$\begin{pmatrix} \frac{dy_1}{dt} & \frac{dy_2}{dt} \\ \frac{dy_3}{dt} & \frac{dy_4}{dt} \end{pmatrix} = \begin{pmatrix} -\mu_b y_1 & -\mu_b y_2 \\ \widetilde{\alpha}(t)y_1 - \mu_m y_3 & \widetilde{\alpha}(t)y_2 - \mu_m y_4 \end{pmatrix}.$$

That is, for each $s \in \mathbb{R}$, the 2×2 matrix $Y(t,s)$ satisfies

$$\frac{d}{dt}Y(t,s) = -V(t)Y(t,s), \quad \forall t \geq s, Y(s,s) = I$$

where I_s is the 2×2 identity matrix. Applying the initial conditions

$$\begin{pmatrix} y_1(s) & y_2(s) \\ y_3(s) & y_4(s) \end{pmatrix} = \begin{pmatrix} 1 & 0 \\ 0 & 1 \end{pmatrix}.$$

Solving for y_1, y_2, y_3 and y_4, we will then have

$$\frac{dy_1}{dt} = -\mu_b y_1$$

$$\Rightarrow y_1 = c_1 e^{-\mu_b t} \text{ where } \quad c_1 = e^c.$$

Applying the initial conditions and solving for the constant c_1 we get $c_1 = e^{\mu_b s}$, therefore

$$y_1(t) = e^{-\mu_b (t-s)}.$$

Similarly,

$$\frac{dy_2}{dt} = -\mu_b y_2$$

$$\Rightarrow y_2 = c_2 e^{-\mu_b t} \text{ where } \quad c_2 = e^c.$$

Applying the initial conditions and substituting for c_2 we get $c_2 = 0$. Hence

$$y_2(t) = 0.$$

$$\frac{dy_4}{dt} = y_2 \widetilde{\alpha}(t) - y_4 \mu_m,$$

$$= -y_4 \mu_m$$

$$\Rightarrow y_4 = c_4 e^{-\mu_m t} \text{ where } \quad c_4 = e^c.$$

Applying the initial conditions and substituting for c_4 give $c_4 = e^{\mu_m s}$. Hence

$$y_4(t) = e^{-\mu_m (t-s)}.$$

Similarly,

$$\frac{dy_3}{dt} + y_3 \mu_m = e^{-\mu_b (t-s)} \widetilde{\alpha}(t).$$

Multiplying throughout by the integrating factor, $I = e^{\mu_m t}$ and simplifying

we get

$$y_3\, e^{\mu_m t-\mu_b s} = \int e^{(\mu_m-\mu_b)t}\widetilde{\alpha}(t)dt, \quad \text{and} \quad \widetilde{\alpha}(t) = \hat{\alpha}\left[1+\bar{\alpha}\sin\left(\frac{2\pi t}{91.25}\right)\right],$$

$$y_3\, e^{\mu_m t-\mu_b s} = \hat{\alpha}\int e^{(\mu_m-\mu_b)t}dt + \hat{\alpha}\bar{\alpha}\int e^{(\mu_m-\mu_b)t}\sin\left(\frac{2\pi t}{91.25}\right)dt$$

$$= \hat{\alpha}\frac{e^{(\mu_m-\mu_b)t}}{\mu_m-\mu_b} + \hat{\alpha}\bar{\alpha}\int \sin\left(\frac{2\pi t}{91.25}\right)e^{(\mu_m-\mu_b)t}dt. \tag{3.4.6}$$

We solve $\int \sin\left(\frac{2\pi t}{91.25}\right)e^{(\mu_m-\mu_b)t}dt$ using integration by parts to obtain,

$$\int e^{(\mu_m-\mu_b)t}\sin\left(\frac{2\pi t}{91.25}\right)dt = \frac{1}{(\mu_m-\mu_t)}\sin\left(\frac{2\pi t}{91.25}\right)e^{(\mu_m-\mu_b)t} - \frac{1}{\mu_m-\mu_t} \times \left(\frac{2\pi t}{91.25}\right)\int \cos\left(\frac{2\pi t}{91.25}\right)e^{(\mu_m-\mu_b)t}dt + C. \tag{3.4.7}$$

Also $$\int \cos\left(\frac{2\pi t}{91.25}\right)e^{(\mu_m-\mu_b)t}dt = \frac{1}{(\mu_m-\mu_b)}e^{(\mu_m-\mu_b)t}\cos\left(\frac{2\pi t}{91.25}\right) + \frac{1}{(\mu_m-\mu_b)} \times \left(\frac{2\pi}{91.25}\right)\int \sin\left(\frac{2\pi t}{91.25}\right)e^{(\mu_m-\mu_b)t}dt + C. \tag{3.4.8}$$

Substituting equation (3.4.1) into equation (3.4.7) and simplifying we get

$$\begin{aligned}\int \sin\left(\frac{2\pi t}{91.25}\right) e^{(\mu_m-\mu_b)t}dt = & \\ & \frac{1}{(\mu_m-\mu_b)}\sin\left(\frac{2\pi t}{91.25}\right)e^{(\mu_m-\mu_b)t} - \frac{1}{\mu_m-\mu_b}\left(\frac{2\pi t}{91.25}\right) \\ & \times\left[\frac{1}{(\mu_m-\mu_b)}e^{(\mu_m-\mu_b)t}\cos\left(\frac{2\pi t}{91.25}\right)\right] \\ & +\left[\frac{1}{(\mu_m-\mu_b)}\left(\frac{2\pi}{91.25}\right)\int \sin\left(\frac{2\pi t}{91.25}\right)e^{(\mu_m-\mu_b)t}dt + C.\right]\end{aligned} \tag{3.4.9}$$

Substituting equation (3.4.9) into equation (3.4.1) and simplifying we get

$$\begin{aligned}y_3\, e^{\mu_m t-\mu_b s} = & e^{(\mu_m-\mu_b)t}\left[\frac{\hat{\alpha}}{(\mu_m-\mu_b)} + \frac{\hat{\alpha}\bar{\alpha}(\mu_m-\mu_b)}{(\mu_m-\mu_b)^2+\left(\frac{2\pi}{91.25}\right)^2}\sin\left(\frac{2\pi t}{91.25}\right)\right] \\ & -e^{(\mu_m-\mu_b)t}\left[\frac{\hat{\alpha}\bar{\alpha}(\mu_m-\mu_b)}{(\mu_m-\mu_b)^2+\left(\frac{2\pi}{91.25}\right)^2}\left(\frac{2\pi}{91.25}\right)\cos\left(\frac{2\pi t}{91.25}\right)\right] + C_1.\end{aligned} \tag{3.4.10}$$

Dividing through by $e^{\mu_m t-\mu_b s}$ and applying the initial condition to solve for the constant C_1

$$\begin{aligned}C_1 = & -e^{(\mu_m-\mu_b)s}\left[\frac{\hat{\alpha}}{(\mu_m-\mu_b)} + \frac{\hat{\alpha}\bar{\alpha}(\mu_m-\mu_b)}{(\mu_m-\mu_b)^2+\left(\frac{2\pi}{91.25}\right)^2}\sin\left(\frac{2\pi s}{91.25}\right)\right] \\ & e^{(\mu_m-\mu_b)s}\left[\frac{\hat{\alpha}\bar{\alpha}(\mu_m-\mu_b)}{(\mu_m-\mu_b)^2+\left(\frac{2\pi}{91.25}\right)^2}\left(\frac{2\pi}{91.25}\right)\cos\left(\frac{2\pi s}{91.25}\right)\right].\end{aligned} \tag{3.4.11}$$

Substituting equation (3.4.11) into equation (3.4.1) to obtain $\widetilde{Y}(t,s)$

where

$$\widetilde{Y}(t,s) = \left[\frac{1}{\mu_m-\mu_b}+\frac{\bar{\alpha}}{\left(\frac{2\pi}{91.25}\right)^2+(\mu_m-\mu_b)^2}\left((\mu_m-\mu_b)\sin\left(\frac{2\pi t}{91.25}\right)-\left(\frac{2\pi}{91.25}\right)\cos\left(\frac{2\pi t}{91.25}\right)\right)\right]$$

$$\times \quad \hat{\alpha}e^{-\mu_b(t-s)}-\hat{\alpha}e^{-\mu_m(t-s)} \quad \times$$

$$\left[\frac{1}{\mu_m-\mu_b}+\frac{\bar{\alpha}}{\left(\frac{2\pi}{91.25}\right)^2+(\mu_m-\mu_b)^2}\left((\mu_m-\mu_b)\sin\left(\frac{2\pi s}{91.25}\right)-\left(\frac{2\pi}{91.25}\right)\cos\left(\frac{2\pi s}{91.25}\right)\right)\right].$$

Therefore,

$$Y(t,s) = \begin{pmatrix} e^{-\mu_b(t-s)} & 0 \\ \widetilde{Y}(t,s) & e^{-\mu_m(t-s)} \end{pmatrix}.$$

We numerically evaluate the next infection operator by

$$(L\phi)(t) = \int_0^\infty Y(t,t-s)F(t-s)\phi(t-s)ds = \int_0^\omega G(t,s)\phi(t-s)ds$$

where

$$\begin{aligned} G(t,s) &\approx \sum_{k=0}^{M} Y(t,t-s-k\omega)F(t-s-k\omega) \\ &\approx \hat{\beta_3}\left(1+\bar{\beta_3}\sin\left(\frac{2\pi(t-s)}{91.25}\right)\right)\sum_{k=0}^{M}\begin{pmatrix} 0 & e^{-\mu_b(s+k\omega)} \\ 0 & \widetilde{Y}(t,t-s-k\omega) \end{pmatrix} \end{aligned}$$

where M is a positive integer. R_0, the basic reproduction number is computed by reducing the operator eigenvalue problem to a matrix eigenvalue problem in the form of $Ax = \lambda x$, where the entries of the function G are used to construct the matrix A. The basic reproduction number R_0 can then be approximated by numerically calculating the spectral radius of the matrix A, see [55] for the methods of calculating R_0.

3.5 Assumptions on disease extinction and persistence

To analysis the disease extinction and persistence of the system 3.3.5 or 3.3.6, we use the following assumptions and then we establish them using Lemma 3.5.1 and 3.5.2. We let the function $\beta_3(t)(1-i_b)m = f(t,i_b,m)$ be the incidence function which determines the rate of generating new infections and the function $\widetilde{\alpha}(t)i_b - \mu_m m = g(t,i_b,m)$ which describes the rate of change for the *Mycobacterium ulcerans* in the environments. Both are differentiable and periodic in time with a common periodic ω. We thus have,

$$f(t+\omega,i_b,m) = f(t,i_b,m) \quad \text{and}$$
$$g(t+\omega,i_b,m) = g(t,i_b,m).$$

To make biological sense, we assume that the functions f and g satisfy the following conditions for all $t \geq 0$,

$$f(t,0,0) = g(t,0,0) = 0. \tag{A1}$$

The assumption (A1) ensures that the model has a unique, constant disease free equilibrium $E^0 = (i_b^0, m^0) = (0,0)$.

$$f(t,i_b,m) \geq 0. \tag{A2}$$

Assumption (A2) ensures a non-negative transmission rate.

$$\frac{\partial f}{\partial i_b}(t,i_b,m) \geq 0, \frac{\partial f}{\partial m}(t,i_b,m) \geq 0, \frac{\partial g}{\partial i_b}(t,i_b,m) \geq 0, \frac{\partial g}{\partial m}(t,i_b,m) \leq 0. \tag{A3}$$

The first two inequalities in (A3) state that the rate of new infection increases with both the infected water bugs and the *Mycobacterium ulcerans* density. The third inequality states that increased water bugs infection and consequently, a higher level of water bugs shedding back to the environments, can contribute to a higher growth rate for the *Mycobacterium ulcerans* in the environment. The last inequality explains that the *Mycobacterium ulcerans* cannot sustain themselves in the environment in the absence of water filtering organism and water-dwelling predators [34, 47].
We also assumed that the incidence function and the *Mycobacterium ulcerans* density

$$f(t,i_b,m) \quad \text{and} \quad g(t,i_b,m) \tag{A4}$$

are both concave for any $t \geq 0$, and the following matrices in equation (3.4.1) are negative semi definite everywhere.

$$D^2 f = \begin{pmatrix} \frac{\partial^2 f}{\partial i_b^2} & \frac{\partial^2 f}{\partial i_b \partial m} \\ \\ \frac{\partial^2 f}{\partial i_b \partial m} & \frac{\partial^2 f}{\partial m^2} \end{pmatrix} \quad \text{and} \quad D^2 g = \begin{pmatrix} \frac{\partial^2 g}{\partial i_b^2} & \frac{\partial^2 g}{\partial i_b \partial m} \\ \\ \frac{\partial^2 g}{\partial i_b \partial m} & \frac{\partial^2 g}{\partial m^2} \end{pmatrix} \tag{3.4.1}$$

The assumption (A4) is based on saturation effect, a common assumption in epidemic models [54].

$$f(t,0,m) > 0 \quad if \quad m > 0; \quad g(t,i_b,0) > 0 \quad if \quad i_b > 0. \tag{A5}$$

The first condition in (A5) implies that a positive *Mycobacterium ulcerans* density can lead to a positive incidence even if $i_b = 0$ initially. The second condition states that infected water bugs will contribute to the growth of the *Mycobacterium ulcerans* in the environments by shedding even if $m = 0$ initially.

Moreover, we introduce an additional regulation on the profiles of the incidence and *Mycobacterium ulcerans* functions for small i_b and m. We assume that

$$\text{There exists} \quad \varepsilon^* > 0 \quad \text{such that when} \quad 0 < i_b < \varepsilon^*, 0 < m < \varepsilon^*, \tag{A6}$$

$$\begin{aligned} f(t,i_b,m) \geq & f(t,0,0) + i_b \frac{\partial f}{\partial i_b}(t,0,0) + m\frac{\partial f}{\partial m}(t,0,0) + \frac{1}{2} i_b^2 \frac{\partial^2 f}{\partial i_b^2}(t,0,0) \\ & + i_b m \frac{\partial^2 f}{\partial i_b \partial m}(t,0,0) + \frac{1}{2} m^2 \frac{\partial^2 f}{\partial m^2}(t,0,0), \end{aligned}$$

and

$$\begin{aligned} g(t,i_b,m) \geq & g(t,0,0) + i_b \frac{\partial g}{\partial i_b}(t,0,0) + m\frac{\partial g}{\partial m}(t,0,0) + \frac{1}{2} i_b^2 \frac{\partial^2 g}{\partial i_b^2}(t,0,0) \\ & + i_b m \frac{\partial^2 g}{\partial i_b \partial m}(t,0,0) + \frac{1}{2} m^2 \frac{\partial^2 g}{\partial m^2}(t,0,0). \end{aligned}$$

Here we make some comments on the assumption (A6) based on the concavity of f (assumption (A4)), the surface of f is below its tangent plane

everywhere. Since the matrix in equation (3.4.1) $D^2 f$ is negative semidefinite everywhere, we obtain the following,

$$\begin{aligned} f(t,0,0) + i_b \frac{\partial f}{\partial i_b}(t,0,0) + m\frac{\partial f}{\partial m}(t,0,0) \geq f(t,0,0) + i_b \frac{\partial f}{\partial i_b}(t,0,0) + m\frac{\partial f}{\partial m}(t,0,0) \\ + \frac{1}{2} i_b^2 \frac{\partial^2 f}{\partial i_b^2}(t,0,0) + i_b m \frac{\partial^2 f}{\partial i_b \partial m}(t,0,0) \\ + \frac{1}{2} m^2 \frac{\partial^2 f}{\partial m^2}(t,0,0). \end{aligned}$$

Assumption (A6) means at least in a small neighbourhood of $i_b = m = 0$, the surface of f lies below its tangent plane and above a concave tangent paraboloid. The result holds for g.

Lemma 3.5.1. (Wang and Zhao, 2008, Theorem 2.1) The following statements are valid:

(i) If $\rho(W(\omega, \lambda)) = 1$ has a positive solution λ_0, then λ_0, is an eigenvalue of operator L, and hence $R_0 > 1$.

(ii) if $R_0 > 1$, then $\lambda = R_0$ is the unique solution of $\rho(W(\omega, \lambda)) = 1$.

(iii) $R_0 = 0$ if and only if $\rho(W(\omega, \lambda)) < 1$. For all $\lambda > 0$.

Lemma 3.5.2. (Wang and Zhao, 2008, Theorem 2.2). The following statements are valid:

(i) $R_0 = 1$ if and only if $\rho(\Phi_{F-V}(\omega)) = 1$.

(ii) $R_0 > 1$ if and only if $\rho(\Phi_{F-V}(\omega)) > 1$.

(iii) $R_0 < 1$ if and only if $\rho(\Phi_{F-V}(\omega)) < 1$.

Thus, the disease-free equilibrium E^0 is locally asymptotically stable if $R_0 < 1$, and unstable if $R_0 > 1$.

3.6 Disease extinction

In this section, we analyse the global stability of disease free equilibrium point for the system (3.3.6), which will also provide a condition for the

extinction of the disease. Suppose we have the matrix function

$$F(t) - V(t) = \begin{pmatrix} \frac{\partial f}{\partial i_b}(t,0,0) - \mu_b & \frac{\partial f}{\partial m}(t,0,0) \\ \\ \frac{\partial g}{\partial i_b}(t,0,0) & \frac{\partial g}{\partial m}(t,0,0) \end{pmatrix}. \tag{3.6.1}$$

Clearly, the matrix function of equation (3.6.1) is irreducible, continuous, cooperative, and ω-periodic. Let $\Phi_{(F-V)}(t)$ be the fundamental solution matrix of the linear ordinary differential system:

$$z' = [F(t) - V(t)]z, \tag{3.6.2}$$

and $\rho(\Phi_{(F-V)}(\omega))$ is the spectral radius of $(\Phi_{(F-V)}(\omega))$. From Lemma 2.1 in [61], we obtain the following result:

Lemma 3.6.1. Let $b = \left(\frac{1}{\omega}\right) \ln \rho(\Phi_{(F-V)}(\omega))$. Then there exists a positive ω-periodic function $v(t)$ such that $e^{bt}v(t)$ is a solution to equation (3.6.2).

Proof. Considering equation (3.3.6), and by using assumption $(A4)$, we have

$$\begin{aligned} \frac{di_b}{dt} &= f(t, i_b, m) - \mu_b i_b \leq \left[i_b \frac{\partial f}{\partial i_b}(t,0,0) + m \frac{\partial f}{\partial m}(t,0,0) \right] - \mu_b i_b, \\ \frac{dm}{dt} &= h(t, i_b, m) \leq i_b \frac{\partial g}{\partial i_b}(t,0,0) + m \frac{\partial g}{\partial m}(t,0,0). \end{aligned}$$

so

$$\frac{d}{dt} \begin{bmatrix} i_b \\ m \end{bmatrix} \leq [F(t) - V(t)] \begin{bmatrix} i_b \\ m \end{bmatrix}. \tag{3.6.3}$$

From Lemma 3.6.1, there exists $v(t)$ such that

$$z(t) = (\widetilde{i}_b(t), \widetilde{m}(t)) = e^{bt}v(t) \tag{3.6.4}$$

is a solution to equation (3.6.2), with $b = \left(\frac{1}{\omega}\right) \ln \rho(\Phi_{(F-V)}(\omega))$. It follows from equations (3.6.2) and (3.6.3) that

$$(i_b(t), m(t)) \leq (\widetilde{i}_b(t), \widetilde{m}(t)) \tag{3.6.5}$$

when t is large. From Lemma 3.5.2, $R_0 < 1$ if and only if $\rho(\Phi_{(F-V)}(\omega)) < 1$. Therefore, $b < 0$. Then, given equation (3.6.4) and (3.6.5), is clear that

$$\lim_{t\to\infty} i_b(t) = 0, \quad \lim_{t\to\infty} m(t) = 0.$$

□

Lemma 3.6.2. The disease free equilibrium E^0 of system (3.3.6) is globally asymptotically stable when $R_0 < 1$ if and only if $\rho(\Phi_{F-V}(\omega)) < 1$ and $\lim_{t\to\infty} z(t) = E^0 = (0,0)$ for all solution $z(t)$ of the system (3.3.6).

Theorem 3.6.2 shows that when $R_0 < 1$ then the disease completely dies out which means reducing and keeping R_0 below the unity would be sufficient to remove BU infection even in fluctuating environments [55].

3.7 Disease persistence

In this section, we consider the dynamics of the BU system (3.3.5) when $R_0 > 1$.

$$X = \mathbb{R}^3_+; \quad X_0 = (s_b, i_b, m) \in X; \quad \partial X_0 = X \setminus X_0.$$

Let $P : X \to X$ be the Poincaré map associated with the system (3.3.5), that is,

$$P(x_0) = u(\omega, x_0), \quad \forall x_0 \in X$$

where ω is the period and $u(t, x_0)$ be the unique solution of the system (3.3.5) with $u(0, x_0) = x_0$.

Definition 3.7.1. The solution of system (3.3.5) is said to be uniformly persistent if there exists some $\varrho > 0$ such that

$$\liminf_{t\to\infty} s_b(t) \geq \varrho, \quad \liminf_{t\to\infty} i_b(t) \geq \varrho, \quad \liminf_{t\to\infty} m(t) \geq \varrho$$

whenever $s_b(0) > 0$, $i_b(0) > 0$, and $m(0) > 0$.

Zhao [62] gave the general definition of uniform persistence. The proof of the theorem below is inspired by the work in [61].

Theorem 3.7.2. *Let $R_0 > 1$ and let (A1)–(A6) hold. Then the solutions of system (3.3.5) are uniformly persistent, and the system (3.3.5) admits at least one positive ω − periodic solution.*

Proof. Let

$$M_\partial = \{(s_b(0), i_b(0), m(0)) \in \partial X_0 : P^n(s_b(0), i_b(0), m(0)) \in \partial X_0, \quad \forall n \geq 0\}.$$

We now show that

$$M_\partial = \{(s_b, 0, 0) \in X : s_b \geq 0\}. \tag{3.7.1}$$

It suffices to prove that for any $M_\partial \supseteq \{(s_b, 0, 0) : s_b \geq 0\}$. Consider any initial values $(s_b(0), i_b(0), m(0)) \in \partial X_0 \setminus \{(s_b, 0, 0) : s_b \geq 0\}$. If $i_b(0) = 0$ and $m(0) > 0$, then $i_b'(0) > 0$ from assumption (A5) and also when $m(0) = 0$ and $i_b(0) > 0$, then $m'(0) > 0$. Thus, it follows that $(s_b(t), i_b(t), m(t)) \notin \partial X_0$ for $0 < t \ll 1$. This implies that $M_\partial \subseteq \{(s_b, 0, 0) : s_b \geq 0\}$, and hence we have (3.7.1).
Now, let us consider the fixed point $E^0 = (1, 0, 0)$ and define $W^s(E^0) = \{x_0 : P^n(x_0) \to E^0, n \to \infty\}$. We show that

$$W^s(E^0) \cap X_0 = \emptyset. \tag{3.7.2}$$

Based on the continuity of solutions with respect to the initial conditions, for any $\epsilon > 0$ and $\epsilon < \epsilon^*$, there exists $\delta > 0$ small enough such that $\forall$ $(s_b(0), i_b(0), m(0)) \in X_0$ with $||(s_b(0), i_b(0), m(0)) - E^0|| \leq \delta$, we have

$$||u(t, (s_b(0), i_b(0), m(0))) - u(t, E^0)|| < \epsilon \quad \forall t \in [0, \omega]. \tag{3.7.3}$$

We claim that

$$\limsup_{n\to\infty} ||P^n(s_b(0), i_b(0), m(0)) - E^0|| \geq \delta \quad \forall (s_b(0), i_b(0), m(0)) \in X_0. \tag{3.7.4}$$

By contradiction, we suppose $\limsup_{n\to\infty} ||P^n(s_b(0), i_b(0), m(0)) - E^0|| < \delta$ for some $(s_b(0), i_b(0), m(0)) \in X_0$. Without the loss of generality, we assume that $||P^n(s_b(0), i_b(0), m(0)) - E^0|| < \delta, \quad \forall n \geq 0$. Thus,

$$||u(t, P^n(s_b(0), i_b(0), m(0))) - u(t, E^0)|| < \epsilon \quad \forall t \in [0, \omega] \quad n \geq 0. \tag{3.6.5}$$

Moreover, for any $t \geq 0$, we can write $t = t_\prime + l\omega$ with $t_\prime \in [0, \omega)$ and l the greatest integer less than or equal to $\frac{t}{\omega}$. Hence,

$$||u(t, (s_b(0), i_b(0), m(0))) - u(t, E^0)|| \tag{3.7.6}$$

$$= ||u(t_\prime, P^n(s_b(0), i_b(0), m(0))) - u(t_\prime, E^0)|| < \epsilon$$

for any $t \geq 0$. Let $(s_b(t), i_b(t), m(t)) = u(t, (s_b(0), i_b(0), m(0)))$. It follows that $1 - \epsilon < s_b(t) < 1 + \epsilon, \quad 0 < i_b(t) < \epsilon$ and $0 < m(t) < \epsilon$. since $\epsilon < \epsilon^*$, based on assumptions (A1) and (A6), we obtain this,

$$\begin{aligned}\frac{di_b}{dt} \geq\ & i_b\frac{\partial f}{\partial i_b}(t,0,0) + m\frac{\partial f}{\partial m}(t,0,0) - \mu_b i_b \\ & + \frac{1}{2}\epsilon i_b\frac{\partial^2 f}{\partial i_b^2}(t,0,0) + \frac{1}{2}\epsilon m\frac{\partial^2 f}{\partial m^2}(t,0,0) - \epsilon i_b\left|\frac{\partial^2 f}{\partial i_b \partial m}(t,0,0)\right| \\ & - \epsilon i_b\frac{\partial f}{\partial i_b}(t,0,0) - \epsilon m\frac{\partial f}{\partial i_b}(t,0,0) - \epsilon^2 i_b\left|\frac{\partial^2 f}{\partial i_b \partial m}(t,0,0)\right|\end{aligned}$$

and

$$\begin{aligned}\frac{dm}{dt} \geq\ & i_b\frac{\partial g}{\partial i_b}(t,0,0) + m\frac{\partial g}{\partial m}(t,0,0) \\ & + \frac{1}{2}\epsilon i_b\frac{\partial^2 g}{\partial i_b^2}(t,0,0) + \frac{1}{2}\epsilon m\frac{\partial^2 g}{\partial m^2}(t,0,0) - \epsilon i_b\left|\frac{\partial^2 g}{\partial i_b \partial m}(t,0,0)\right|.\end{aligned}$$

That is,

$$\frac{d}{dt}\begin{bmatrix} i_b \\ m \end{bmatrix} \geq [F - V - \epsilon K]\begin{bmatrix} i_b \\ m \end{bmatrix}, \tag{3.67.7}$$

Where $F - V$ is given in (3.6.1) and

$$\epsilon K = -\epsilon\begin{bmatrix} \frac{1}{2}\frac{\partial^2 f}{\partial i_b^2}(t,0,0) - \frac{\partial f}{\partial i_b}(t,0,0) & 0 \\ -(1+\epsilon)\left|\frac{\partial^2 f}{\partial i_b \partial m}(t,0,0)\right| & \frac{1}{2}\frac{\partial^2 f}{\partial m^2}(t,0,0) - \frac{\partial f}{\partial m}(t,0,0) \\ \frac{1}{2}\frac{\partial^2 g}{\partial i_b^2}(t,0,0) - \left|\frac{\partial^2 g}{\partial i_b \partial m}(t,0,0)\right| & \frac{1}{2}\frac{\partial^2 g}{\partial m^2}(t,0,0) \end{bmatrix}. \tag{3.7.8}$$

From Lemma 3.5.2, $R_0 > 1$ if and only if $\rho(\Phi_{F-V}(\omega)) > 1$. Thus, for $\epsilon > 0$ small enough, we have $\rho(\Phi_{F-V-\epsilon K}(\omega)) > 1$. With the help of Lemma 3.6.1 and by the comparison principle, we obtain as follows:

$$\lim_{t\to\infty} i_b(t) = \infty \quad \lim_{t\to\infty} m(t) = \infty, \tag{3.7.9}$$

this is a contradiction. Hence, E^0 is acyclic in M_∂, and P is uniformly persistent with respect to $(X_0, \partial X_0)$, which implies the uniform persistence of the solutions to the equation (3.7.6). Consequently, the Poincaré map P has a fixed point $(\widetilde{s}_b(0), \widetilde{i}_b(0), \widetilde{m}(0)) \in X_0$, clearly $\widetilde{s}_b(0) \neq 0$. Thus, $(\widetilde{s}_b(0), \widetilde{i}_b(0), \widetilde{m}(0)) \in \{s_b, i_b, m \in X\}$ and
$(\widetilde{s}_b(t), \widetilde{i}_b(t), \widetilde{m}(t)) = u(t, (\widetilde{s}_b(0), \widetilde{i}_b(0), \widetilde{m}(0))$ is a positive $\omega-$periodic solution of the system. □

3.8 Simulations

In this section we provide some simulations for the system (3.3.2). These simulations were done using Python software. We set our time in days and give our period-ω to be 91.25 days. We computed the basic reproduction number R_0 and the time-averaged basic reproduction number $([R_0])$ for various values of $\beta_3(t)$ and $\widetilde{\alpha}(t)$. For both rates to be positive, we set $0 < \bar{\beta_3} < 1$ and $0 < \bar{\alpha} < 1$, we focus on the variation of $\beta_3(t)$ here. In Figure 3.2, we vary $\hat{\beta_3}$ and $\bar{\beta_3}$, respectively, while keeping the values of other parameters fixed. The initial condition of the susceptible water bugs, infected water bugs and *Mycobacterium ulcerans* was estimated in proportion to be 0.6, 0.4, and 0.2 respectively. For the mortality rate μ_h, we assume that the life expectancy of the human population is 61 years, in Ghana [49] and is indeed applicable to sub-Saharan Africans. This becomes $\mu_h = 0.0166$ per year and 4.5×10^{-5} per day. Since BU is a vector borne disease we estimate using some of the parameters based on literature of vector borne diseases. Recovery rates of vector borne disease is from 1.6×10^{-5} to 0.5 per day [44]. Also, the mortality rate for water bugs is not completely known, it is assumed to be 0.15 per day [2]. For vector borne disease the loss of immunity ranges between 0 and 1.1×10^{-2} per day [44]. The rest of the parameters were carefully estimated based on assumptions about the disease; see Table 3.2 for details of parameters used.

Table 3.2: Model parameters, values and source used.

Parameter	Value(day^{-1})	Source
β_3	0.09	[14]
β_1	1×10^{-5}	[14]
β_2	2×10^{-7}	[14]
μ_h	4.5×10^{-5}	[49]
μ_b	0.8	[14]
μ_m	0.15	[2]
$\widetilde{\alpha}$	0.00615	[14]
θ	$0 - 1.1 \times 10^{-2}$	[44]
γ	$1.6 \times 10^{-5} - 0.5$	[44]
δ	0.08 – 0.4	[14]

Table 3.2 gives model parameters, values and source used.

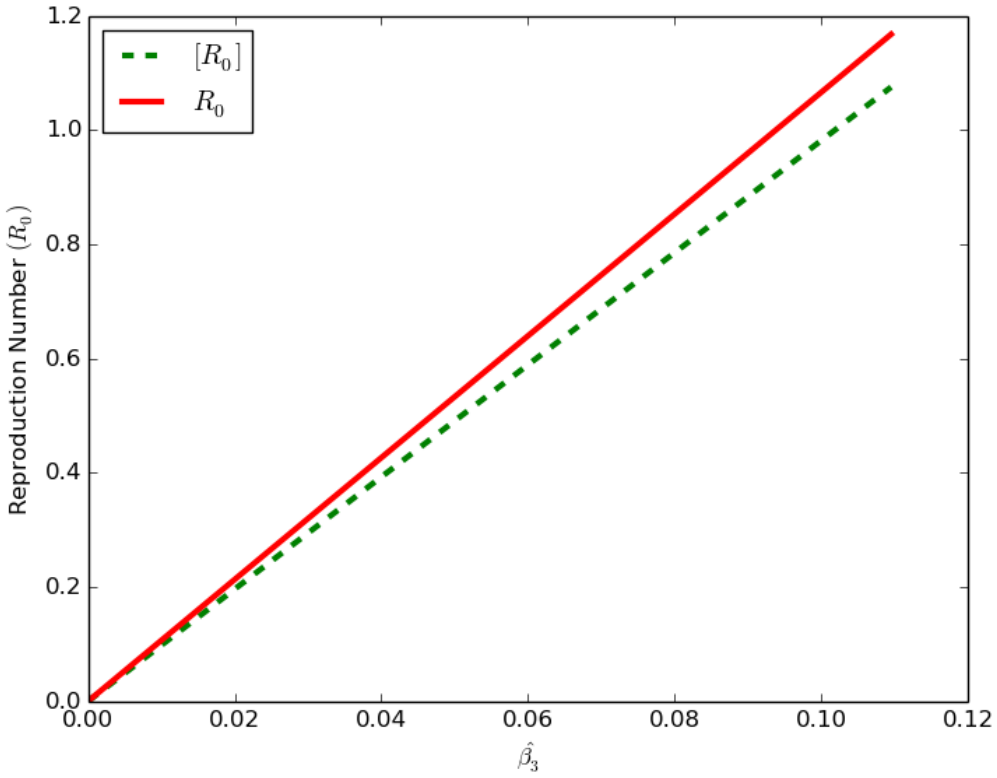

Figure 3.2: A plot of the periodic threshold of the two basic reproduction numbers of system 3.3.2 for various $\hat{\beta}_3$ with other parameters as in Table 3.2 to be constant. $R_0 = 1$ when $\hat{\beta}_3 \approx 0.0931$ and $[R_0] = 1$ when $\hat{\beta}_3 \approx 0.1021$. The time-averaged reproduction number $[R_0]$, shows inaccuracy in predicting the number of infections.

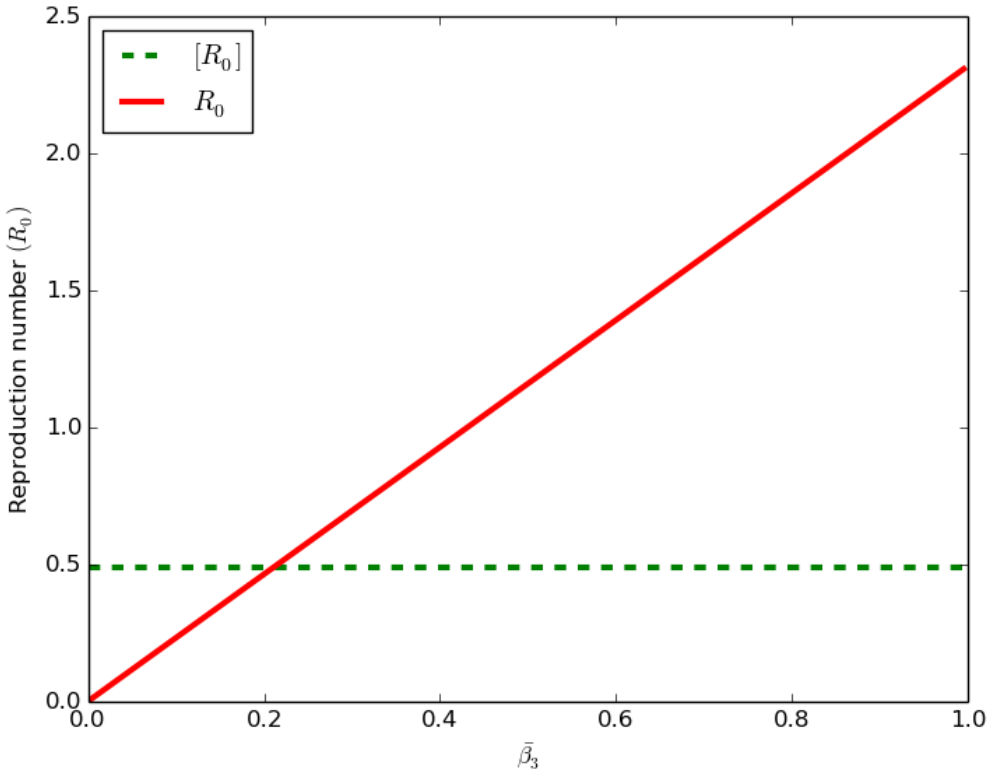

Figure 3.3: A plot of the periodic threshold of the two basic reproduction numbers of system 3.3.2 for various $\bar{\beta}_3$ with other parameters as in Table 3.2 to be constant. When $R_0 = 1$ then $\bar{\beta}_3 \approx 0.4402$ and $[R_0] = 0.500$ for all $\bar{\beta}_3$. The time-averaged reproduction number $[R_0]$, shows inaccuracy in predicting the number of infections.

When varying the model parameters $\hat{\beta}_3$ and $\bar{\beta}_3$ with other parameters in two reproduction numbers constant. Figure 3.2 shows that the time-averaged reproduction number underestimates the infection risk as compared to the basic reproduction number. With $R_0 = 1$ when $\hat{\beta}_3 \approx 0.0899$ and $[R_0] = 1$ when $\hat{\beta}_3 \approx 0.099$. In Figure 3.3 also with $R_0 = 1$ when $\bar{\beta}_3 \approx 0.410$ and $[R_0] = 0.50$ for all $\bar{\beta}_3$, the time-averaged reproduction number shows inaccuracy in predicting the number of infections.

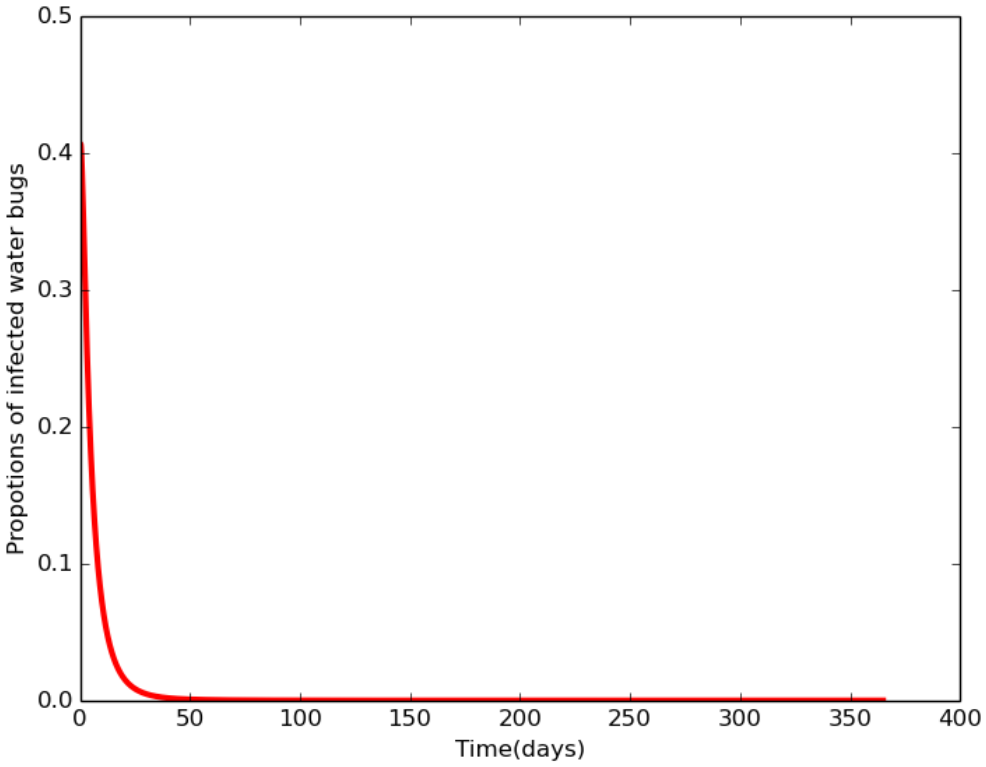

Figure 3.4: An infection curve for proportions of infected water bugs when $R_0 < 1$, in model 3.1 for a period of 365 days. Initial condition $i_b(0) = 0.4$ and with other parameters as in Table 3.2 to be constant. The solution converges to the disease free equilibrium.

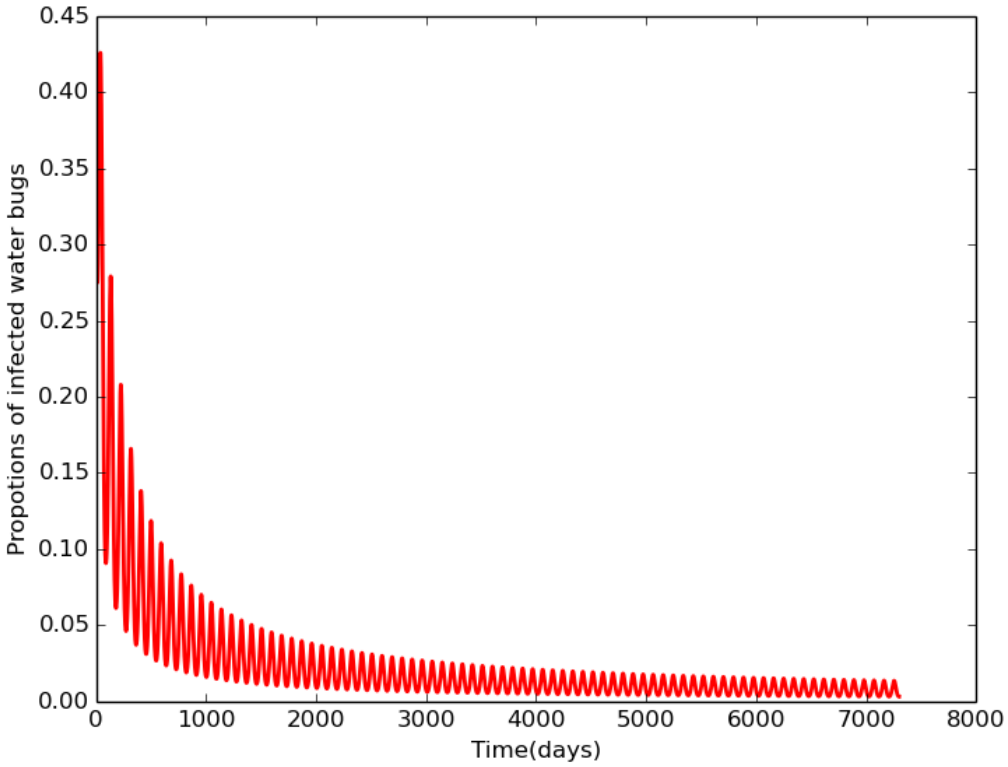

Figure 3.5: An infection curve for proportions of infected water bugs when $R_0 > 1$, in model 3.1. Initial condition $i_b(0) = 0.2$ and with other parameters as in Table 3.2 to be constant. The disease persists and a periodic solution with $\omega = 91.25$ days forms after a long transient.

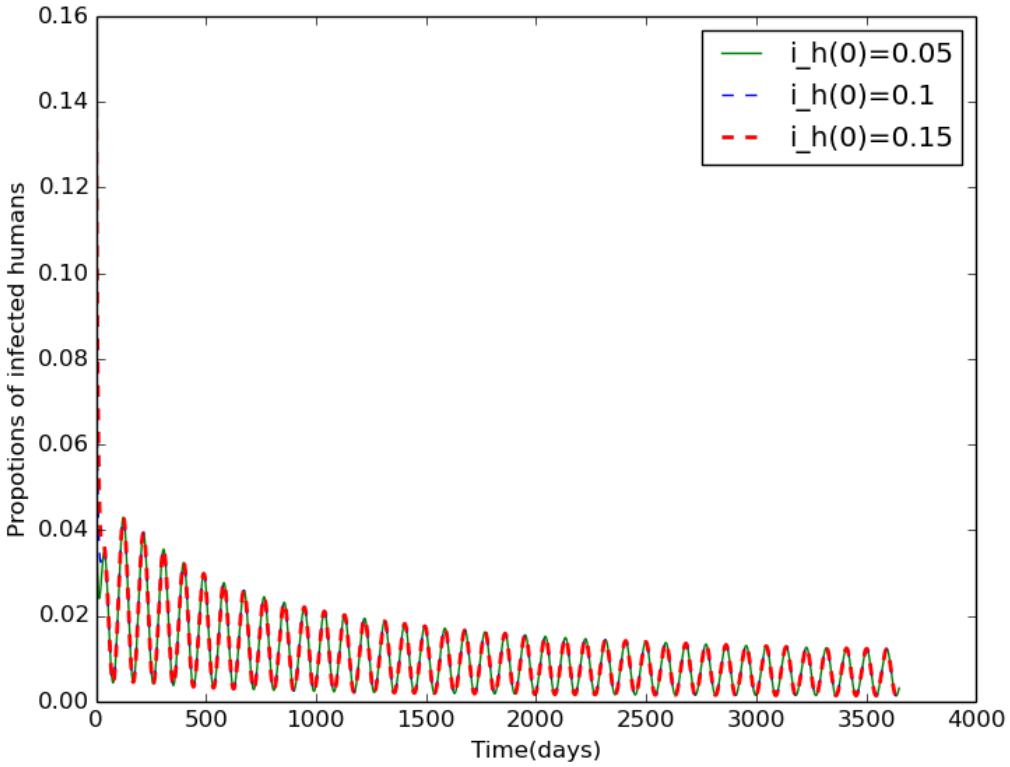

Figure 3.6: Proportions of infected humans when $R_0 > 1$, in model 3.1. Different initial conditions; $i_h(0) = 0.05, 0.1$ and 0.2 and with other parameters as in Table 3.2 to be constant. The disease persists and a periodic solution with $\omega = 91.25$ days forms after a long transient.

When $R_0 < 1$, the proportions of infected water bug population i_b turns to zero. The disease completely dies out, and similar patterns were observed for various initial conditions (result not shown), this provides some evidence that the disease free equilibrium is globally stable in Figure 3.4. When $R_0 > 1$, the disease persists after a long oscillating transient and the infection approaches a positive $\omega-$periodic solution in Figure 3.5. The disease also persists (see Figure 3.6) for the proportion of infected humans and after a long oscillating transient the infection approaches a positive $\omega-$periodic solution.

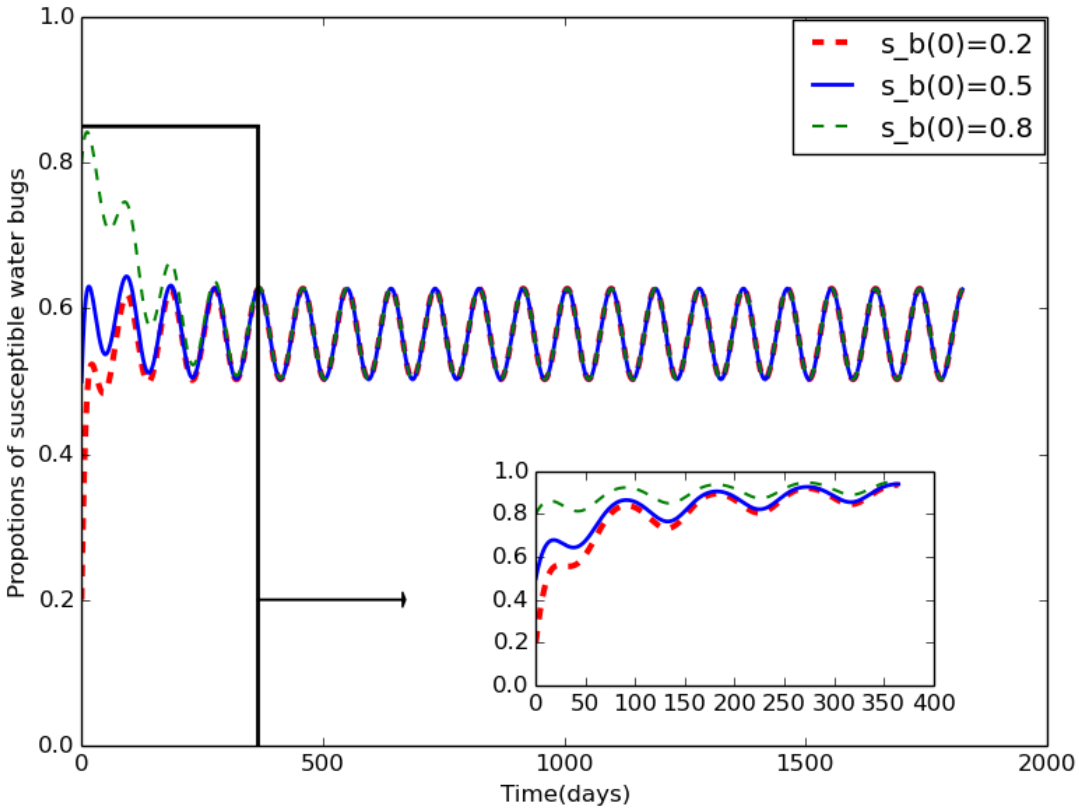

Figure 3.7: Proportions of susceptible water bugs over a period of 1825 days for disease persistence in model 3.1. Different initial conditions; $s_b(0) = 0.2, 0.5, 0.8$ and with rest of the parameters as defined in Table 3.2 to be constant. The inset plot shows proportions of susceptible water bugs over a period of 365 days.

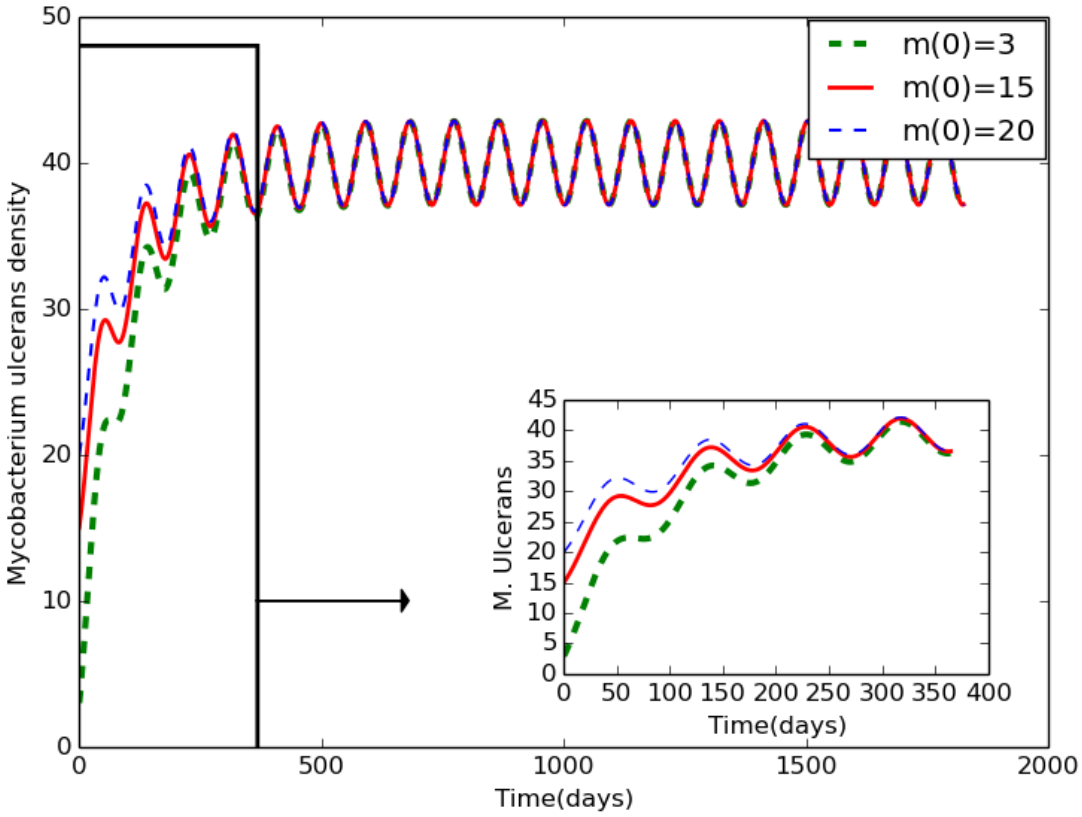

Figure 3.8: *Mycobacterium ulcerans* density over a period of 1825 days for disease persistence in model 3.1. Different initial conditions; $m(0) = 3, 15, 20$ and with rest of the parameters as defined in Table 3.2 to be constant. The inset plot shows *Mycobacterium ulcerans* density over a period of 365 days.

The long-term behaviors when $R_0 > 1$ and the sub graph shows the global stability of the disease free equilibrium E^0 when $R_0 < 1$ for proportions of susceptible water bugs (see Figure 3.7) and the *Mycobacterium ulcerans* density (see Figure 3.8) respectively. Given different initial conditions for the long-term behavior and the disease free equilibrium, it exhibited the same patterns showing a long oscillating transient and infection approaches a positive $\omega-$solution respectively.

3.9 Summary

In this chapter, we investigated the transmission of BU in fluctuating environments using deterministic model by considering our disease transmission pathways and the *Mycobacterium ulcerans* density to vary seasonally.
Our mathematical analysis results of the timed-averaged reproduction number obtained shows that Buruli ulcer epidemic is driven by the dynamics of the environments. We also found out that the time-averaged reproduction number $[R_0]$ shows inaccuracy in predicting the number of infections.
Model simulations confirm that when $R_0 < 1$ and $R_0 > 1$ the solution converges to the disease free and endemic equilibrium point respectively. It also confirms that if $R_0 > 1$ the infection is sustained seasonally.
Our simulations also indicated that BU epidemic depends mostly on the environmental dynamics, that is the shedding rate of the water bugs α and the transmission rate of the water bugs β_3 which influences the basic reproduction number R_0. Any increase in these parameters leads to an increase in the BU epidemic. We also observed that controlling of water bugs will be helpful in decreasing BU epidemic.
Our model outcome suggests that environmental fluctuation should be taken into consideration in designing policies aimed at Buruli ulcer control and management.

The model presented in this chapter can be improved by considering social interventions in the human population and inclusion of treatment delays. Also introduction of logistic function in the *Mycobacterium ulcerans* density to model it's evolution to see how such a change impacts the BU epidemic. In the next chapter relook at the transmission of BU using *STELLA* with

some social dynamics.

Chapter 4

A system dynamic model for BU transmission in both fluctuating and non-fluctuating environments

4.1 Introduction

In this chapter we relook at the model presented in Chapter 3 using *STELLA*. The advantages of using *STELLA* are many but few are noted below based on our problem:

- *STELLA* modelling is easy to understand and usable by non-mathematicians. This is important since many of the policy markers and individuals involved in BU control and management have little or no exposure to mathematical formulations.
- *STELLA* modelling allows us to add more information like intervention strategies and social dynamics which may not be done using mathematical formulations since analysis becomes difficult when many parameters are involved.

In Section 4.7 we improved our model in Chapter 3 by considering some social dynamics in the human population such as educational campaign and treatment delays. We also, introduce a logistic function in the *Mycobacterium ulcerans* density to model it's evolution to see how such a change impacts the BU disease.

4.2 Model formulation

We present below the systems dynamic model for the transmission of BU in both fluctuating and non-fluctuating environments. The human population size NH, comprises of susceptible individuals SH, infectious individuals IH, those under treatment TH and the recovered RH. Thus, the population at any time t is

$$NH = SH + IH + TH + RH.$$

Similarly, the water bugs population size NWB, includes susceptible water bugs SWB and infectious water bugs IWB, so that, the population of water bugs at any time t is

$$NWB = SWB + IWB.$$

The compartment, MU represents *Mycobacterium ulcerans* in the environment whose carrying capacity is K_M.

4.3 Causal loop diagram for the transmission of BU

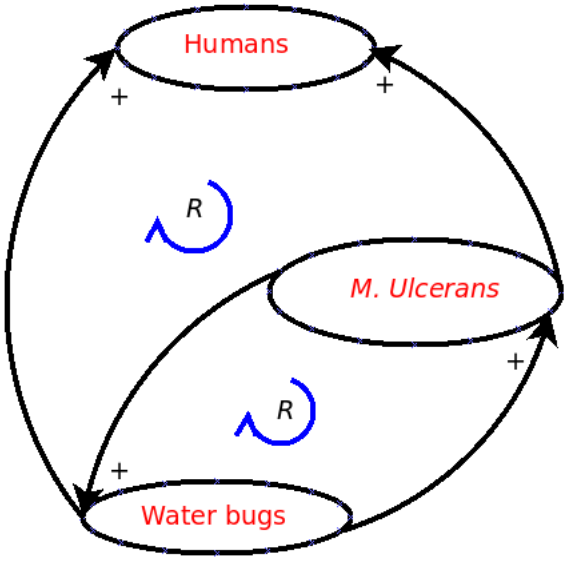

Figure 4.1: Causal loop diagram for the transmission of Buruli ulcer. The lines with arrow head moving from one variable to another with a positive sign on indicate the relationship between them. The curves with arrow head with the text R indicate reinforcing loop and the sign "$+$ " indicates the loops polarity.

Figure 4.1 represents the causal loop diagram for the transmission of BU. The causal diagram helps in picturing the different variables in the system that are interrelated. The nodes include the humans, *Mycobacterium ulcerans* and the water bugs as the variables, the edge with arrows are the link that represent connections. Figure 4.1 is a reinforcing loop because the effect of a variation in any variable propagates through the loop and returns to the variable reinforcing the initial deviation, meaning if a variable increases in a reinforcing loop the effect through the cycle will return an increase to the same variable and vice versa [40, 51, 57]. A link marked

positive indicates a positive relation which means the two nodes change in the same direction. From our preliminary 1.7.1, a closed cycle is either defined as a reinforcing or balancing loop. In Figure 4.1 humans with an open cut when have direct contact with *Mycobacterium ulcerans* in the environments result in BU infection, which indicates a positive relation. The *Mycobacterium ulcerans* and the water bugs have a positive relation since the water bugs shed back increasing the *Mycobacterium ulcerans* density in the environment. Similarly, water bugs bite the humans which in turns transmit the disease, indicating a positive relation.

4.4 SD *STELLA* model

We let the stocks be SH, IH, TH, RH, SWB, IWB and MU, the flows represent the rates at which people move from one stock to another stock and the other rates are converters (represented by circles) that denote the rules or conditions controlling the stocks and the flows through the use of connectors (represented by single lines with arrows). Figure 4.2 represent a *STELLA* model for the transmission of Buruli ulcer.
LI is the loss of immunity for the recovered individual. All death rates here are assumed to be natural mortality and TR means transmission rate.

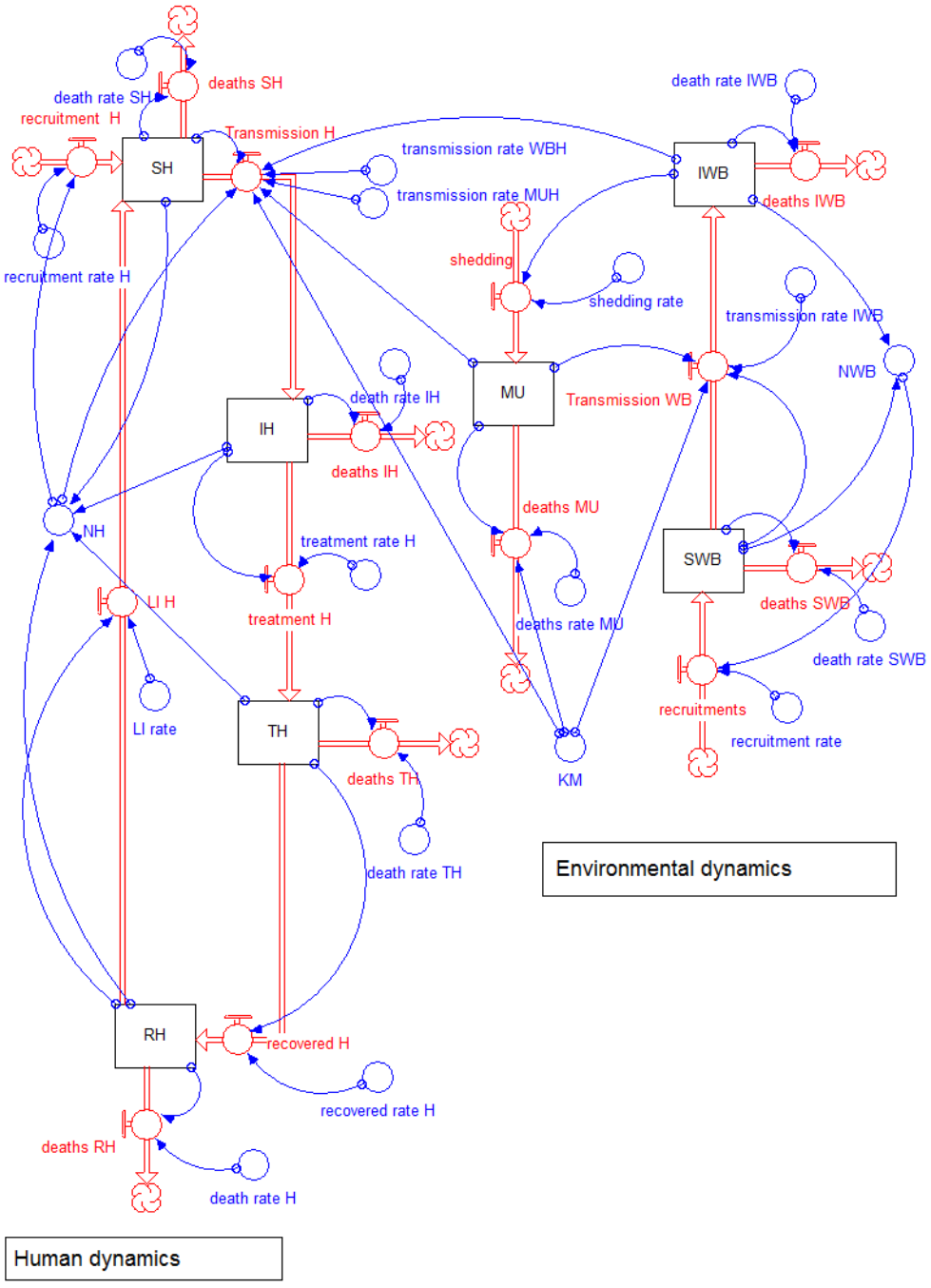

Figure 4.2: A *STELLA* model for the transmission of Buruli ulcer. The rectangles; SH, IH, TH, RH, SWB, IWB and MU represent stocks, the circles represent converters, the double lines with arrow represent flows and the single lines with arrow represent connectors connecting the flows and the stocks. The flows indicates movement and the connectors indicate contact.

4.4.1 System dynamic equations

From the above *STELLA* model the following system dynamic are derived to describe the dynamics of the transmission of BU in both non fluctuating and fluctuating environments:

$$\left.\begin{aligned}
S_H(t) &= S_H(t-dt) + (recruitment_H + LI_H - Transmission_H - deaths_{SH}) * dt \\
I_H(t) &= I_H(t-dt) + (Transmission_H - deaths_{IH} - treatment_H) * dt, \\
T_H(t) &= T_H(t-dt) + (treatment_H - recovered_H - deaths_{TH}) * dt, \\
R_H(t) &= R_H(t-dt) + (recovered_H - LI_H - deaths_{RH}) * dt, \\
S_{WB}(t) &= S_{WB}(t-dt) + (recruitment_{WB} - Transmission_{WB} - deaths_{SWB}) * dt, \\
I_{WB}(t) &= I_{WB}(t-dt) + (Transmission_{WB} - deaths_{IWB} - treatment_H) * dt, \\
MU(t) &= MU(t-dt) + (shedding - deaths_{MU}) * dt
\end{aligned}\right\} \tag{4.4.0}$$

where disease transmission pathways for humans and water bugs in non fluctuating environments is defined below,

$$\text{Transmission}_H = \left(TR_{WBH} \times \left(\frac{IWB}{N_H}\right) + TR_{MUH} \times \left(\frac{MU}{(K_{50} + MU)}\right)\right).$$

The parameters TR_{WBH} and TR_{MUH} are the effective contact rates of susceptible humans with the water bugs and *Mycobacterium ulcerans* in the environments, respectively. Here TR_{WBH} is the product of the biting frequency of water bugs on humans, density of water bugs per human host, and the probability that a bite will result in an infection also TR_{MUH} is the product of density of *Mycobacterium ulcerans* per human host and the probability that a contact will result in an infection. The parameter K_{50} gives the concentration of *Mycobacterium ulcerans* in the environment that is assumed to yield 50% chance of infection with BU.

$$\text{Transmission}_{WB} = TR_{IWB} \times \left(\frac{MU}{K_{50}}\right),$$

$$\text{Shedding} = SR_{MUIWB} \times I_{WB}.$$

TR_{IWB} is infection rate of water bugs by *Mycobacterium ulcerans* and SR_{MUIWB} means the shedding rate of *Mycobacterium ulcerans* by water bugs in the environments; see equation (6) for detail model equations. We defined our basic reproduction number R_0 in non fluctuating environments as derived in Chapter 3 below,

$$R_0 = \frac{TR_{IWB} \times SR_{MUIWB}}{\text{deaths rate MU} \times \text{deaths rate WB}}.$$

4.5 Parameter estimation

The Buruli ulcer is a vector borne disease and some of the model parameters were estimated based on literature on vector borne diseases and on the assumption of the disease because not much of the disease is understood [59]. For the mortality rate of human, we assume that life expectancy of human population in sub-Saharan Africans is 61 year, which is 4.5×10^{-5} days. Recovery rates of vector borne disease is from 1.6×10^{-5} to 0.5 per day [44]. The mortality rate for water bugs is not completely known, it is assumed to be 0.15 per day [2]. For vector borne disease the loss of immunity ranges between 0 and 1.1×10^{-2} per day [44]. See Table 4.1 for details of model parameters and variables for our simulations. Simulations were done using *STELLA* software and we set our time in days.

Table 4.1: Model parameter values and source used

Parameter	Value(day^{-1})	Source
TR_{IWB}	0.09	[14]
TR_WBH	1×10^{-5}	[14]
TR_MUH	2×10^{-7}	[14]
death rate WB	0.8	[14]
deaths rate MU	0.15	E [2]
SR_{MUIWB}	0.00615	[14]
LI	1.1×10^{-2} – 0	[44]
Recovery rate	1.6×10^{-5} – 0.5	[44]
Death/birth rate H	4.5×10^{-5}	[12]
Treatment rate	0.08 – 0.4	[14]

Table 4.1 gives model parameters, values and source used.

4.5.1 Simulation for model without fluctuations

4.5.1.1 Plots of disease free equilibrium

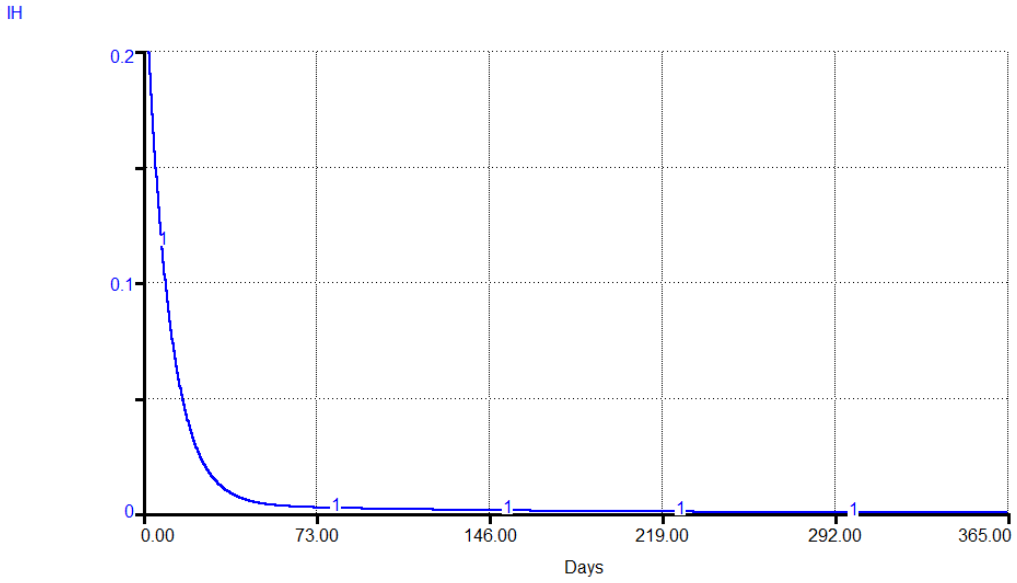

(a) Plot of proportions of infected humans when $R_0 < 1$.

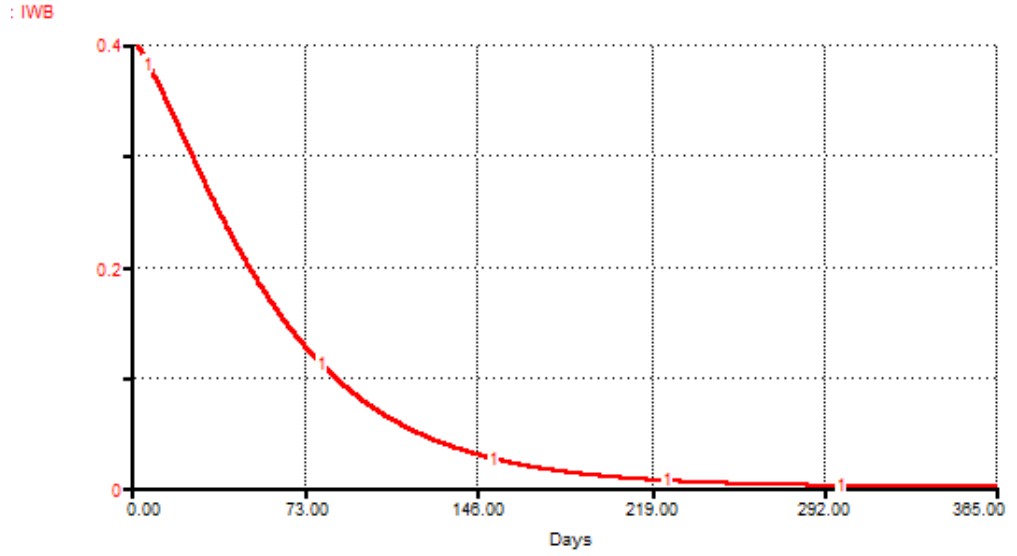

(b) Plot of proportions of infected water bugs when $R_0 < 1$.

Figure 4.3: Plot of proportions of infected humans(I_H) and water bugs(I_{WB}) when $R_0 < 1$ respectively, in model 4.2 for a period of 365 days. Initial conditions; $I_H(0) = 0.2$, $I_{WB}(0) = 0.4$ and with other parameters as in Table 4.1 to be constant. The solution converges to the disease free equilibrium with $(I_H^0, I_{WB}^0) = (0, 0)$.

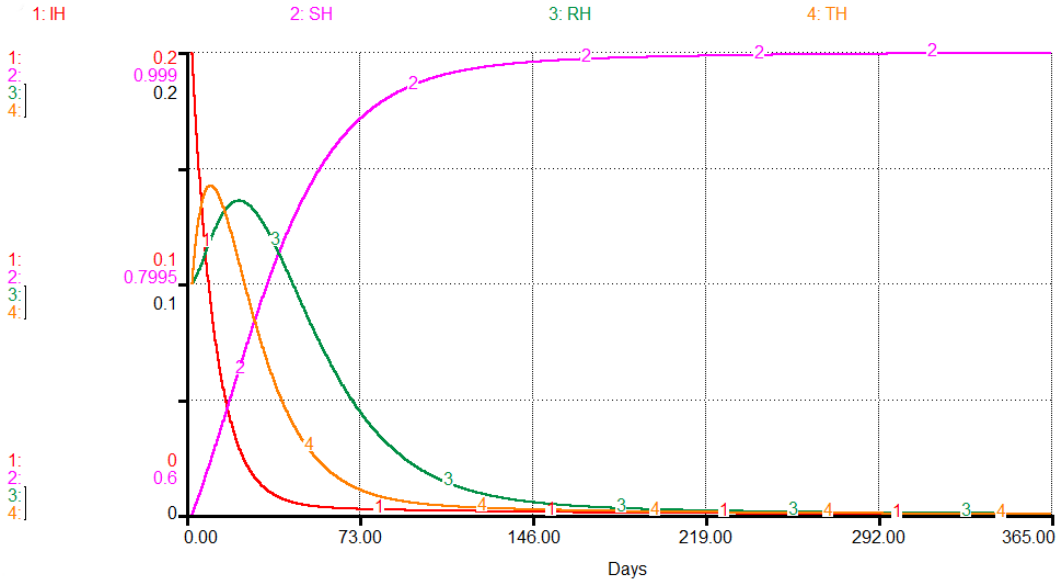

(a) Plot of proportions of humans population dynamics when $R_0 < 1$.

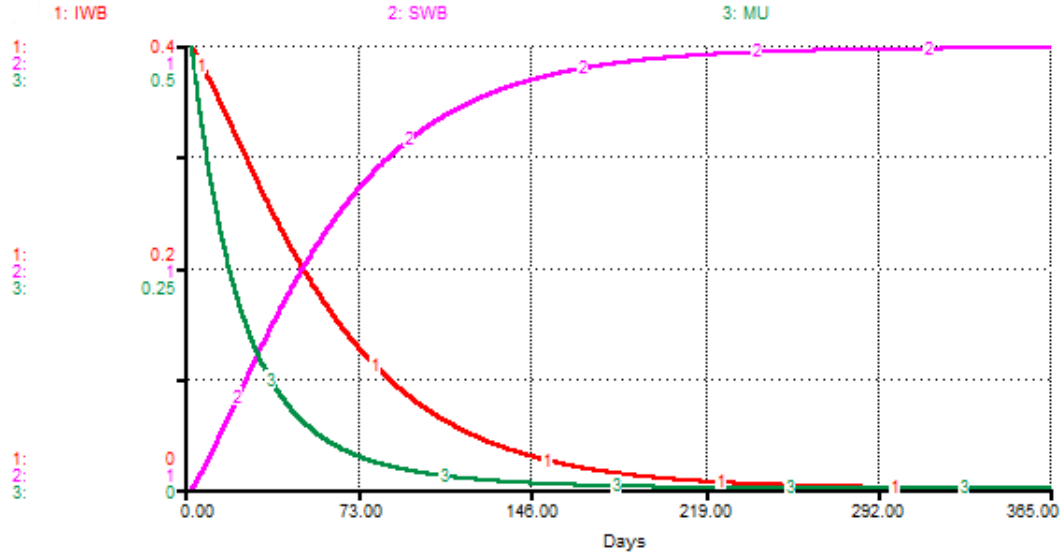

(b) Plot of the environmental daynamics when $R_0 < 1$.

Figure 4.4: Plot of proportions of humans and the environmental population dynamics when $R_0 < 1$ respectively, in model 4.2 for a period of 365 days. Initial conditions; $S_H(0) = 0.6$, $T_H(0) = 0.1$, $R_H(0) = 0.1$, $S_{WB}(0) = 0.6$, $MU(0) = 0.5$ and with other parameters as in Table 4.1 to be constant. The solution converges to the disease free equilibrium with $S_H^0 = 1$, $T_H^0 = 0$, $R_H^0 = 0$, $S_{WB}^0 = 1$, $MU^0 = 0$.

When $R_0 < 1$, the proportions of infected humans(I_H) and water bugs(I_{WB}) turns to zero respectively, showing that the disease completely dies out in each Figure. In Figure 4.4a and 4.4b, the proportions of both the humans and environmental dynamics turns to its disease free equilibrium point respectively. This provides some evidence that the disease free equilibrium is globally asymptotically stable.

4.5.1.2 Plots of endemic equilibrium

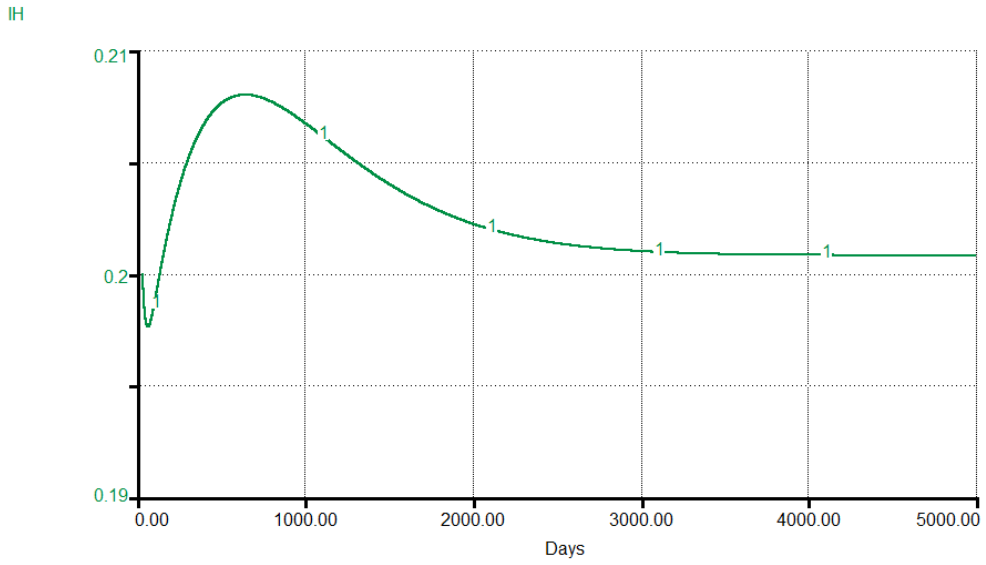

(a) Plot of proportions of infected humans when $R_0 > 1$.

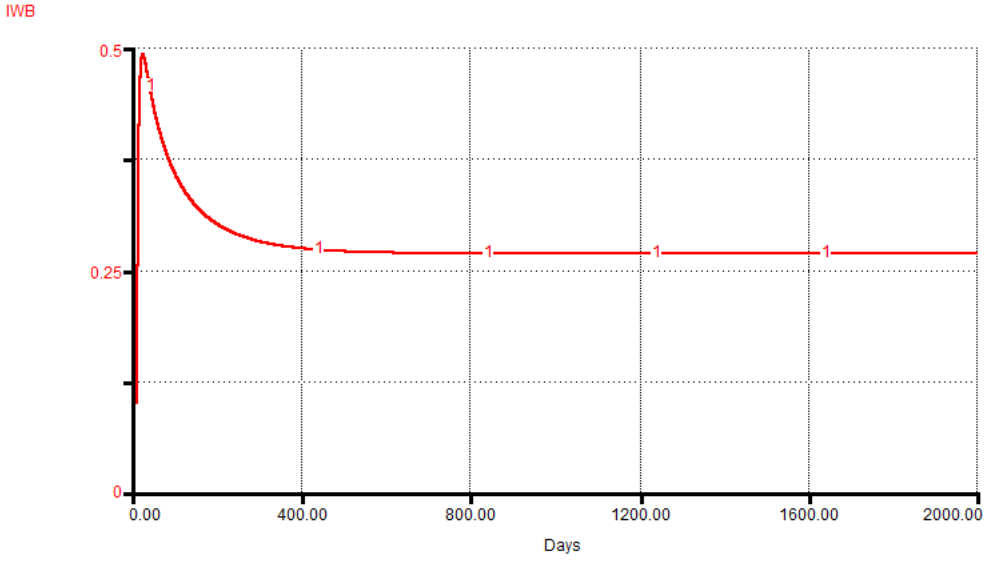

(b) Plot of proportions of infected water bugs when $R_0 > 1$.

Figure 4.5: Plot of proportions of infected humans(I_H) and water bugs(I_{WB}) when $R_0 > 1$ respectively, in model 4.2. Initial conditions; $I_H(0) = 0.2$, $I_{WB}(0) = 0.1$ and with other parameters as in Table 4.1 to be constant. The disease persist even after 365 days and solution converges to the endemic equilibrium.

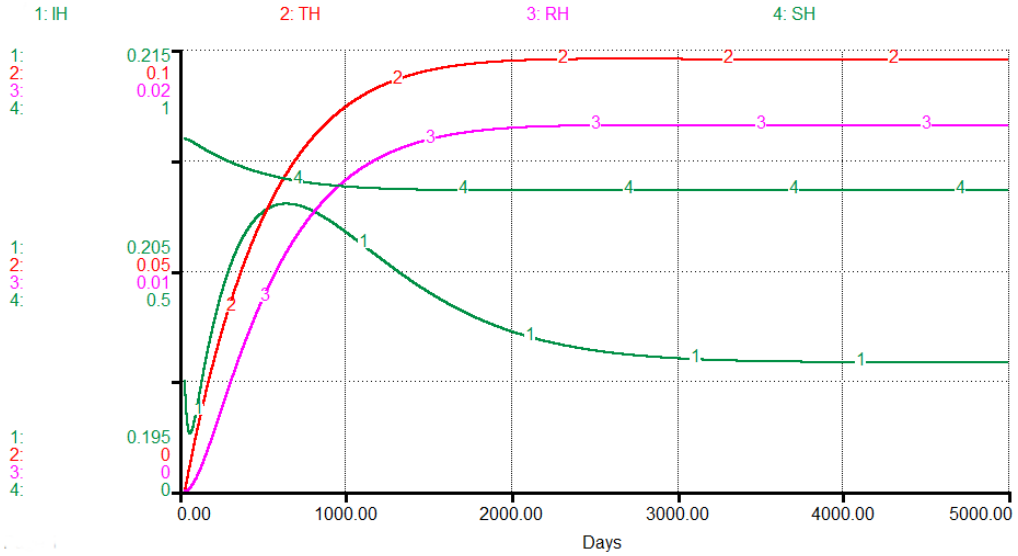

(a) Plot of proportions of humans population dynamics when $R_0 > 1$.

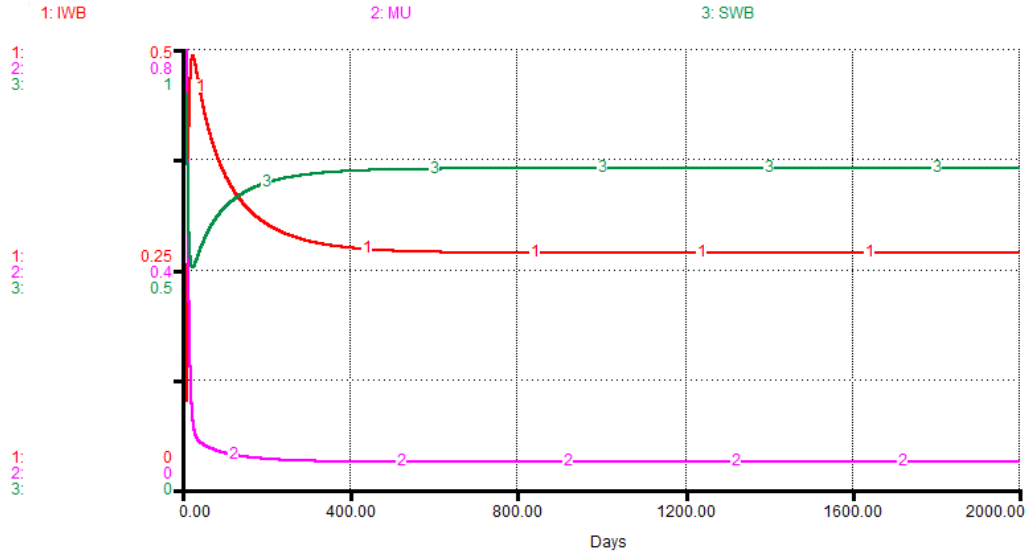

(b) Plot of proportions of environmental population dynamics when $R_0 > 1$.

Figure 4.6: Plot of proportions of humans and environmental population dynamics when $R_0 > 1$ respectively, in model 4.2. Initial conditions; $S_H(0) = 0.8$, $I_H(0) = 0.2$, $T_H(0) = 0$, $R_H(0) = 0$, $S_{WB}(0) = 0.9$, $I_{WB}(0) = 0.1$, $MU(0) = 0.8$ and with other parameters as in Table 4.1 to be constant. The disease persist even after 365 days and solution converges to the endemic equilibrium.

When $R_0 > 1$, the proportions of infected humans(I_H) and water bugs(I_{WB})

turns to it endemic equilibrium point. The proportions of humans and environmental population dynamics turns to their endemic equilibrium point respectively, after a long term the disease persist in Figure 4.6a-4.6b.

4.6 Fluctuating environments

In this section, based on the *STELLA* model we can incorporate periodicity in the disease transmission pathways $(\text{Transmission}_H(t), \text{Transmission}_{WB}(t))$ and also in the *Mycobacterium ulcerans* density (Shedding(t)). These are both periodic functions of time with a common period, $\omega = \frac{365}{4} = 91.25$ days. Periodic transmission is often assumed to be sinusoidal, from equation 4.4.1, we defined our new disease transmission for both humans and water bugs population in fluctuating environments to be as follows:

$$\begin{aligned}&\text{Transmission}_H(t) = \\ &\left(TR_{WBH} \times SINWAVE(amplitude, period) \times \left(\frac{I_{WB}}{N_H}\right)\right) \\ &+ \left(TR_{MUH} \times SINWAVE(amplitude, period) \times \left(\frac{MU}{(K_{50} + MU)}\right)\right),\end{aligned} \tag{4.6.1}$$

$$\text{Transmission}_{WB}(t) = TR_{IWB} \times SINWAVE(amplitude, period) \times \left(\frac{MU}{K_{50}}\right),$$

$$\text{Shedding(t)} = SR_{MUIWB} \times SINWAVE(amplitude, period) \times I_{WB}.$$

SR_{MUIWB} means the shedding rate of *Mycobacterium ulcerans* by the water bugs in the environments. To ensure that both rates be positive, we require that

$$0 < amplitude < 1 \quad \text{and} \quad period = 91.25.$$

We defined basic reproduction number R_0 with periodicity as derived in Chapter 3 to be,

$$R_0 = \frac{TR_{IWB}(SINWAVE(amplitude, period)) \times SR_{MUIWB}(SINWAVE(amplitude, period))}{\text{deaths rate MU} \times \text{deaths rate WB}}.$$

4.6.1 Plots in fluctuating environments

4.6.1.1 Disease free equilibrium

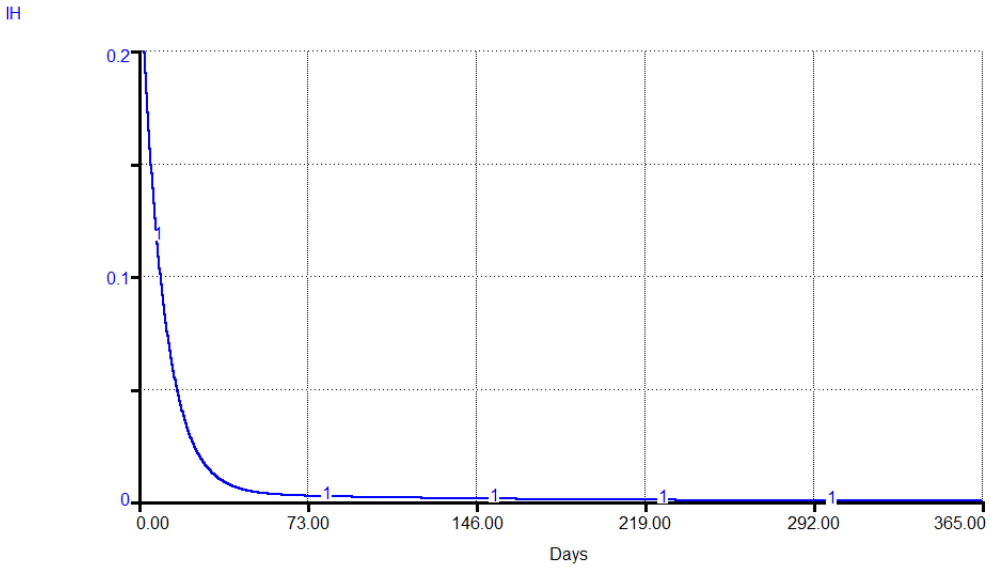

(a) An infection curve of humans when $R_0 < 1$.

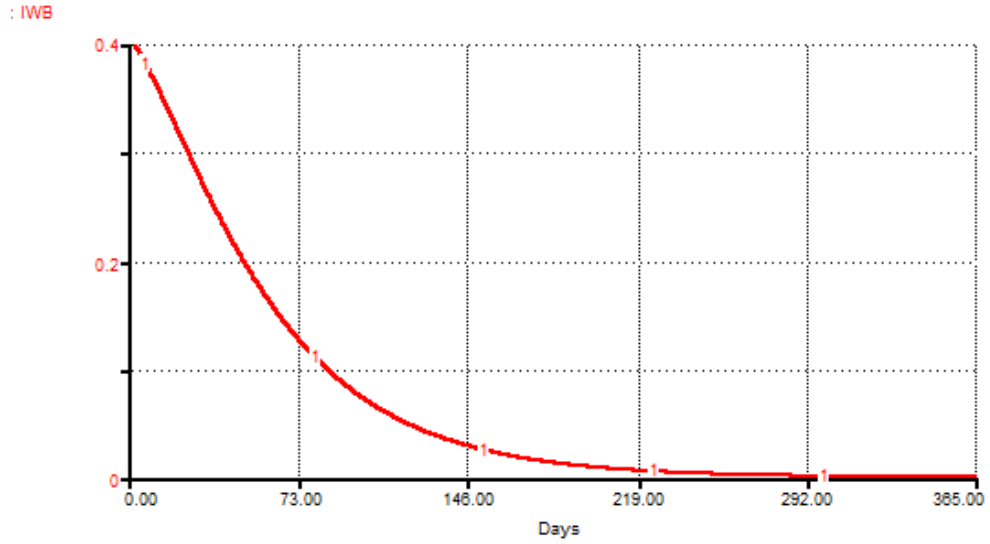

(b) An infection curve of water bugs when $R_0 < 1$.

Figure 4.7: Plot of proportions of infected humans(I_H) and water bugs(I_{WB}) when $R_0 < 1$ respectively, in model 4.2 for a period of 365 days. Initial conditions; $I_H(0) = 0.2$, $I_{WB}(0) = 0.4$ and with other parameters as in Table 4.1 to be constant. The solution converges to the disease free equilibrium with $I_H^0 = 0$, $I_{WB}^0 = 0$.

4.6.1.2 Endemic equilibrium

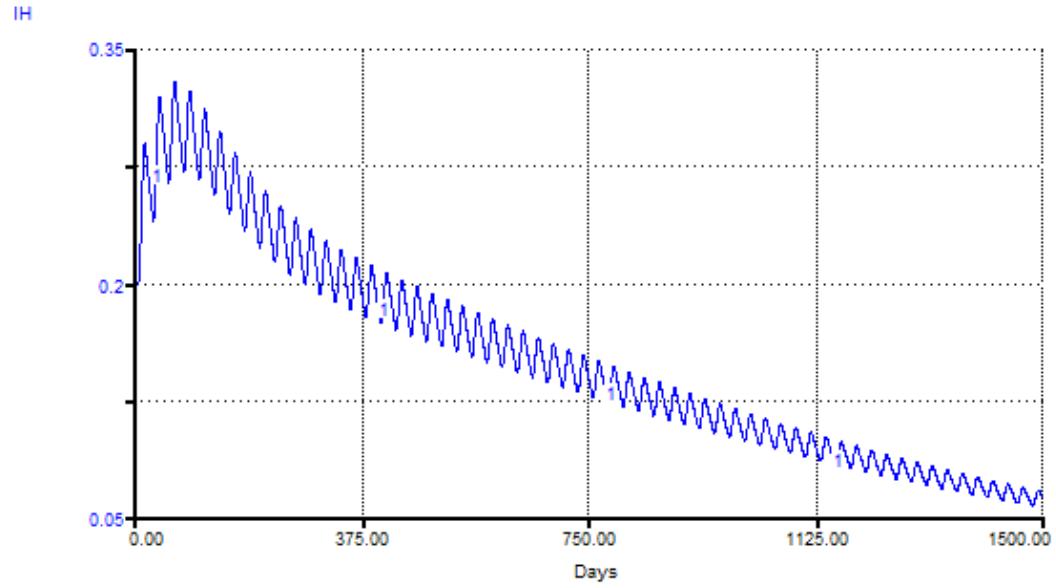

(a) An infection curve for proportions of humans when $R_0 > 1$.

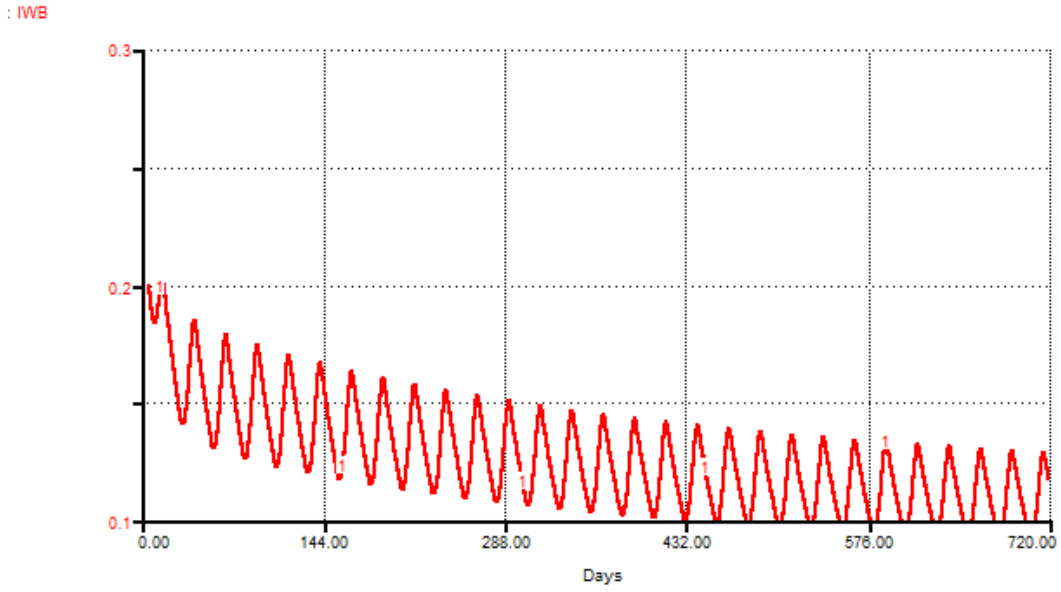

(b) An infection curve for proportions of infected water bugs when $R_0 > 1$.

Figure 4.8: Plot of proportions of infected humans(I_H) and water bugs(I_{WB}) when $R_0 > 1$ respectively, in model 4.2. Initial conditions; $I_H(0) = 0.2$, $I_{WB}(0) = 0.2$ and with other parameters as in Table 4.1 to be constant. The disease persist and a periodic solution with $\omega = 91.25$ days forms after a long transient.

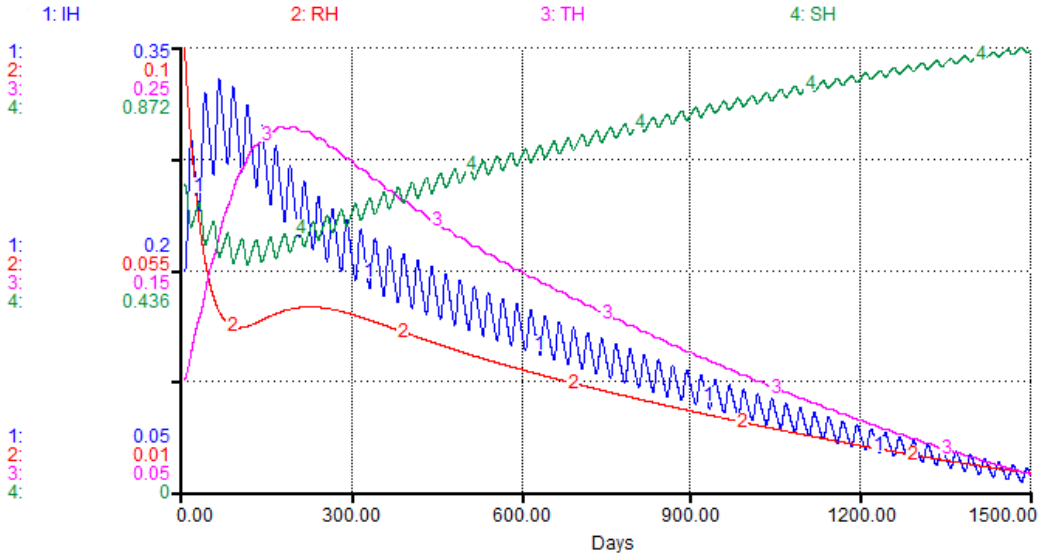

(a) Infection curves for the proportions of human population when $R_0 > 1$.

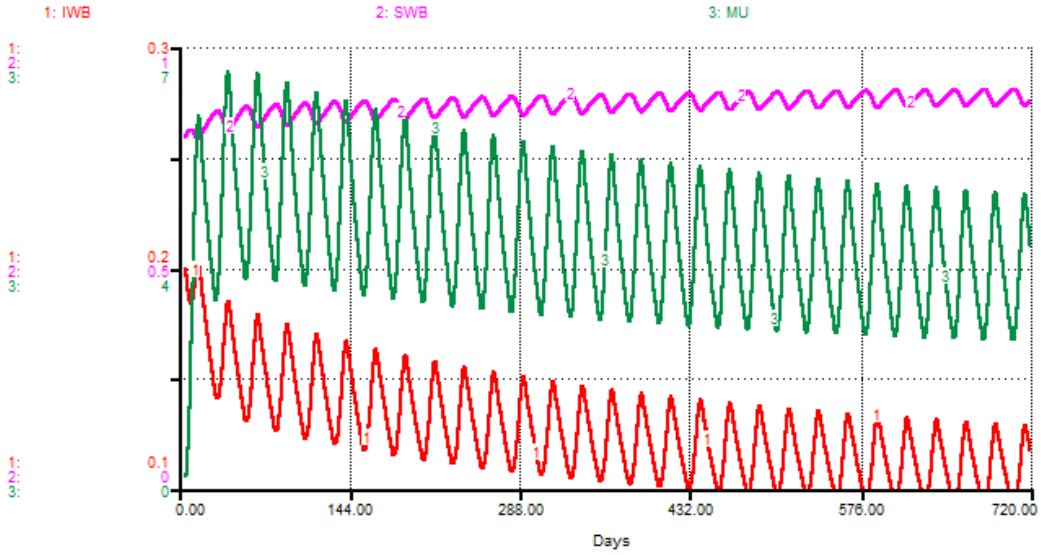

(b) Infection curves for the environmental population dynamic when $R_0 > 1$.

Figure 4.9: Plot of proportions of humans and environmental population dynamics when $R_0 > 1$ respectively, in model 4.2. Initial conditions; $S_H(0) = 0.6$, $I_H(0) = 0.2$, $T_H(0) = 0.1$, $R_H(0) = 0.1$, $S_{WB}(0) = 0.8$, $I_{WB}(0) = 0.2$, $MU(0) = 0$ and with other parameters as in Table 4.1 to be constant. The disease persist and a periodic solution with $\omega = 91.25$ days forms after a long transient.

When $R_0 < 1$, the proportions of infected humans(I_H) and infected water bugs population (I_{WB}) decreases to zero respectively, showing that the

disease dies out. This gives an evidence that the disease free equilibrium is globally asymptotically stable (see Figure 4.7a-4.7b). In Figure 4.8a-4.9b illustrates typical infection curves for the human and environmental dynamics respectively, when $R_0 > 1$. In this case the disease persist after a long oscillating transient the infection approaches a positive $\omega-$periodic solution.

4.7 *STELLA* model for the transmission of BU with social dynamics

In this section, we explore the effect of social dynamics in the transmission of BU disease such as; the effect of educational campaigns, treatment delays and logistic function to the *Mycobacterium ulcerans* density. We first treated them separately and then combined them to see it effectiveness on the disease endemic population.

4.7.1 Eduction campaigns and delay treatments

Studies to identify factors contributing to delayed presentation indicate that awareness of the disease is generally good in endemic regions, but wide variation exists in perceived cause of the disease and the role of sorcery in its transmission and treatment [56]. The use of traditional healers as first line therapy also contributes to delayed treatment, as do lack of awareness about the availability of effective treatment and financial concerns. Epidemiological data from existing BU control programs indicate that active educational campaigns are successful in increasing understanding and decreasing infection rate and disease progression [38, 56]. In this section we add educational campaign to our *STELLA* model 4.10. We define our new human transmission as the force of the infection in the fluctuating environments already defined in equation (4.6.1) with the education function, we express this below

$$\text{New transmission}_H(t) = \text{Transmission}_H(t) \times education$$

where new transmission is due to the changes in the disease transmission pathway of the humans with the effect from the educational campaign. We express education as $(1 - m)$ and m is the efficacy of it. In addition to

the *STELLA* model 4.10 we added a delay function. The delay function in *STELLA* helps us to monitor treatment delays, we define the delay function as follows:

$$\text{delay}_T = DELAY(input, \text{delay duration}[, initial]),$$

$$\text{treatment}_H = \text{treatment rate H} \times T_H \times \text{delay}_T.$$

Here we model the effect of treatment delays for 30 days and 60 days respectively. See appendix for the rest of model equations (6).

4.7.2 Environmental degradation through mining

An aquatic environment is not the only factor that has been linked to the prevalence of *Mycobacterium ulcerans*. It has been observed that if, in addition, high levels of arsenic (As) concentration prevail in such environments, the occurrence of *Mycobacterium ulcerans* is enhanced. Duker et al. [2, 22] have advanced the hypothesis that As may play a significant role in the spatial distribution of BU [2, 23]. Concentration of As in surface and ground water in areas where BU is a serious health threat has been noted to be higher than average. Aidoo and Osei [2] asset that, in Ghana, West Africa, the Amansie West District which accounts for high BU cases coincides with the highest levels of As, possibly released into rivers and lakes and ground water by intensive gold mining activities [2, 23]. Furthermore, a convenient specification for the change in the *Mycobacterium ulcerans* density is the logistic function(LF). We again included LF into *STELLA* model 4.10 to monitor the density of the *Mycobacterium ulcerans* in the environment. We define LF below,

$$\triangle MU = R \times MU \times \left(1 - \frac{MU}{K_M(t)}\right)$$

where the constant R defines the growth rate and K_M is the carrying capacity. K_M is not constant over time because of the seasonal fluctuations in the environments. For simplicity, we assume that these seasonal fluctuations occur along a sinewave around the carrying capacity. We define carrying capacity as

$$K_M(t) = K_M + SINWAVE(amplitude, period),$$

therefore our *Mycobacterium ulcerans* dynamics is given as

$$MU(t) = MU(t - dt) + (shedding + LF - deaths_{MU}) * dt.$$

We present below a *STELLA* model for the transmission of Buruli ulcer with social dynamics as described above; see *STELLA* model 4.10.

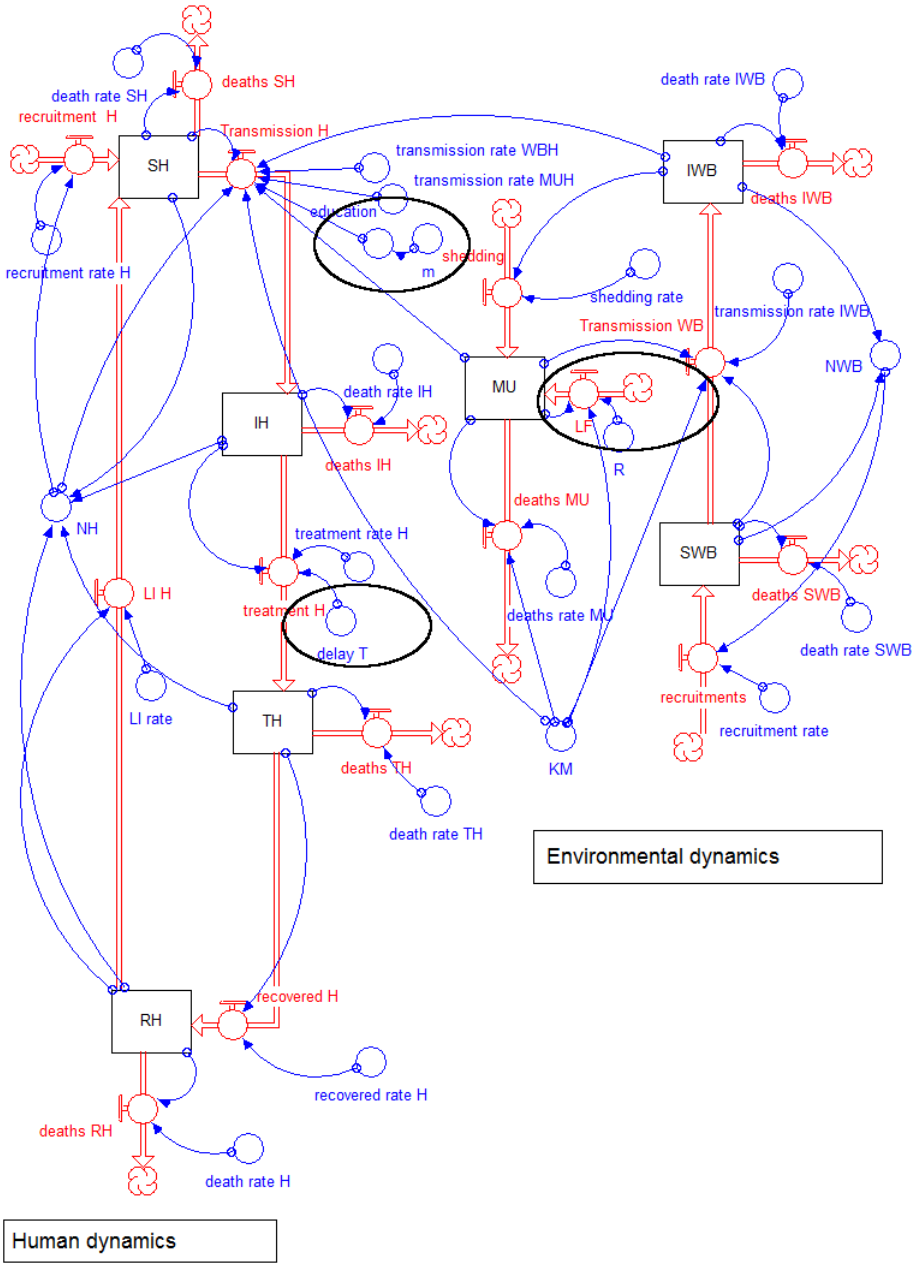

Figure 4.10: A *STELLA* model for the transmission of Buruli ulcer with social dynamics. Where the highlighted ellipse are the added social dynamics: education, treatment delays and LF. The rectangles; SH, IH, TH, RH, SWB, IWB and MU represent stocks, the circles represent converters, the double lines with arrow represent flows and the single lines with arrow represent connectors which connect the flows and the stocks. The flows indicates movement and the connectors indicates contact.

4.7.2.1 Results of education campaigns

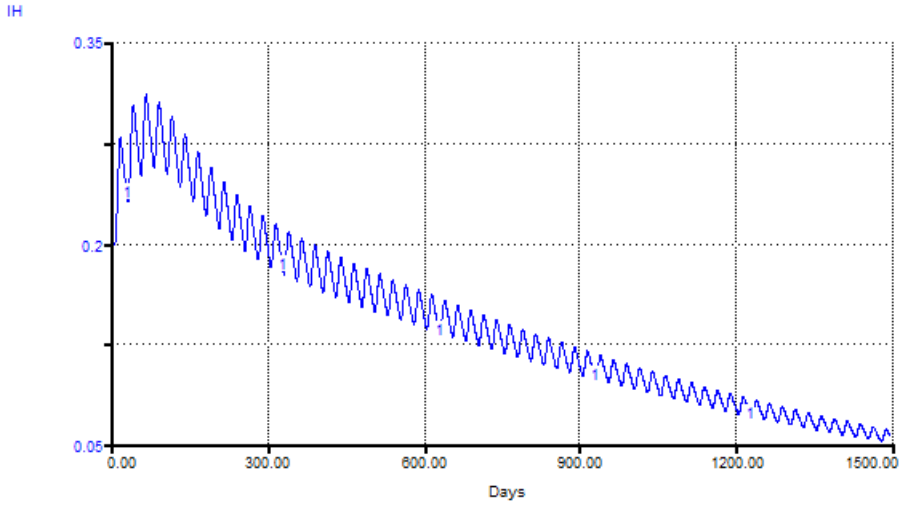

(a) An infection curve for proportions of humans with education efficacy of 0.1 or 10%.

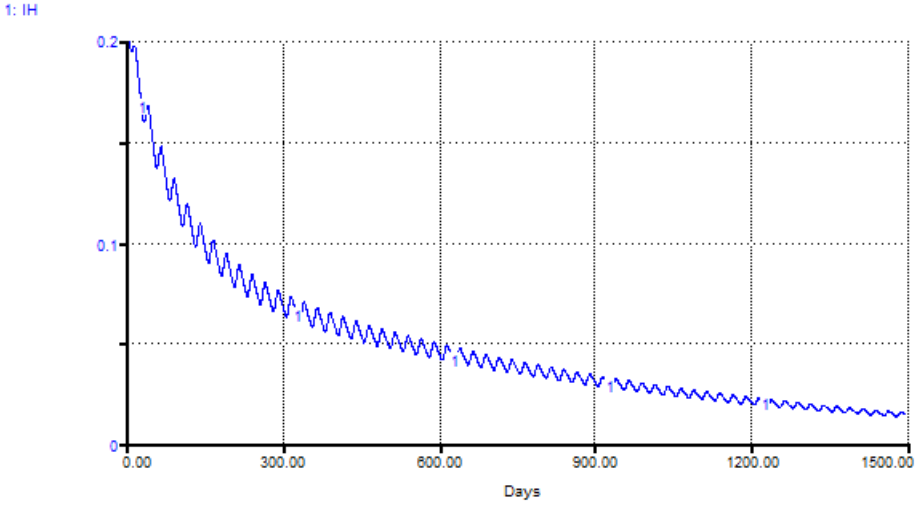

(b) An infection curve for proportions of humans with education efficacy of 0.8 or 80%.

Figure 4.11: An infection curve for proportions of humans with education efficacy of 0.1 and 0.8 respectively, in model 4.10. With an initial condition $I_H(0) = 0.2$, and with rest of the parameters as defined in Table 4.1 to be constant. The disease persist and a periodic solution with $\omega = 91.25$ days forms after a long transient.

With the inclusion of educational campaign in the model 4.10, there is no

much difference in the infection rate when the efficacy is less than 50% as seen in Figure 4.11a. When the education efficacy is between $(50-80)\%$, or more it reduces the disease infection rate since individuals become aware of BU disease and its transmission mode as seen in Figure 4.11b. In Figure 4.11a-4.11b the disease persists after a long oscillating transient the infection approaches a positive $\omega-$periodic solution.

4.7.2.2 Effects of treatment delays

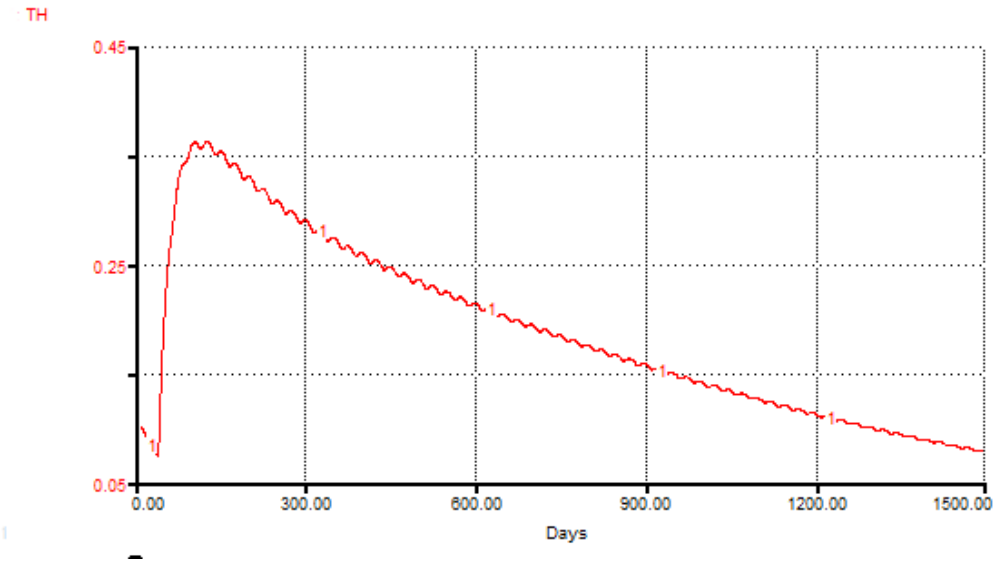

(a) Plot of treatment delays for 30 days.

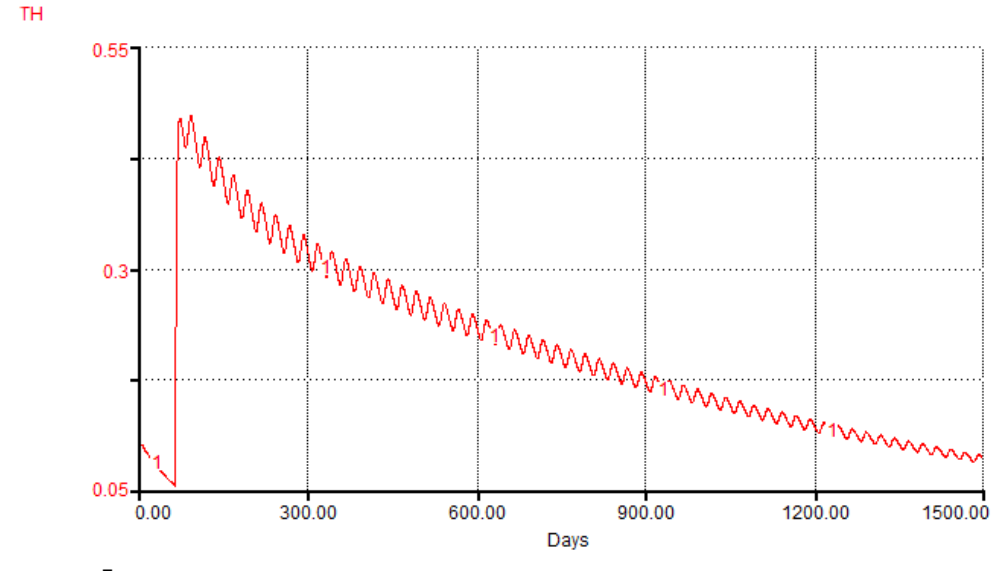

(b) Plot of treatment delays for 60 days.

Figure 4.12: Treatment delays for 30 and 60 days respectively, in model 4.10, with an initial condition $T_H(0) = 0.1$. The rest of the parameters as defined in Table 4.1 to be constant, the disease persists and a periodic solution with $\omega = 91.25$ days forms after a long transient.

Considering Figure 4.12, we analyse the effect of inclusion of treatment delays without educational campaign. In Figure 4.12b when treatment delays

for more than 30 days, it increases treatment rate and the disease persists even after long time and after a long oscillating transient the infection approaches a positive $\omega-$periodic solution.

4.7.2.3 Effect of environmental degradation through mining

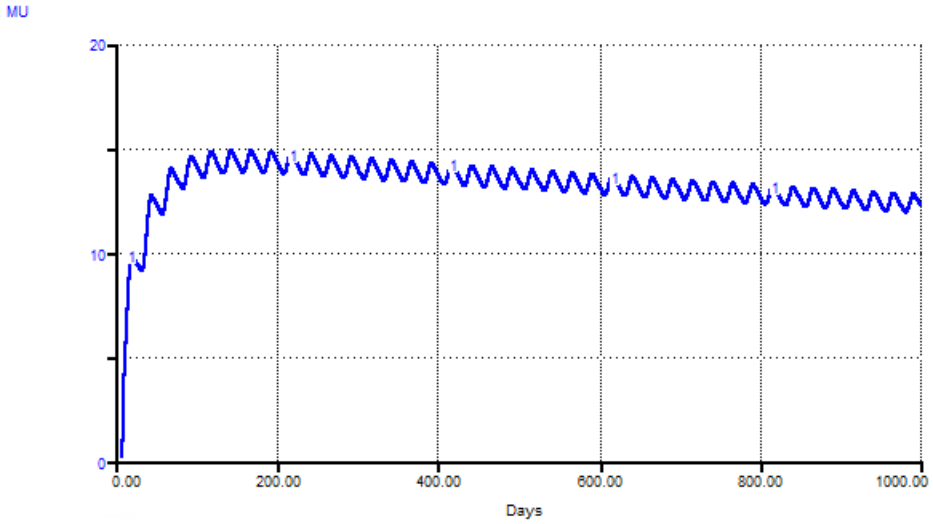

Figure 4.13: Plot of *Mycobacterium ulcerans* density with low or no environmental degradation through mining, with initial conditions $MU(0) = 0$ and $K_M(0) = 0.4$. The rest of the parameters as defined in Table 4.1 to be constant, the disease persists and a periodic solution with $\omega = 91.25$ days forms after a long transient.

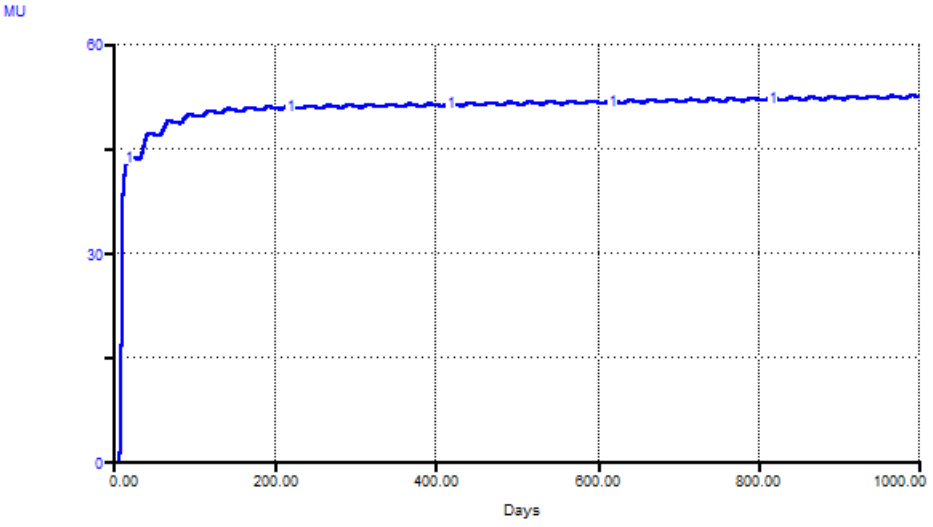

Figure 4.14: Plot of *Mycobacterium ulcerans* density with environmental degradation through intensive mining, with initial conditions $MU(0) = 0$ and $K_M(0) = 40$. The rest of the parameters as defined in Table 4.1 to be constant, the disease persists and a periodic solution with $\omega = 91.25$ days forms after a long transient.

With the inclusion of Logistic function and exclusive of educational campaigns and treatment delays in the model 4.10, we noted that when the carrying capacity K_M is increased by environmental degradation through mining, the *Mycobacterium ulcerans* density in the environment increases. Figure 4.14 indicates that high levels of arsenic (As) concentration positively induces the growth and spread of *Mycobacterium ulcerans* in the environment. This cause disease to persists and a periodic solution with $\omega = 91.25$ days forms after a long transient.

4.7.3 All social dynamics

Here we analyse all the social dynamics together, by plotting both the good and bad scenarios of *STELLA* model 4.10. In the good scenarios we considered high educational efficacy, no treatment delays and no or low environmental degradation through mining (see Figure 4.15) also in the bad scenarios we considered low educational efficacy, treatment delays and environmental degradation through mining (see Figure 4.16).

4.7.3.1 Good scenarios

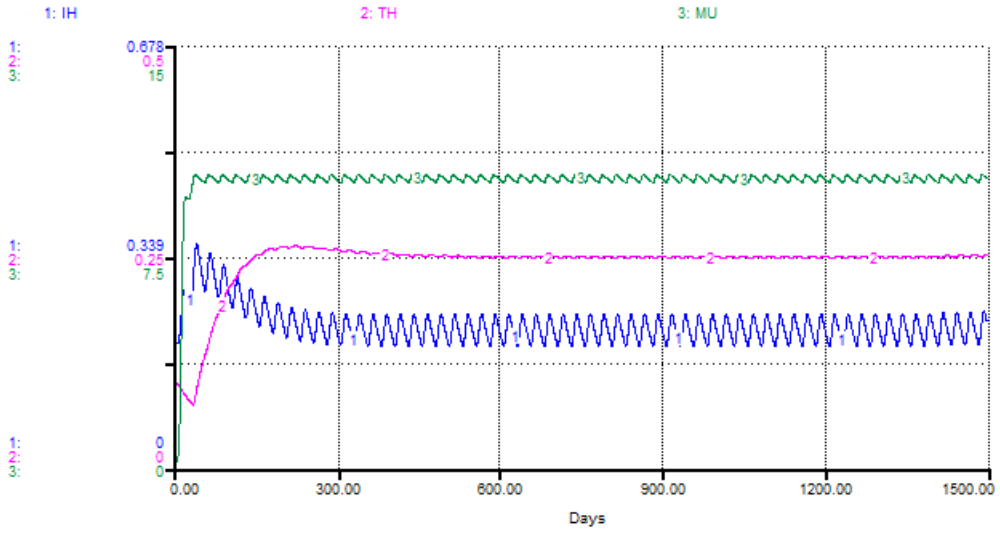

Figure 4.15: Plot of good social dynamics with initial conditions; $I_H(0) = 2, T_H = 0, MU(0) = 0$ and $K_M(0) = 0.4$. The rest of the parameters as defined in Table 4.1 to be constant, the disease persists and a periodic solution with $\omega = 91.25$ days forms after a long transient.

With the inclusion of all social dynamics into the *STELLA* model 4.10. We increased the education efficacy to 80%, gave no treatment delays and no environmental degradation through mining. In Figure 4.15 the infection rate decreases, treatment rate minimise and the *Mycobacterium ulcerans* density also decreases respectively. Our results implies that the BU disease can be reduce over time with the above social dynamics being considered.

4.7.4 Worst scenarios

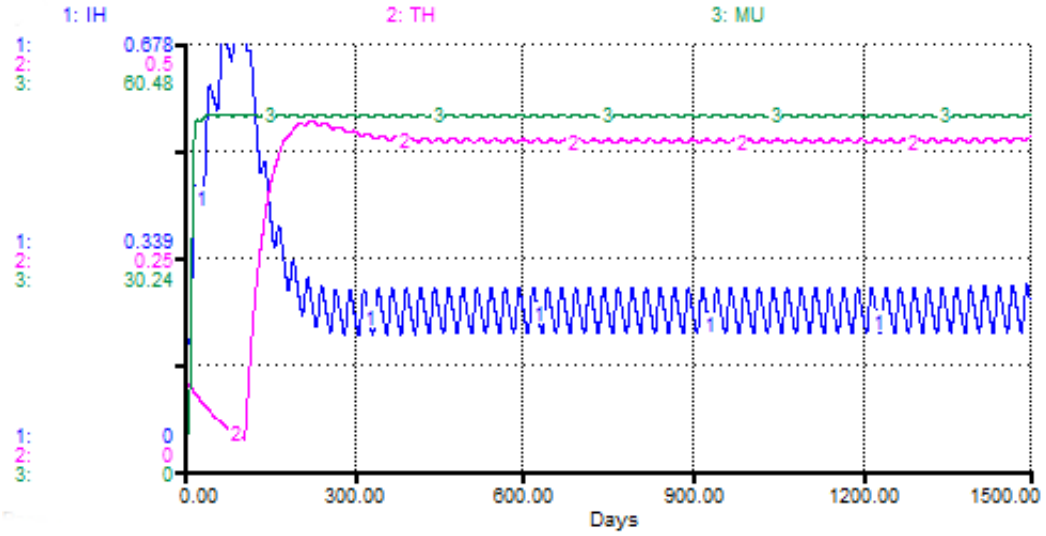

Figure 4.16: Plot of bad social dynamics with initial conditions; $I_H(0) = 2, T_H = 0, MU(0) = 0$ and $K_M(0) = 40$. The rest of the parameters as defined in Table 4.1 to be constant, the disease persists and a periodic solution with $\omega = 91.25$ days forms after a long transient.

We again in Figure 4.16 plotted the effect of educational campaign, treatment delays and a logistic function to the *Mycobacterium ulcerans* density (see model 4.10). We noted that when the efficacy of educational campaign is low such as less than 50%, treatment delays for more than 30 days and there are intensive mining activities in the environments this increases the carrying capacity K_M. Figure 4.16 indicates that the infection rate increases, treatment rate increases and the *Mycobacterium ulcerans* density also increases. This causes BU disease to persist even for a very long time. Our results from model 4.16 indicates that not only shedding back

of *Mycobacterium ulcerans* by water bugs increases the density of the *Mycobacterium ulcerans* in the environment but also through intensive mining activities.

4.8 Summary

In this chapter we relooked at the model presented in Chapter 3, we notice that similar results were obtained by using both the deterministic model and *STELLA* model. We extended the model developed in Chapter 3 to include social dynamic functions.
We investigated the effect of educational campaigns, treatment delays and logistic function to the *Mycobacterium ulcerans* density, through environmental degradation such as mining. We treated them separately to see its effectiveness on the disease endemic population. We noticed that when educational campaigns have more than 50% efficacy it reduces the disease infection rate since individuals now becomes aware of the prevention strategies (by wearing protective apparel and boots) and early detection of the disease. With the use of the delay function in *STELLA* we detected that if treatment delays for more than 30 days it increases the treatment rates and causes the infection to persists. From our simulation results *Mycobacterium ulcerans* density can also be increased through environmental degradation and not water bugs shedding back only. Environmental degradation through mining causes the bacteria carry capacity K_M to increase.
However, our simulations again confirm that clearance of water bugs from the environments will decrease BU disease but this is not practically feasible. Research on malaria now looks at vector control, sterilisation, and genetic modification of the mosquito. Such an approach could be beneficial with regard to the control of water bugs. However, models presented in this project can be used to suggest the type of data that should be collected as research on the ulcer intensifies.

Chapter 5

Discussion

A model for the transmission of BU in periodic environments was presented. It incorporated periodic changes in the environments that results in periodicity in the disease transmission pathway and density of *Mycobacterium ulcerans* The model properties are summarized as the time-averaged reproduction number and the basic reproduction number in the presence of periodicity. Conditions for disease extinction and persistence are established. Numerical simulations are carried out for cases with the basic reproduction number below and above unit.

We found that the time-averaged basic reproduction number $[R_0]$ depends on the life spans of the water bugs and *Mycobacterium ulcerans* in the environments, shedding rate, and infection rates of the water bugs. We further found the basic reproduction number of the system (3.3.6) by using the next infection operator introduced in [55] ($R_0 = \rho(L)$ where L is the next infection operator). We proved that the unique disease free equilibrium E^0 is globally asymptotically stable if $R_0 < 1$. However, when $R_0 > 1$ the disease uniformly persists implying there exists at least one positive periodic solution. Numerical simulations show that there is only one positive periodic solution which is globally asymptotically stable in the case of $R_0 > 1$ (see Figure 3.5). The basic reproduction numbers $[R_0]$ and R_0 were compared under various conditions by varying the baseline value $\hat{\beta}_3$ and the amplitude $\bar{\beta}_3$. It was clearly seen that the basic reproduction number R_0 is slightly less than the time-averaged reproduction number $[R_0]$ in $\hat{\beta}_3$ and greater in $\bar{\beta}_3$ implying that the time-averaged reproduction number shows inaccuracy in predicting risk of infection in BU transmission.

Our results on reproduction numbers, recapitulates that the management

of BU depends mostly on the environmental management; that is, clearance of the bacteria from the environments and by reducing the shedding of the water bugs. This in turn will reduce the infection of the water bugs that transmit the infection to humans. The intricacy of modelling the BU lies in the fact that, apart from humans being victims, the transmission dynamics are subject to seasonal variations. Thus the construction of a realistic mathematical model lies in the consideration of ecological dynamics, climatic and environmental changes.

Finally a system dynamic for the transmission of BU in both fluctuating and non fluctuating environments using *STELLA* was presented. The main aim was to capture the two modes of transmission. It incorporates seasonal variation in the disease transmission pathways and the *Mycobacterium ulcerans* density. The *STELLA* model analysis was carried out using the basic reproduction number R_0 derived from the model in Chapter 3. Model parameters were estimated based on literature on vector borne diseases and some assumptions. This was because not much of the disease is understood. Our results have established R_0 as a sharp threshold for BU dynamics; i.e. disease completely dies out if $R_0 < 1$ and persists if $R_0 > 1$. A good agreement was obtained when comparing the deterministic and *STELLA* model. Our simulation results confirms that BU can be prevented through community health education, early detection and treatment of the disease. Patients should be made aware of the disturbing conditions in their surroundings (by wearing protective apparel and boots). Early detection of the major symptoms of the disease such as identification of any small lesions, nodules or plaques on one's body would help aid in early diagnosis and possible prevention of ulcers and disabilities. The model presented in this thesis is a very simplified caricature of a interaction of the environments (water bugs and *Mycobacterium ulcerans*) and humans. It therefore has some limitations. The model incorporates periodicity only to the contact rates and the shedding rate but the rest of the parameters are still constant. There is also insufficient of experimental data for model verification. Despite these limitations, the model results have significant impact on BU epidemic control. Our model outcome suggests that environmental fluctuations should be taken into consideration in designing policies aimed at BU control and management.

The models presented in this project echoes the attempts to model the BU

with the incorporation of seasonal variations. The results have implications on designing more social interventions like poverty reduction, provision of social services and policies geared towards the eradication of the BU in the presence of fluctuations. The populations considered here are constant. It would be interesting also to investigate on how a non-constant population model will evolve. Moreover, the studies suggests that the model, developed with *STELLA*, has great potentials as a modelling tool for effective investigations of the transmission dynamics of BU due to its simplicity.

Chapter 6

Appendix

STELLA equations

IH(t) = IH(t - dt) + (Transmission_H - deaths_IH - treatment_H) * dt
INIT IH = 0.2
INFLOWS:
- Transmission_H = ((transmission_rate_WBH*(IWB/NH)+transmission_rate_MUH*(MU/(MU+KM)))*SH)*educatio n

OUTFLOWS:
- deaths_IH = death_rate_IH*IH
- treatment_H = treatment_rate_H*IH*delay_T

IWB(t) = IWB(t - dt) + (Transmission_WB - deaths_IWB) * dt
INIT IWB = 0.4
INFLOWS:
- Transmission_WB = transmission_rate_IWB*SWB*(MU/KM)

OUTFLOWS:
- deaths_IWB = IWB*death_rate_IWB

MU(t) = MU(t - dt) + (shedding + LF - deaths_MU) * dt
INIT MU = 1
INFLOWS:
- shedding = shedding_rate*IWB
- LF = R*MU*(1-MU/KM)

OUTFLOWS:
- deaths_MU = (MU/KM)*deaths_rate_MU

RH(t) = RH(t - dt) + (recovered_H - LI_H - deaths_RH) * dt
INIT RH = 0.1
INFLOWS:
- recovered_H = recovered_rate_H*TH

OUTFLOWS:
- LI_H = RH*LI_rate
- deaths_RH = RH*death_rate_H

SH(t) = SH(t - dt) + (recruitment__H + LI_H - Transmission_H - deaths_SH) * dt
INIT SH = 0.6
INFLOWS:
- recruitment__H = NH*recruitment_rate_H
- LI_H = RH*LI_rate

OUTFLOWS:
- Transmission_H = ((transmission_rate_WBH*(IWB/NH)+transmission_rate_MUH*(MU/(MU+KM)))*SH)*educatio n
- deaths_SH = SH*death_rate_SH

SWB(t) = SWB(t - dt) + (recruitments - Transmission_WB - deaths_SWB) * dt
INIT SWB = 0.6
INFLOWS:
- recruitments = NWB*recruitment_rate

OUTFLOWS:
- Transmission_WB = transmission_rate_IWB*SWB*(MU/KM)
- deaths_SWB = SWB*death_rate_SWB

TH(t) = TH(t - dt) + (treatment_H - recovered_H - deaths_TH) * dt
INIT TH = 0.1
INFLOWS:

treatment_H = treatment_rate_H*IH*delay_T

OUTFLOWS:

recovered_H = recovered_rate_H*TH

deaths_TH = death_rate_TH*TH

deaths_rate_MU = 0.02

death_rate_H = 0.00045

death_rate_IH = 0.00045

death_rate_IWB = 0.025

death_rate_SH = 0.00045

death_rate_SWB = 0.025

death_rate_TH = 0.00045

delay_T = DELAY(0.3,30,0)

education = 1-m

KM = 0.4

LI_rate = 0.011

m = 0.1

NH = TH+RH+IH+SH

NWB = SWB+IWB

R = 0.1

recovered_rate_H = 0.00016

recruitment_rate = 0.025

recruitment_rate_H = 0.00045

shedding_rate = 0.5*SINWAVE(0.5,2*1460*PI/365)

transmission_rate_IWB = 0.009*SINWAVE(0.5,2*1460*PI/365)

transmission_rate_MUH = 0.25*SINWAVE(0.5,2*1460*PI/365)

transmission_rate_WBH = 0.25*SINWAVE(0.5,2*1460*PI/365)

treatment_rate_H = 0.04

List of References

[1] Buruli ulcer disease (Mycobacterium ulcerans infection). *Fact SheetNul99, WorldHealth Organization*, Accessed 2015.

[2] A. Y. Aidoo and B. Osei. Prevalence of aquatic insects and arsenic(As) concentration determine the geographical distribution of *Mycobacterium ulcerans* infection. *Computational and Mathematical Methods in Medicine*, 8:235–244, 2007.

[3] L. Allen. An intoduction to mathematical biology. *Department of Mathematics and Statistics, Texas Tech University*, (32):747–763, 2007.

[4] R. M. Anderson and R. M. May. *Infectious Diseases of Humans*. Oxford, 1991.

[5] J. L. Aron and I. B. Schwartz. Seasonality and period-doubling bifurcations in an epidemic model. *Journal of Theoretical Biology*, 110:665–679, 1984.

[6] K. Asiedu and S. Etuaful. Socio-economic implications of Buruli ulcer in Ghana: a three-year review. *American Journal of Tropical Medicine and Hygiene*, 59:1015–1022, 1998.

[7] N. Bacaër. Approximation of the basic reproduction number for vector-borne disease with periodic vector population. *Bulletin of Mathematical Biology*, 69:1067–1091, 2007.

[8] N. Bacaër. Approximation of the basic reproduction number R_0 for vector-borne diseases with a periodic vector population. *Bulletin of Mathematical Biology*, 69:1067–1091, 2007.

[9] N. Bacaër and S. Guernaoui. The epidemic threshold of vector-borne disease with seasonality. *Journal of Mathematical Biology*, 53:421–436, 2006.

[10] Z. Bai and Y. Zhou. Threshold dynamics of a baillary dysentery model with seasonal fluctuations. *Discrete and Continuous Dynamical Systems - Series B*, 15(2):1–14, 2011.

[11] Z. Bai and Y. Zhou. Global dynamics of an seirs epidemic model with periodic vaccination and seasonal contact rate. *Nonlinear Analysis: Real World Applications*, 13(2):1060–1068, 2012.

[12] The World Bank. *The World Bank (Data)*. http://data.worldbank.org/region/SSA, Accessed 2015.

[13] O. N. Bjornstad, B. F. Finkenstadt, and B. T. Grenfell. Dynamics of measles epidemics: Estimating scaling of transmission rates using a time series SIR model. *Ecological Monographs*, 72:169–184, 2002.

[14] E. Bonyah, I. Dontwi, and F. Nyabadza. A theoretical model for the transmission dynamics of the Buruli ulcer with saturated treatment. *Computational and Mathematical Methods in Medicine*, 2014:1–14, 2014.

[15] P. J. Converse, E. L. Nuermberger, D. V. Almeida, and J. H. Grosset. Treating Mycobacterium ulcerans disease (Buruli ulcer): from surgery to antibiotics, is the pill mightier than the knife? *Future Microbiology*, 6(10):1185–1198, 2011.

[16] H. Darie, T. Le Guyadec, and J. E. Touze. Epidemiological and clinical aspects of Buruli ulcer in Ivory Coast. *Bulletin de la Societe de pathologie exotique et de ses filiales*, 86:272–276, 1993.

[17] J. M. Debacker, C. Zinsou, J. Aguiar, W. M. Meyers, and F. Portaels. First case of Mycobacterium ulcerans disease (Buruli ulcer) following a human bite. *Clinical Infectious Diseases*, 36(5):e67–e68, 2003.

[18] P. Van den Driessche and J. Watmough. Reproduction numbers and subthreshold endemic equilibria for compartmental models of disease transmission. *Mathematical Biosciences*, 180:29–48, 2002.

[19] J. Diamond. *STELLA* modelling of a zombies invasion. *https://www.scribd.com/doc/24096872/STELLA-Modelling-of-a-Zombie-Invasion*, pages 1–6, Accessed 2015.

[20] O. Diekmann, J. A. P. Heesterbeek, and J. A. J. Metz. On the definition and the computation of the basic reproduction ratio in models for infectious diseases in heterogeneous populations. *Journal of Mathathematical Biology*, 28:365, 1990.

[21] S. F. Dowell. Seasonal variation in host susceptibility and cycles of certain infectious diseases. *Emerging Infectious Disease Journal*, 7:365–382, 2001.

[22] A. A. Duker, M. J. E. Carranza, and M. Hale. Spatial dependency of Buruli ulcer prevalence on arsenic- enriched domains in Amansie-West District, Ghana: implications for arsenic mediation in Mycobacterium ulcerans infection. *International Journal of Health Geographics*, 69(3):1–19, 2004.

[23] A. A. Duker, M. J. E. Carranza, and M. Hale. Spatial relation between arsenic in drinking water and Mycobacterium ulcerans infection in Amansie West District, Ghana, Mineralogical Magazine. *PLoS Neglected Tropical Diseases*, 69(2):707–717, 2005.

[24] A. A. Duker, F. Portaels, and M. Hale. Pathways of Mycobacterium ulcerans infection: A review. *Environment International*, 32:567–573, 2006.

[25] S. M. Garba, A. B. Gumel, and M. R. A. Bakar. Backward bifurcations in dengue transmission dynamics. *Mathematical Biosciences*, 215:11–25, 2008.

[26] N. C. Grassly and C. Fraser. Seasonal infectious disease epidemiology. *Proceedings of the Royal Society B*, 273:2541–2550, 2006.

[27] K. P. Grietens, A. U. Boock, H. Peeters, S. Hausmann-Muela, E. Toomer, and et al. It is me who endures but my family that suffers: social isolation as a consequence of the household cost burden of Buruli ulcer free of charge hospital treatment. *PLoS Neglected Tropical Diseases*, 13(2):p1–7, 2008.

[28] S. Gui-Quan, Z. Toa, and J. Zhen. Positive periodic solutions of an epidemic model with seasonality. *The Scientific World Journal*, 2013:p1–10, 2013.

[29] K. Jacobsen and J. Padgett. Risk factors for Mycobacterium ulcerans infection. *International Journal of Infectious Diseases*, 14:667–681, 2010.

[30] M. J. Keeling, P. Rohani, and B. T. Grenfell. Seasonally forced disease dynamics explored as switching between attractors. *Physica Dynamics*, 148:665–679, 2001.

[31] W. London and J. A. Yorke. Recurrent outbreaks of measles, chickenpox and mumps. i. seasonal variation in contact rates. *The American Journal of Epidemiology*, 98:453–468, 1973.

[32] L. Luju, X-Q. Zhao, and Y. Zhou. A tuberculosis model with seasonality. *Bulletin of Mathematical Biology*, 72:931–952, 2010.

[33] L. Marsollier, R. Robert, J. Aubry, J-P. S. André, H. Kouakou, P. Legras, A-L. Manceau, C. Mahaza, and B. Carbonnella. Aquatic insects as a vector for Mycobacterium ulcerans. *Applied and Environmental Microbiology*, 439(12):4623–4628, 2002.

[34] M. Mcintosh, H. Williamson, M. E. Benbow, R. Kimbirauskas, C. Quaye, D. Boakye, P Small, and R. Merritt. Associations between Mycobacterium ulcerans and acquatic plant communuties of West Africa: implications for Buruli ulcer disease. *Journal of Public Health Medicine - Ecology & Health*, 11:184–196, 2014.

[35] R. W. Merritt, E. D. Walker, P. L. Small, J. R. Wallace, Johnson P. D, M. E. Benbow, and D. A. Boakye. Ecology and transmission of Buruli ulcer disease: A systematic review. *PLoS Neglected Tropical Diseases*, 4(12), 2010.

[36] P. Munz, I. Hudea, J. Imad, and R. J. Smith? When zombies attack!: Mathematical modelling of an outbreak of zombie infection. *Infectious Disease Modelling Research Progress, J.M. Tchuenche and C. Chiyaka, eds.*, NY:133–156, 2009.

[37] World Health Organization. Buruli ulcer disease, fact sheet nul99, World Health Organization. *http://www.who.int/buruli/en/.*, 2007.

[38] World Health Organization. Buruli ulcer. *http://www.who.int/mediacentre/factsheets/fs199/en/.*, accessed 2015.

[39] World Health Organization. *Buruli ulcer disease (Mycobacterium ulcerans infection) Fact Sheet Nnl99*. http://www.unicef.org, www.ghanainfo.org, Accessed 2015.

[40] N. Osgood. A glimpse of system dynamics models of infectious disease. *Institute for Systems Sciences and Health*, Accessed 2015.

[41] F. Portaels. Epidemiology of ulcers Mycobacterium ulcerans. *Annales de la Societe Belge de Medecine Tropicale*, 96:91–103, 1989.

[42] D. Posny and J. Wang. Modelling cholera in periodic environments. *Journal of Biological Dynamics*, 8(1):1–19, 2014.

[43] M. J. Radzicki and R. A. Taylor. "origin of system dynamics: Jay W. Forrester and the history of system dynamics". in: U. S. Department of Energy's introduction to system dynamics. 2008.

[44] G. Rascalou, D. Potier, F. Menu, and S. Gourbiére. Emergence and prevalence of human vector-borne disease in sink vector populations. *PLoS ONE*, 326(7):1–16, 2012.

[45] J. Ravensway, M. Benbow, A. Tsonis, and et al. Climate and landscape factors associated with Buruli ulcer incidence in Victoria, Australia. *PLoS ONE*, 7:1–12, 2012.

[46] C. Rebelo, A. Margheri, and N. Bacaër. Persistence in seasonally forced epidemiological models. *Journal of Mathematical Biology*, 64:933–949, 2012.

[47] M. T. Silva, F. Portaels, and J. Pedrosa. Aquatic insects and Mycobacterium ulcerans: An association relevant to Buruli ulcer control. *PLOS Medicine*, 102:969–978, 2008.

[48] G. E. Sopoh, Y. T. Barogui, R. C. Johnson, A. D. Dossou, M. Makoutodé, S.Y. Anagonou, L. Kestens, and F. Portaels. Family relationship, water contact and occurrence of Buruli ulcer in Benin. *PLOS Neglected Tropical Diseases*, 4:p1–6, 2010.

[49] Ghana statistical Service. http://www.statsghana.gov.gh/. Accessed 2015.

[50] Isee Systems. Technical document for the iThink and *STELLA* software. Accessed 2015.

[51] Thwink.org. Feedback loop. *http://www.thwink.org/sustain/glossary/FeedbackLoop.*, Accessed 2015.

[52] J. van Ravensway, M. E. Benbow, A. A. Tsonis, S. J. Pierce, L. P. Campbell, J. A. M. Fyfe, J. A. Hayman, P. D. R. Johnson, J. R. Wallace, and J. Qi. Climate and landscape factors associated with Buruli ulcer incidence in Victoria, Australia. *PLOS one*, 7(12):144–147, 2012.

[53] D. Walsh, F. Portaels, and W. Meyers. Buruli ulcer (Mycobacterium ulcerans infection. *Transactions of the Royal Society of Tropical Medicine and Hygiene*, 102(10):969–978, 2008.

[54] J. Wang and S. Liao. A generalized cholera model and epidemic-endemic analysis. *Journal of Biological Dynamics*, 6:568–589, 2012.

[55] W. Wang and X-Q. Zhao. Threshold dynamics for compartmental epidemic models in periodic environments. *Journal of Dynamics and Differential Equations*, 20:699–717, 2008.

[56] B. J. Webb, F. R. Hauck, E. Houp, and F. Portaels. Buruli ulcer in West Africa: strategies for early detection and treatment in the antibiotic era. *Journal of Public Health*, 6(2):144–147, 2009.

[57] Wikipedia. Causal loop diagram. *https://en.wikipedia.org/wiki/Causalloopdiagram*, Accessed 2015.

[58] H. R. Williamson, M. E. Benbow, L. P. Campbell, R. Johnson Christian, Sopoh Ghislain, Barogui Yves, W. Merritt Richard, and P. L. C. Small. Detection of Mycobacterium ulcerans in the environment predicts prevalence of Buruli ulcer in benin. *PLOS Neglected Tropical Diseases*, 6(3):P1–9, 2012.

[59] H. Yang, H. Wei, and X. Li. Global stability of an epidemic model for vector-borne disease. *Journal of Systems Science and Complexity*, 23(2):276–292, 2010.

[60] O. Ying., E. Z. Jia, and L. Dian. A *STALLA* model for the estimation of atrazine runoff, leaching, adsorption, and degradation from an agricultural land. *Journal of Soils and Sediments*, (10):263–271, 2010.

[61] F. Zang and X-Q. Zhao. A periodic epidemic model in a patchy environment. *Journal of Mathematical Analysis and Applications*, 325:496–516, 2007.

[62] X-Q. Zhao. Uniform persistence in processes with application to non-autonomous competitive modes. *Journal of Mathematical Analysis and Applications*, 258:87–101, 2001.

To appear in the *Journal of Biological Dynamics*
Vol. 00, No. 00, Month 20XX, 1–24

Modelling the transmission of the Buruli ulcer in fluctuating environments

Belthasara Assan[†*], Farai Nyabadza[†], Pietro Landi[†] and Cang Hui [† ‡]

[†]*Department of Mathematical Sciences, Stellenbosch University, Private Bag X1, Matieland, 7602, South Africa.*

[‡] *African Institute for Mathematical sciences (AIMS), Cape Town 7945, South Africa.*

(*v5.0 released March 2015*)

The transmission dynamics of Buruli ulcer largely depends on environmental changes. In this paper a deterministic model for the transmission of Buruli ulcer in fluctuating environments is proposed. The model incorporates periodicity in the disease transmission pathways and the *Mycobacterium ulcerans* density that are thought to vary seasonally. Two reproduction numbers, the time-averaged reproduction number $[R_0]$ and the basic reproduction number R_0 are determined and compared. The time-averaged reproduction number obtained shows that the Buruli ulcer epidemic is driven by the dynamics of the environments. The time-averaged reproduction number shows inaccuracy in predicting the number of infections. Numerical simulations confirmed that if $R_0 > 1$ the infection is sustained seasonally. The model outcome suggests that environmental fluctuation should be taken into consideration in designing policies aimed at Buruli ulcer control and management.

Keywords: Buruli ulcer, time-averaged reproduction number, basic reproduction number, extinction, persistence.

1. Introduction

Buruli ulcer (**BU**) is a neglected tropical disease caused by *Mycobacterium ulcerans* [15, 22, 23]. BU is the third most common mycobacterial disease which belongs to the same group with tuberculosis and leprosy [1]. In most cases the disease occurs in children between the ages of 4 and 15 years. It however, affects all ages and sexes. The infection in most instances occurs as painless lumps under the skin often resulting in scars, contractual deformities, amputations, and disabilities [2, 15, 23]. In West Africa, gender distribution of the disease also varies, males with 52% and females 48% [13]. About 37.8% of the recorded cases require surgery while 48% of those affected are children under 15 years [13]. It is a poorly understood disease that has emerged dramatically since the 1980's. It has been driven by speedy environmental changes, coupled together with deforestation, eutrophication, construction of dams, irrigation, farming, mining, and habitat fragmentations [10, 11, 23]. These factors affect the survival of the pathogens and their transmission in the environments. Fundamental aspects of the ecology and epidemiology of *Mycobacterium ulcerans,* including its environmental distribution, niche, host range, and mode of transmission and infection, are poorly understood [7]. Epidemiological studies show that this mycobacteriosis is mainly found and also endemic near wetlands and

*Corresponding author. Email: Belthasara@aims.ac.za

areas with slow-moving rivers. *Mycobacterium ulcerans* survives best under low oxygen tensions, such as in the mud or the bottom of swamps [9].

The likely mode of transmission of BU is driven by two processes: firstly, it occurs through direct contact with *Mycobacterium ulcerans* in the environments [3, 4, 13] and secondly, Portaels et al. [9] hypothesised that some water-filtering organisms such as fish and mollusks concentrate the *Mycobacterium ulcerans* present in water or mud and release the *Mycobacterium ulcerans* into the environments. It is then ingested by water-dwelling predators such as beetles and water bugs. These insect may end up transmitting the disease by biting humans [9, 12, 15]. The likely mode of transmission in humans however, occurs through contact with the environments and not human-to-human transmission.

Few mathematical models have been designed to study the dynamics of BU in order to understand the transmission dynamics of the disease, effective control measures and also to determine adequate prevention [12, 15]. Aidoo and Osei [12], use SIR model to explain the transmission of *Mycobacterium ulcerans* and its dependence on the arsenic (As) environments and the biting frequency of the water bugs. In particular, the higher the rate of ingestion of *Mycobacterium ulcerans* by water bugs, the higher the infectiousness. Furthermore, Bonyah, Dontwi and Nyabadza [15] gave a theoretical model for the transmission dynamics of the BU which considered the effect of treatment. The transmission of the BU is hypothesised to be in two modes: by direct contact with the environments and the biting by the water bugs. They concluded that the BU epidemic is highly influenced by shedding of *Mycobacterium ulcerans* into the environments. One limitation of these models, however, is that all assumed that the model parameters are constant in time meaning that the disease contact rate, recovery rate, *Mycobacterium ulcerans* growth rate , etc., all take fixed values independent of time.

On the other hand, environmental forcing, such as floods, rainfall, dry seasons, temperatures and other climatic factors, is often seasonal and could significantly affects BU disease dynamics. A series of epidemiological studies show seasonal variations in the appearance of BU cases. The number of cases increases during dry periods or after inundations [5, 6]. These conditions are probably favourable for the development of *Mycobacterium ulcerans*, because of the density of possible vectors in areas that are frequently visited by humans. For example if we consider Ghana where BU is endemic, this country experience a typical tropical climate. Where in December to February is Harmattan (dry and dusty weather), March is the hottest month, through April to June they experience major rainfall, July to October there is small rains and in the month of November there is mild and dry weather [39]. Such field observations underline the limitation of all current BU models and imply that mathematical insights into BU seasonality has largely lagged behind. It is thus important for mathematical BU studies to incorporate these seasonal factors to gain deeper quantitative understanding of the short and long-term evolution of BU.

The objective of this paper is to propose a general BU model in a fluctuating environments by extending the model proposed in [15], by incorporating periodicity in the environments and the disease transmission pathways. That is the incidence and the rate of change for the *Mycobacterium ulcerans* density are subject to periodicity. Following [20], we analysed the basic reproduction number, R_0, for this BU model and establish that R_0 is a sharp threshold for BU dynamics in fluctuating environments: when $R_0 < 1$, the disease free equilibrium (DFE) is globally asymptotically stable, and the disease completely dies out; when $R_0 > 1$, the system admits a positive periodic solution, and the disease is uniformly persistent. The method of analysis for extinction and persistence results for periodic epidemic systems is inspired by the research done in [16, 29–32, 38]

The outline of this paper is as follows. In section 2, we introduce the BU model in fluctuating environments. In section 3, the basic reproduction is derived, we introduce the underlying assumptions and further consideration on the model which are the global stability analysis of the disease extinction in Section 4. The existence and uniform persistence of an endemic periodic solution are analysed in Section 5. Some numerical results on the behaviour of the periodic model are presented in section 6. The paper is then discussed in Section 7.

2. Model Formulation

Building on the BU model in [15], we present below compartmental diagram for the transmission of BU in fluctuating environments.

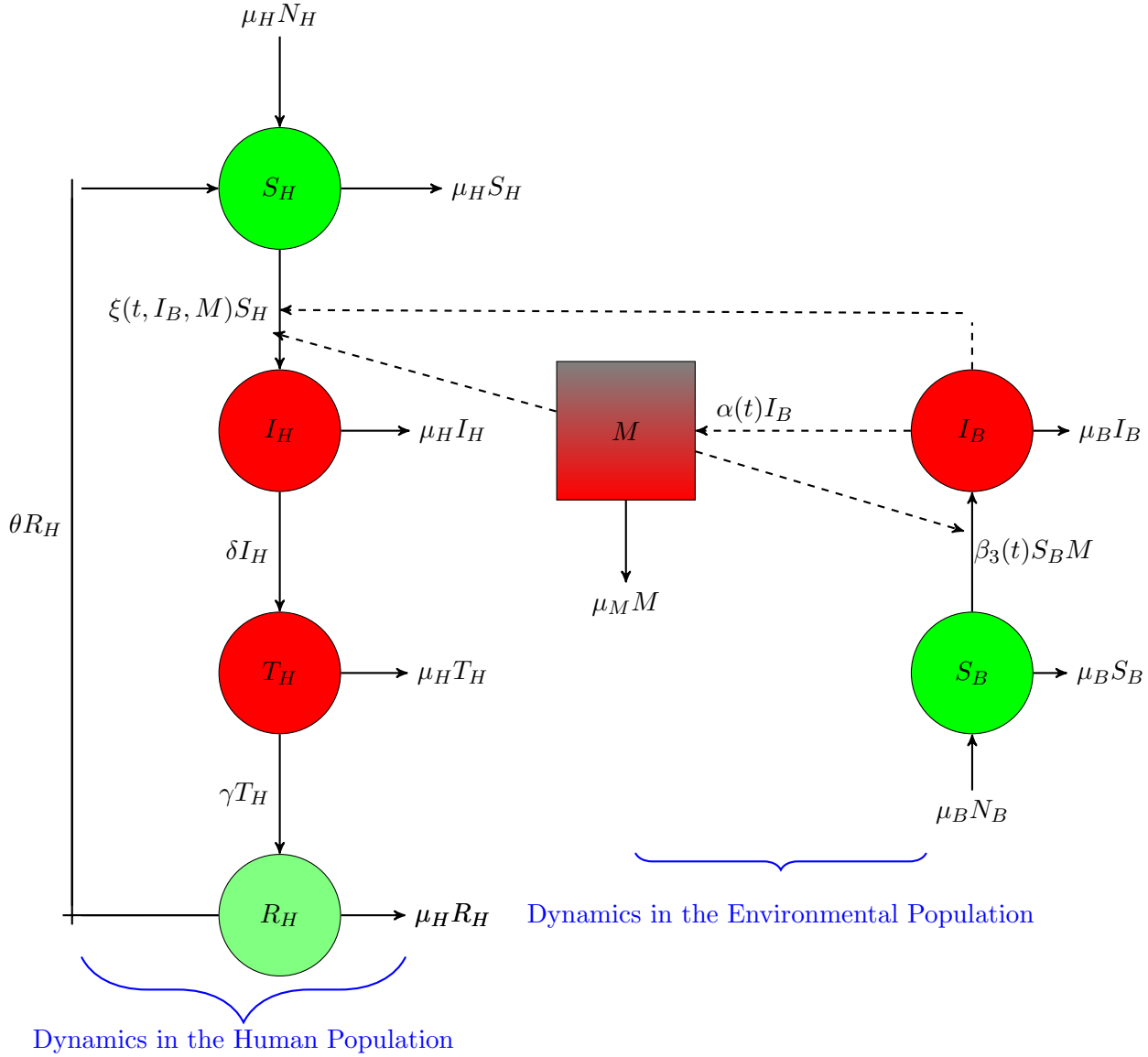

Figure 1. Compartmental diagram for the transmission of BU in fluctuating environments. We have in the human population susceptible human(S_H), infected humans(I_H), individuals in treatments(T_h) and the recovered humans(R_H). Thus, the population at any time t is $N_H = S_H + I_H + T_H + R_H$. In the environmental population S_B is the susceptible water bugs, I_B is the infected water bugs. That is, the population at any time t is $N_B = S_B + I_B$ and M is the *Mycobacterium ulcerans* in the environment. We have used the dashed lines with arrow head to indicates contact and solid lines with arrow head to indicates movement (Table 1 for details).

From the above compartmental diagram the following dynamical system are derived

Table 1. Description of diagram variables and parameters

Variables	Interpretation
S_H	Susceptible humans
I_H	Infected humans
T_H	Treated humans
R_H	Recovered humans
S_B	Susceptible water bugs
I_B	Infected water bugs
M	*Mycobacterium ulcerans* in the environments
Parameters	**Interpretation**
δ	Treatment rate of infected humans
γ	Recovery rate of infected humans
K_M	Carrying capacity of the *Mycobacterium ulcerans*
θ	Lost of immunity by the recovered humans
$\beta_1(t)$	Effective contact rates between susceptible humans with the water bugs in periodic environments
$\beta_2(t)$	Effective contact rates between susceptible humans with the *Mycobacterium ulcerans* in periodic environments
$\beta_3(t)$	The effective contact rate between the water bugs and the *Mycobacterium ulcerans* in periodic environments
$\xi(t, I_B, M)$	The disease transmission rate for humans dependent on time, infected water bugs and *Mycobacterium ulcerans*
μ_H	Natural mortality/birth rate for humans
μ_B	Natural mortality/birth rate for water bugs
μ_M	Natural mortality rate for *Mycobacterium ulcerans*
$\widetilde{\alpha}(t)$	Rate of shedding of *Mycobacterium ulcerans* into the environments
N_H	Total number of human population
N_B	Total number of water bugs population.

to describe the dynamics of the transmission of BU in fluctuating environments:

$$\left.\begin{aligned}
\frac{dS_H}{dt} &= \mu_H N_H + \theta R_H - \xi(t, I_B, M) S_H - \mu_H S_H, \\
\frac{dI_H}{dt} &= \xi(t, I_B, M) S_H - (\mu_H + \delta) I_H, \\
\frac{dT_H}{dt} &= \delta I_H - (\mu_H + \gamma) T_H, \\
\frac{dR_H}{dt} &= \gamma T_H - (\mu_H + \theta) R_H, \\
\frac{dS_B}{dt} &= \mu_B N_B - \mu_B S_B - \beta_3(t) S_B \frac{M}{K_M}, \\
\frac{dI_B}{dt} &= \beta_3(t) S_B \frac{M}{K_M} - \mu_B I_B, \\
\frac{dM}{dt} &= \alpha(t) I_B - \mu_B \frac{M}{K_M},
\end{aligned}\right\} \tag{1}$$

where,

$$\xi(t, I_B, M) = \beta_1(t)\frac{I_B}{N_H} + \beta_2(t)\frac{M}{(K_{50} + M)}.$$

The incidence function $\xi(t, I_B, M)$ determines the rate at which new cases of BU are generated and $\alpha(t)$ the shedding rate of *Mycobacterium ulcerans* by the water bugs in the environments. K_{50} gives the density of *Mycobacterium ulcerans* in the environment that yield 50% chance of infection. The rates $\beta_1, \beta_2, \beta_3$ and α are periodic functions of time with a common period, $\omega = \frac{365}{4} = 91.25$ days. Periodic transmission is often assumed to be sinusoidal, such that

$$\beta_i(t) = \hat{\beta}_i\left[1 + \bar{\beta}_i \sin\left(\frac{2\pi t}{91.25}\right)\right] \quad \text{and} \quad \alpha(t) = \hat{\alpha}\left[1 + \bar{\alpha}\sin\left(\frac{2\pi t}{91.25}\right)\right],$$

where $i = 1, 2, 3$. $\hat{\beta}\bar{\beta}_i$ and $\hat{\alpha}\bar{\alpha}$ are the amplitude of the periodic oscillations in $\beta_i(t)$ and $\alpha(t)$. There is no periodic infections when $\bar{\beta}_i = \bar{\alpha} = 0$. Here $\hat{\beta}_i$ and $\hat{\alpha}$ is the baseline values or the time average. The following change of variables transform system (1) into a dimensionless system,

$$\begin{aligned} s_h &= \frac{S_H}{N_H},\ i_h = \frac{I_H}{N_H}, \tau_h = \frac{T_H}{N_H}, r_h = \frac{R_H}{N_H}, \\ s_b &= \frac{S_B}{N_B},\ i_b = \frac{I_B}{N_B}, m = \frac{M}{K_M}, p = \frac{N_B}{N_H}. \end{aligned}$$

Since we have constant populations, $r_h = 1 - (s_h + i_h + \tau_h)$, $s_b = 1 - i_b$ and the system becomes,

$$\left.\begin{aligned} \frac{ds_h}{dt} &= (\mu_h + \theta)(1 - s_h) - \theta(i_h + \tau_h) - \widetilde{\xi}(t, i_b, m)s_h, \\ \frac{di_h}{dt} &= \widetilde{\xi}(t, i_b, m)s_h - \delta i_h - \mu_h i_h, \\ \frac{d\tau_h}{dt} &= \delta i_h - (\mu_h + \gamma)\tau_h, \\ \frac{di_b}{dt} &= \beta_3(t)(1 - i_b)m - \mu_b i_b, \\ \frac{dm}{dt} &= \widetilde{\alpha}(t)i_b - \mu_m m, \end{aligned}\right\} \tag{2}$$

where,

$$\widetilde{\xi}(t, i_b, m) = \beta_1(t)p(N_B, N_H)i_b + \beta_2(t)\frac{m}{\widetilde{K} + m}, \quad \widetilde{\alpha}(t) = \frac{\alpha(t)N_B}{K_m}, \quad \widetilde{K} = \frac{K_{50}}{K_m}.$$

because the total number of bites made by the water bugs must be equal to the number of bites received by "humans" $p(N_B, N_H)$ is a constant. In this case $p(N_B, N_H) = p$ [15].

2.1. *Basic Properties of the Model*

Positivity of the solution

We need to ensure that the state variables remain non-negative and solutions of the system remain positive for all $t \geq 0$ given positive initial conditions i.e. to establish the long term behaviour of the solutions. We thus have the following lemma.

LEMMA 2.1 *Given the initial conditions* $s_h(0) \geq 0, i_h(0) \geq 0, \tau_h(0) \geq 0, i_b(0) \geq 0$ *and* $m(0) \geq 0$ *then the solution of* $s_h(t), i_h(t), \tau_h(t), i_b(t)$ *and* $m(t)$ *remain positive for all* $t \geq 0$.

Proof. Assume that $\hat{t} = \sup\{t > 0 : s_h(0) \geq 0, i_h(0) \geq 0, \tau_h(0) \geq 0, i_b(0) \geq 0, m(0) \geq 0\} \in [0, t]$, implying $\hat{t} \geq 0$. From the first equation we have,

$$\frac{ds_h}{dt} \geq -[(\mu_h + \theta) + \widetilde{\xi}(t, i_b, m)]s_h.$$

Simple integration yields,

$$s_h(t) \geq s_h(0) \exp^{-(\mu_h+\theta)t + \int_0^t \widetilde{\xi}(\tau, i_b, m)d\tau} \geq 0.$$

The solution $s_h(t)$ will thus always be positive even for a non constant force of infection $\widetilde{\xi}(t, i_b, m)$.

From the second equation we have,

$$\frac{di_h}{dt} \geq -[(\delta + \mu_h)i_h],$$

which results in

$$i_h(t) \geq i_h(0) \exp^{-(\delta+\mu_h)t} \geq 0.$$

The remaining equations give $\tau_h(t) \geq \tau_h(0) \exp^{-(\gamma+\mu_h)t} \geq 0$, $i_b(t) \geq i_b(0) \exp^{-\mu_b t} \geq 0$, and $m(t) \geq m(0) \exp^{-\mu_m t} \geq 0$. Thus all the state variables are positive for any non-negative initial conditions. ■

Invariant Region

Since the model monitors changes in the populations of humans and water bugs and the density of *Mycobacterium ulcerans* in the environment, the model parameters and variables are non-negative. The biological feasible region for the system (2) is in $\mathbb{R}^5_+$ and is represented by the following invariant region:

$$\Omega = \left\{(s_h, i_h, \tau_h, i_h, m) \in \mathbb{R}^5_+ | 0 \leq s_h + i_h + \tau_h \leq 1, 0 \leq i_b \leq 1, 0 \leq m \leq m^*\right\},$$

where the basic properties of local existence, uniqueness, and continuity of solutions are valid for the Lipschitzian systems above. The total population sizes for the human and water bug are assumed to be constant over the modelling time.We can easily establish

the positive invariance of Ω. Given that,

$$\frac{dm}{dt} = \widetilde{\alpha}(t)i_b - \mu_m m \leq \widetilde{\alpha}(t) - \mu_m m, \tag{3}$$

we have $m \leq m^*$ where $m^* = \left\{ \frac{\hat{\alpha}}{\mu_m} + \hat{\alpha}\bar{\alpha} \left[\frac{(91.25)^2\mu_m + (2\pi)^2\mu_m}{(91.25\mu)^2 + (2\pi)^2} \right] \sin\left(\frac{2\pi t}{91.25}\right) \right\}$. The solutions of systems (2) starting in Ω remain in Ω for all $t > 0$. The ω-limit sets of systems (2) are contained in Ω. It thus suffices to consider the dynamics of our system in Ω, where the model is epidemiologically and mathematically well posed.

3. Model Analysis

In this section, for comparison, we first calculate the time-averaged reproduction number, denoted by $[R_0]$, for the *autonomous* form of our system (2). It is then followed by the next infection operator which is the basic reproduction number for the *non-autonomous* system (2). It is easy to see that system (2) has one disease free equilibrium in the non-negative feasible region $\mathbb{R}^5_+$; $E^0 = (s_h^0, i_h^0, \tau_h^0, i_b^0, m^0) = (1, 0, 0, 0, 0)$.

3.1. *Basic Reproduction Number*

The basic reproduction number, R_0, is defined as the expected number of secondary infections in a population of susceptible individuals arising from a single individual during the entire infectious period [25]. R_0 often serves as the threshold parameter that predicts whether an infection will spread or not. Using the standard next-generation matrix theory [25], we consider only the infective classes.

$$\begin{pmatrix} \frac{di_h}{dt} \\ \frac{d\tau_h}{dt} \\ \frac{di_b}{dt} \\ \frac{dm}{dt} \end{pmatrix} = \begin{pmatrix} \widetilde{\xi}(t, i_b, m)s_h \\ 0 \\ \beta_3(1 - i_b)m \\ 0 \end{pmatrix} - \begin{pmatrix} (\delta + \mu_h)i_h \\ -\delta i_h + (\mu_h + \gamma)\tau_h \\ \mu_b i_b \\ -\widetilde{\alpha} i_b + \mu_m m \end{pmatrix} = \mathcal{F} - \mathcal{V},$$

where $\mathcal{F}$ denotes the occurrence rate of new infections and $\mathcal{V}$ the rate of transfer of individuals into or out of each compartments. For any continuous periodic function $h(t)$ with period ω, we define its average as

$$[h] = \frac{1}{\omega} \int_0^\omega h(t)dt$$

we defined the time-averaged matrices of $F(t)$ and $V(t)$ for our BU system (2) as the following, respectively,

$$[F] = D\mathcal{F}(E^0) = \begin{pmatrix} 0 & 0 & 0 & 0 \\ 0 & 0 & 0 & 0 \\ \beta_1 p & 0 & 0 & 0 \\ \frac{\beta_2}{K} & 0 & \beta_3 & 0 \end{pmatrix} \text{ and } [V] = D\mathcal{V}(E^0) = \begin{pmatrix} \delta + \mu_h & -\delta & 0 & 0 \\ 0 & (\mu_h + \gamma) & 0 & 0 \\ 0 & 0 & \mu_b & -\widetilde{\alpha} \\ 0 & 0 & 0 & \mu_m \end{pmatrix},$$

and where E^0 is the disease free equilibrium of the model defined in system (2). The time-averaged reproduction number of system (2) is defined as the spectral radius of the time-averaged next-generational matrix $[F][V]^{-1}$, and is given by

$$[R_0] = \rho([F][V]^{-1}) = \frac{\widehat{\beta_3 \widetilde{\alpha}}}{\mu_b \mu_m}. \tag{4}$$

We interpreted our $[R_0]$ to be the number of secondary cases of infected water bugs generated by the shedded *Mycobacterium ulcerans* in the environments. The time-averaged basic reproduction number $[R_0]$ is independent of the parameters of the human population but only dependent on the life spans of the water bugs and *Mycobacterium ulcerans* in the environments, shedding rate and the infection rate of the water bugs. From this we can conclude that the infection is driven by the water bug population and the density of the *Mycobacterium ulcerans* in the environments. It has been noted, however, that $[R0]$ may overestimate or underestimate the infection risk for a non-autonomous epidemiological system see [32, 34]. From the above conclusion on our time-average reproduction number, it is enough to only consider the water bugs and *Mycobacterium ulcerans* compartments for the following analysis on the transmission of BU in fluctuating environments.

Now we consider our environmental dynamics for the following analysis.

$$\left.\begin{aligned} \frac{ds_b}{dt} &= \mu_b - \mu_b s_b - \beta_3(t) s_b m, \\ \frac{di_b}{dt} &= \beta_3(t) s_b m - \mu_b i_b, \\ \frac{dm}{dt} &= \widetilde{\alpha}(t) i_b - \mu_m m, \end{aligned}\right\} \tag{5}$$

By setting $s_b = 1 - i_b$ we have,

$$\left.\begin{aligned} \frac{di_b}{dt} &= \beta_3(t)(1 - i_b)m - \mu_b i_b, \\ \frac{dm}{dt} &= \widetilde{\alpha}(t) i_b - \mu_m m, \end{aligned}\right\} \tag{5i}$$

Let the function $\beta_3(t)(1 - i_b)m = f(t, i_b, m)$ be the incidence function which determines

the rate of generating new infections and the function $\widetilde{\alpha}(t)i_b - \mu_m m = g(t, i_b, m)$ which describes the rate of change for the *Mycobacterium ulcerans* in the environments. Both are differentiable and periodic in time with period ω. We thus have,

$$f(t+\omega, i_b, m) = f(t, i_b, m) \quad \text{and} \quad g(t+\omega, i_b, m) = g(t, i_b, m).$$

To make biological sense, we assume that the functions f and g satisfy the following conditions for all $t \geq 0$, see [16]

$$f(t, 0, 0) = g(t, 0, 0) = 0. \tag{A1}$$

The assumption (A1) ensures that the disease free equilibrium of the model is unique and constant $E^0 = (i_b^0, m^0) = (0, 0)$.

$$f(t, i_b, m) \geq 0. \tag{A2}$$

Assumption (A2) ensures a non-negative transmission rate.

$$\frac{\partial f}{\partial i_b}(t, i_b, m) \geq 0, \frac{\partial f}{\partial m}(t, i_b, m) \geq 0, \frac{\partial g}{\partial i_b}(t, i_b, m) \geq 0, \frac{\partial g}{\partial m}(t, i_b, m) \leq 0. \tag{A3}$$

The first two inequalities in assumption (A3) state that the rate of new infection increases with both the infected water bugs and the *Mycobacterium ulcerans* density. The third inequality states that increased water bugs infection and consequently, a higher level of water bugs shedding back to the environments, can contribute to a higher growth rate for the *Mycobacterium ulcerans* in the environments. The last inequality explains that the *Mycobacterium ulcerans* cannot sustain themselves long in the environments in the absence of water filtering organisms and water-dwelling predators since they are the main carriers of the bacteria [9, 12, 24]. We also assumed that the incidence function and the change in *Mycobacterium ulcerans*,

$$f(t, i_b, m) \quad \text{and} \quad g(t, i_b, m) \tag{A4}$$

are both concave for any $t \geq 0$, and the following matrices (6) are negative semi definite everywhere.

$$D^2 f = \begin{pmatrix} \frac{\partial^2 f}{\partial i_b^2} & \frac{\partial^2 f}{\partial i_b \partial m} \\ \\ \frac{\partial^2 f}{\partial i_b \partial m} & \frac{\partial^2 f}{\partial m^2} \end{pmatrix} \quad \text{and} \quad D^2 g = \begin{pmatrix} \frac{\partial^2 g}{\partial i_b^2} & \frac{\partial^2 g}{\partial i_b \partial m} \\ \\ \frac{\partial^2 g}{\partial i_b \partial m} & \frac{\partial^2 g}{\partial m^2} \end{pmatrix} \tag{6}$$

Assumption (A4) is based on saturation effects, a common assumption in epidemic models [16, 37].

$$f(t, 0, m) > 0 \quad if \quad m > 0; \quad g(t, i_b, 0) > 0 \quad if \quad i_b > 0. \tag{A5}$$

The first condition in assumption (A5) implies that a positive *Mycobacterium ulcerans* density can lead to a positive incidence even if $i_b = 0$ initially. The second condition states that infected water bugs will contribute to the growth of the *Mycobacterium ulcerans* in the environments by shedding even if $m = 0$ initially. Moreover, we introduce

an additional regulation on the profiles of the incidence and *Mycobacterium ulcerans* functions for small i_b and m. We assume that

$$\text{There exists} \quad \varepsilon^* > 0 \quad \text{such that when} \quad 0 < i_b < \varepsilon^*, 0 < m < \varepsilon^*, \tag{A6}$$

$$\begin{aligned} f(t, i_b, m) \geq & f(t,0,0) + i_b \frac{\partial f}{\partial i_b}(t,0,0) + m\frac{\partial f}{\partial m}(t,0,0) + \frac{1}{2} i_b^2 \frac{\partial^2 f}{\partial i_b^2}(t,0,0) \\ & + i_b m \frac{\partial^2 f}{\partial i_b \partial m}(t,0,0) + \frac{1}{2} m^2 \frac{\partial^2 f}{\partial m^2}(t,0,0), \end{aligned}$$

and

$$\begin{aligned} g(t, i_b, m) \geq & g(t,0,0) + i_b \frac{\partial g}{\partial i_b}(t,0,0) + m\frac{\partial g}{\partial m}(t,0,0) + \frac{1}{2} i_b^2 \frac{\partial^2 g}{\partial i_b^2}(t,0,0) \\ & + i_b m \frac{\partial^2 g}{\partial i_b \partial m}(t,0,0) + \frac{1}{2} m^2 \frac{\partial^2 g}{\partial m^2}(t,0,0). \end{aligned}$$

We make some comments on assumption (A6), from assumption (A4) since the surface of f is below its tangent plane everywhere based on it concavity and the matrix (6) $D^2 f$ is negative semidefinite everywhere, we obtain the following,

$$\begin{aligned} f(t,0,0) + i_b \frac{\partial f}{\partial i_b}(t,0,0) + m\frac{\partial f}{\partial m}(t,0,0) \geq & f(t,0,0) + i_b \frac{\partial f}{\partial i_b}(t,0,0) + m\frac{\partial f}{\partial m}(t,0,0) \\ & + \frac{1}{2} i_b^2 \frac{\partial^2 f}{\partial i_b^2}(t,0,0) + i_b m \frac{\partial^2 f}{\partial i_b \partial m}(t,0,0) \\ & + \frac{1}{2} m^2 \frac{\partial^2 f}{\partial m^2}(t,0,0). \end{aligned}$$

Assumption (A6) means at least in a small neighbourhood of $i_b = m = 0$, the surface of f lies below its tangent plane and above a concave tangent paraboloid. This result also holds for g.

3.2. *Basic reproduction number using the next infection operator L*

The definition of the basic reproduction number of a general non-autonomous model system, however, is still an open question. Bacaër and Guernaoui introduced R_0 for periodic epidemic models (including ODE and PDE systems) as the spectral radius of an integral operator [27] related work for some periodic ODE systems was also discussed in [26]. In addition, Wang and Zhao [20] extended the framework in [25] to include epidemiological model in periodic environments. Let $\Phi_{-V}(t)$ and $\rho(\Phi_{-V}(\omega))$ be the monodromy matrix of the linear $\omega-$periodic system $\frac{dz}{dt} = -V(t)z$ and the spectral radius of $\Phi_{-V}(\omega)$, respectively. Assume $Y(t,s), t \geq s$, is the evolution operator of the linear $\omega-$periodic system

$$\frac{dy}{dt} = -V(t)y. \tag{7}$$

That is, for each $s \in \mathbb{R}$, the 2×2 matrix $Y(t,s)$ satisfies

$$\frac{d}{dt}Y(t,s) = -V(t)Y(t,s), \quad \forall t \geq s, Y(s,s) = I, \tag{8}$$

where I is the 2×2 identity matrix. Thus, the monodromy matrix $\Phi_{-V}(t)$ of equation (7) is equal to $Y(t,0), t \geq 0$.

In view of the fluctuating environments, we assume that $\phi(s)$, $\omega-$periodic in s, is the initial distribution of infectious individuals. Then $F(s)\phi(s)$ is the rate of new infections produced by the infected individuals who were introduced at time s. Given $t \geq s$, then $Y(t,s)F(s)\phi(s)$ gives the distribution of those infected individuals who were newly infected at time s and remain in the infected compartments at time t. It follows that

$$\lambda(t) := \int_{-\infty}^{t} Y(t,s)F(s)\phi(s)ds = \int_{0}^{\infty} Y(t,t-s)F(t-s)\phi(t-s)ds$$

is the cumulative number of new infections at time t produced by all those infected individuals $\phi(s)$ introduced at time previous to t.

Let C_ω be the ordered Banach space of all $\omega-$periodic functions from $\mathbb{R}$ to $\mathbb{R}^2$, which is equipped with the maximum norm $||.||$ and the positive cone $C_\omega^+ := \{\phi \in C_\omega : \phi(t) \geq 0, \forall t \in \mathbb{R}\}$. Then we can define a linear operator $L : C_\omega \to C_\omega$ by

$$(L\phi)(t) = \int_{0}^{\infty} Y(t,t-s)F(t-s)\phi(t-s)ds, \quad \forall t \in \mathbb{R}, \phi \in C_\omega. \tag{9}$$

Following [20], we call L the next infection operator, and define the basic reproduction number as $R_0 := \rho(L)$, the spectral radius of L. We define our new $F(t)$ and $V(t)$ to be,

$$F(t) = \begin{pmatrix} 0 & \beta_3(t) \\ 0 & 0 \end{pmatrix}, \quad V(t) = \begin{pmatrix} \mu_b & 0 \\ -\widetilde{\alpha}(t) & \mu_m \end{pmatrix},$$

$$Y(t,s) = \begin{pmatrix} e^{-\mu_b(t-s)} & 0 \\ \widetilde{Y}(t,s) & e^{-\mu_m(t-s)} \end{pmatrix},$$

where

$$\begin{aligned}\widetilde{Y}(t,s) = &\left[\frac{1}{\mu_m - \mu_b} + \frac{\bar{\alpha}}{\left(\frac{2\pi}{91.25}\right)^2 + (\mu_m - \mu_b)^2}\left((\mu_m - \mu_b)\sin\left(\frac{2\pi t}{91.25}\right) - \left(\frac{2\pi}{91.25}\right)\cos\left(\frac{2\pi t}{91.25}\right)\right)\right] \\ &\times \hat{\alpha}e^{-\mu_b(t-s)} - \hat{\alpha}e^{-\mu_m(t-s)} \times \\ &\left[\frac{1}{\mu_m - \mu_b} + \frac{\bar{\alpha}}{\left(\frac{2\pi}{91.25}\right)^2 + (\mu_m - \mu_b)^2}\left((\mu_m - \mu_b)\sin\left(\frac{2\pi s}{91.25}\right) - \left(\frac{2\pi}{91.25}\right)\cos\left(\frac{2\pi s}{91.25}\right)\right)\right].\end{aligned}$$

We numerically evaluate the next infection operator by

$$(L\phi)(t) = \int_0^\infty Y(t, t-s)F(t-s)\phi(t-s)ds = \int_0^\omega G(t,s)\phi(t-s)ds,$$

where

$$\begin{aligned} G(t,s) &\approx \sum_{k=0}^{M} Y(t, t-s-k\omega)F(t-s-k\omega) \\ &\approx \hat{\beta}_3\left(1+\bar{\beta}_3 \sin\left(\frac{2\pi(t-s)}{91.25}\right)\right)\sum_{k=0}^{M}\begin{pmatrix} 0 & e^{-\mu_b(s+k\omega)} \\ 0 & \widetilde{Y}(t, t-s-k\omega) \end{pmatrix}, \end{aligned}$$

where M is a large positive integer. R_0, the basic reproduction number is computed by reducing the operator eigenvalue problem to a matrix eigenvalue problem in the form of $Ax = \lambda x$, where the entries of the function G are used to construct the matrix A. The basic reproduction number R_0 can then be approximated by numerically calculating the spectral radius of the matrix A : [20, 26] for the methods of calculating R_0.

4. Disease Extinction

In this section, we analyse the global stability of disease free equilibrium point for the system (5i), this gives condition for disease extinction. Suppose we have the matrix function

$$F(t) - V(t) = \begin{pmatrix} \frac{\partial f}{\partial i_b}(t,0,0) - \mu_b & \frac{\partial f}{\partial m}(t,0,0) \\ \frac{\partial g}{\partial i_b}(t,0,0) & \frac{\partial g}{\partial m}(t,0,0) \end{pmatrix}, \tag{10}$$

Clearly,the matrix function of equation (10) is irreducible, continuous, cooperative, and ω-periodic. Let $\Phi_{(F-V)}(t)$ be the fundamental solution matrix of the linear ordinary differential system:

$$z' = [F(t) - V(t)]z, \tag{11}$$

and $\rho(\Phi_{(F-V)}(\omega))$ is the spectral radius of $(\Phi_{(F-V)}(\omega))$. From Lemma 2.1 in [32], we obtain the following result:

LEMMA 4.1 *Let $b = \left(\frac{1}{\omega}\right)\ln\rho(\Phi_{(F-V)}(\omega))$. Then there exists a positive ω-periodic function $v(t)$ such that $e^{bt}v(t)$ is a solution to equation* (11).

Proof. Considering system (5i), and using assumption $(A4)$, we have

$$\begin{aligned} \frac{di_b}{dt} &= f(t, i_b, m) - \mu_b i_b \leq \left[i_b\frac{\partial f}{\partial i_b}(t,0,0) + m\frac{\partial f}{\partial m}(t,0,0)\right] - \mu_b i_b, \\ \frac{dm}{dt} &= h(t, i_b, m) \leq i_b\frac{\partial g}{\partial i_b}(t,0,0) + m\frac{\partial g}{\partial m}(t,0,0). \end{aligned}$$

so

$$\frac{d}{dt}\begin{bmatrix} i_b \\ m \end{bmatrix} \leq [F(t) - V(t)] \begin{bmatrix} i_b \\ m \end{bmatrix}. \tag{12}$$

From Lemma 4.1, there exists $v(t)$ such that

$$z(t) = (\widetilde{i}_b(t), \widetilde{m}(t)) = e^{bt}v(t) \tag{13}$$

is a solution to equation (11), with $b = \left(\frac{1}{\omega}\right) \ln \rho(\Phi_{(F-V)}(\omega))$. It follows from equations (11) and (12) that

$$(i_b(t), m(t)) \leq (\widetilde{i}_b(t), \widetilde{m}(t)) \tag{14}$$

when t is large. From [Theorem 2.2, [20]] $R_0 < 1$ if and only if $\rho(\Phi_{(F-V)}(\omega)) < 1$. Therefore, $b < 0$. Then, given equation (13) and (14), it is clear that

$$\lim_{t\to\infty} i_b(t) = 0, \quad \lim_{t\to\infty} m(t) = 0. \tag{15}$$

■

THEOREM 4.2 *The disease free equilibrium E^0 of system* (5i) *is globally asymptotically stable when $R_0 < 1$ if and only if $\rho(\Phi_{F-V}(\omega)) < 1$.*

Theorem 4.2 shows that when $R_0 < 1$ then the disease completely dies out which means reducing and keeping R_0 below the unity would be sufficient to remove BU infection even in fluctuating environments.

5. Disease Persistence

In this section, we consider the dynamics of the BU system in (5) when $R_0 > 1$.

$$X = \mathbb{R}^3_+; \quad X_0 = (s_b, i_b, m) \in X; \quad \partial X_0 = X \setminus X_0.$$

Let $P : X \to X$ be the Poincaré map associated with the system (5), that is,

$$P(x_0) = u(\omega, x_0), \quad \forall x_0 \in X,$$

where ω is the period and $u(t, x_0)$ be the unique solution of the system (5) with $u(0, x_0) = x_0$.

Definition 5.1 The solution of system (5) is said to be uniformly persistent if there exists some $\varrho > 0$ such that

$$\liminf_{t\to\infty} s_b(t) \geq \varrho, \quad \liminf_{t\to\infty} i_b(t) \geq \varrho, \quad \liminf_{t\to\infty} m(t) \geq \varrho$$

whenever $s_b(0) > 0$, $i_b(0) > 0$, and $m(0) > 0$.

Zhao [33] has given the general definition of uniform persistence. The proof of the theorem below is inspired by the work in [16, 32].

THEOREM 5.2 *Let $R_0 > 1$ and let (A1)–(A6) hold. Then the solutions of system (5) are uniformly persistent, and the system (5) admits at least one positive $\omega-$periodic solution.*

Proof. Let

$$M_\partial = \{(s_b(0), i_b(0), m(0)) \in \partial X_0 : P^n(s_b(0), i_b(0), m(0)) \in \partial X_0, \quad \forall n \geq 0\}.$$

We now show that

$$M_\partial = \{(s_b, 0, 0) \in X : s_b \geq 0\}. \tag{16}$$

It suffices to prove that for any $M_\partial \supseteq \{(s_b, 0, 0) : s_b \geq 0\}$. Consider any initial values $(s_b(0), i_b(0), m(0)) \in \partial X_0 \setminus \{(s_b, 0, 0) : s_b \geq 0\}$. If $i_b(0) = 0$ and $m(0) > 0$, then $i_b'(0) > 0$ from assumption $(A5)$ and also when $m(0) = 0$ and $i_b(0) > 0$, then $m'(0) > 0$. Thus, it follows that $(s_b(t), i_b(t), m(t)) \notin \partial X_0$ for $0 < t \ll 1$. This implies that $M_\partial \subseteq \{(s_b, 0, 0) : s_b \geq 0\}$, we obtain equation (16). Taking the fixed point $E^0 = (1, 0, 0)$ and define $W^s(E^0) = \{x_0 : P^n(x_0) \to E^0, n \to \infty\}$. We show that

$$W^s(E^0) \cap X_0 = \emptyset. \tag{17}$$

Based on the continuity of solutions with respect to the initial conditions, for any $\epsilon > 0$ and $\epsilon < \epsilon^*$, there exists $\delta > 0$ small enough such that $\forall\ (s_b(0), i_b(0), m(0)) \in X_0$ with $||(s_b(0), i_b(0), m(0)) - E^0|| \leq \delta$, we have

$$||u(t, (s_b(0), i_b(0), m(0))) - u(t, E^0)|| < \epsilon \quad \forall t \in [0, \omega]. \tag{18}$$

We assert that

$$\limsup_{n\to\infty} ||P^n(s_b(0), i_b(0), m(0)) - E^0|| \geq \delta \quad \forall (s_b(0), i_b(0), m(0)) \in X_0. \tag{19}$$

By contradiction, we suppose $\limsup_{n\to\infty} ||P^n(s_b(0), i_b(0), m(0)) - E^0|| < \delta$ for some $(s_b(0), i_b(0), m(0)) \in X_0$. Without the loss of generality, we assume that $||P^n(s_b(0), i_b(0), m(0)) - E^0|| < \delta, \quad \forall n \geq 0$. Thus,

$$||u(t, P^n(s_b(0), i_b(0), m(0))) - u(t, E^0)|| < \epsilon \quad \forall t \in [0, \omega] \quad n \geq 0. \tag{20}$$

Moreover, for any $t \geq 0$, we can write $t = t_\prime + l\omega$ with $t_\prime \in [0, \omega)$ and l the greatest integer less than or equal to $\frac{t}{\omega}$. Hence,

$$||u(t, (s_b(0), i_b(0), m(0))) - u(t, E^0)|| = ||u(t_\prime, P^n(s_b(0), i_b(0), m(0))) - u(t_\prime, E^0)|| < \epsilon \tag{21}$$

for any $t \geq 0$. Let $(s_b(t), i_b(t), m(t)) = u(t, (s_b(0), i_b(0), m(0)))$. It follows that $1 - \epsilon < s_b(t) < 1 + \epsilon, \quad 0 < i_b(t) < \epsilon$ and $0 < m(t) < \epsilon$. Since $\epsilon < \epsilon^*$, based on assumptions $(A1)$ and $(A6)$, we obtain this,

$$\begin{aligned}\frac{di_b}{dt} &\geq i_b\frac{\partial f}{\partial i_b}(t,0,0)+m\frac{\partial f}{\partial m}(t,0,0)-\mu_b i_b\\ &+\frac{1}{2}\epsilon i_b\frac{\partial^2 f}{\partial i_b^2}(t,0,0)+\frac{1}{2}\epsilon m\frac{\partial^2 f}{\partial m^2}(t,0,0)-\epsilon i_b\left|\frac{\partial^2 f}{\partial i_b\partial m}(t,0,0)\right|\\ &-\epsilon i_b\frac{\partial f}{\partial i_b}(t,0,0)-\epsilon m\frac{\partial f}{\partial i_b}(t,0,0)-\epsilon^2 i_b\left|\frac{\partial^2 f}{\partial i_b\partial m}(t,0,0)\right|\end{aligned}$$

and

$$\begin{aligned}\frac{dm}{dt} &\geq i_b\frac{\partial g}{\partial i_b}(t,0,0)+m\frac{\partial g}{\partial m}(t,0,0)\\ &+\frac{1}{2}\epsilon i_b\frac{\partial^2 g}{\partial i_b^2}(t,0,0)+\frac{1}{2}\epsilon m\frac{\partial^2 g}{\partial m^2}(t,0,0)-\epsilon i_b\left|\frac{\partial^2 g}{\partial i_b\partial m}(t,0,0)\right|.\end{aligned}$$

That is,

$$\frac{d}{dt}\begin{bmatrix}i_b\\ m\end{bmatrix}\geq[F-V-\epsilon K]\begin{bmatrix}i_b\\ m\end{bmatrix},$$

Where $F-V$ is given in (10) and

$$\epsilon K=-\epsilon\begin{bmatrix}\frac{1}{2}\frac{\partial^2 f}{\partial i_b^2}(t,0,0)-\frac{\partial f}{\partial i_b}(t,0,0) & 0\\ -(1+\epsilon)\left|\frac{\partial^2 f}{\partial i_b\partial m}(t,0,0)\right| & \frac{1}{2}\frac{\partial^2 f}{\partial m^2}(t,0,0)-\frac{\partial f}{\partial m}(t,0,0)\\ \frac{1}{2}\frac{\partial^2 g}{\partial i_b^2}(t,0,0)-\left|\frac{\partial^2 g}{\partial i_b\partial m}(t,0,0)\right| & \frac{1}{2}\frac{\partial^2 g}{\partial m^2}(t,0,0)\end{bmatrix}. \tag{22}$$

From [Theorem 2.2 [20]], $R_0>1$ if and only if $\rho(\Phi_{F-V}(\omega))>1$. Thus, for $\epsilon>0$ small enough, we have $\rho(\Phi_{F-V-\epsilon K}(\omega))>1$. With the help of Lemma 4.1 and by the comparison principle, we obtain as follows:

$$\lim_{t\to\infty} i_b(t)=\infty \quad \lim_{t\to\infty} m(t)=\infty, \tag{23}$$

this is a contradiction. Hence, E^0 is acyclic in M_∂, and P is uniformly persistent with respect to $(X_0,\partial X_0)$, which implies the uniform persistence of the solutions to the equation (21). Consequently, the Poincaré map P has a fixed point $(\widetilde{s}_b(0),\widetilde{i}_b(0),\widetilde{m}(0))\in X_0$, clearly $\widetilde{s}_b(0)\neq 0$. Thus, $(\widetilde{s}_b(0),\widetilde{i}_b(0),\widetilde{m}(0))\in\{s_b,i_b,m\in X\}$ and $(\widetilde{s}_b(t),\widetilde{i}_b(t),\widetilde{m}(t))=u(t,(\widetilde{s}_b(0),\widetilde{i}_b(0),\widetilde{m}(0))$ is a positive $\omega-$periodic solution of the system (5i). ■

6. Simulations

In this section we provide some simulations for the system (2). This simulations were done using Python software. We set our time in days and given our period-ω to be 91.25 days. We computed the basic reproduction number (R_0) and the time-averaged

basic reproduction number ($[R_0]$) for various values of $\beta_3(t)$ and $\widetilde{\alpha}(t)$. For both rates to be positive, we set $0 < \bar{\beta}_3 < 1$ and $0 < \bar{\alpha} < 1$, we focus on the variation of $\beta_3(t)$ here. In Figure 2, we vary $\hat{\beta}_3$ and $\bar{\beta}_3$, respectively, while keeping the values of other parameters fixed. The initial condition of the susceptible water bugs, infected water bugs and *Mycobacterium ulcerans* was estimated in proportion to be $0.6, 0.4$, and 2 respectively. For the mortality rate μ_h, we assume that the life expectancy of the human population is 61 years, in Ghana [39] and is indeed applicable to sub-Saharan Africans. This becomes $\mu_h = 0.0166$ per year and 4.5×10^{-5} per day. Since BU is a vector borne disease we estimate using some of the parameters based on literature of vector borne diseases. Recovery rates of vector borne disease is from 1.6×10^{-5} to 0.5 per day [15, 36]. Also, the mortality rate for water bugs is not completely known, it is assumed to be 0.15 per day [12]. For vector borne disease the loss of immunity ranges between 0 and 1.1×10^{-2} per day [15, 36]. In [15] it was assume that we have more water bugs than humans so that $p > 1$. The rest of the parameters were carefully estimated based on literature on vector borne diseases and on assumptions about the disease, see Table 2 for details of parameters.

Table 2. Model parameters and variable

Parameter/variables	Value(day^{-1})	Source
β_3	0.09	[15]
β_1	1×10^{-5}	[15]
β_2	2×10^{-7}	[15]
μ_h	4.5×10^{-5}	[39]
μ_b	0.8	[15]
μ_m	0.15	[12]
$\widetilde{\alpha}$	0.00615	[15]
θ	$1.1 \times 10^{-2} - 0$	[36]
γ	$1.6 \times 10^{-5} - 0.5$	[36]
δ	$0.08 - 0.4$	[15]

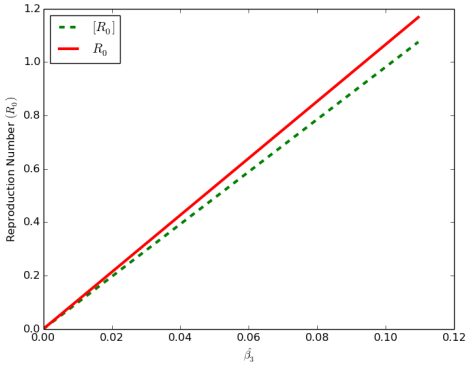

(a) Plot of periodic threshold for various $\hat{\beta}_3$.

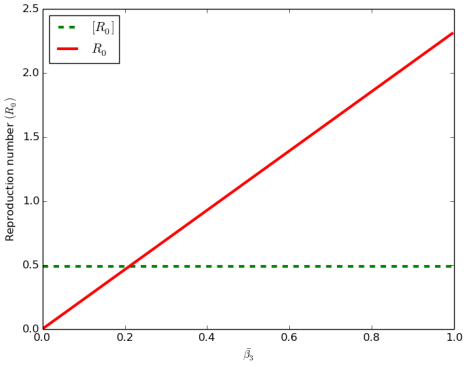

(b) Plot of periodic threshold for various $\bar{\beta}_3$.

Figure 2. A periodic threshold for various $\hat{\beta}_3$ and $\bar{\beta}_3$, of the two basic reproduction numbers of system 2 with other parameters as in Table 2 to be constant.

The time-averaged reproduction number underestimates the infection risk as compared to the basic reproduction number in Figure 2a with $R_0 = 1$ when $\hat{\beta}_3 \approx 0.0899$ and $[R_0] = 1$ when $\hat{\beta}_3 \approx 0.099$. In Figure (2b) $R_0 = 1$ when $\bar{\beta}_3 \approx 0.41$, and $[R_0] = 0.50$ for all $\bar{\beta}_3$. $[R_0]$ shows inaccuracy in predicting the number of infections.

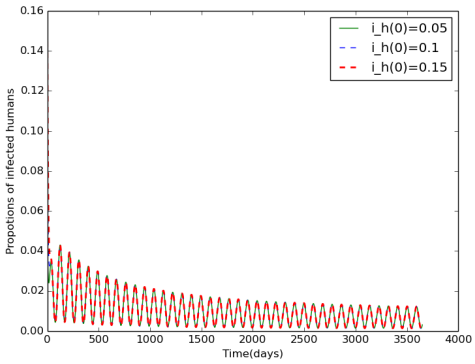

Figure 3. Proportions of infected humans when $R_0 > 1$, in model 1. Different initial conditions; $i_h(0) = 0.05, 0.1$ and 0.15 and with other parameters as in Table 2 to be constant. The disease persists and a periodic solution with $\omega = 91.25$ days forms after a long transient.

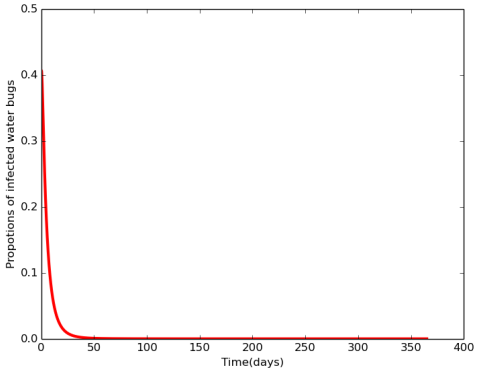

(a) An infection curve when $R_0 < 1$.

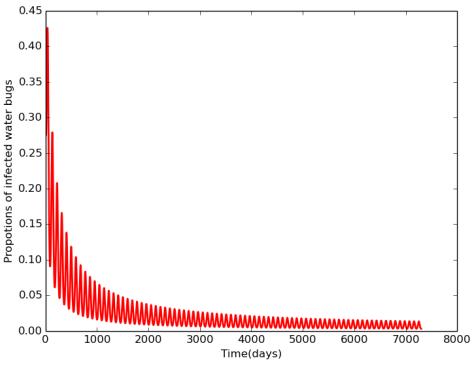

(b) An infection curve $R_0 > 1$.

Figure 4. An infection curve for proportions of infected water bugs when $R_0 < 1$, and $R_0 > 1$, in model 1. For a period of 365 days, initial condition $i_b(0) = 0.4$ and with other parameters as in Table 2 to be constant in Figure 4a. The solution converges to the disease free equilibrium and initial condition $i_b(0) = 0.2$ and with other parameters as in Table 2 to be constant in Figure 4b. The disease persists and a periodic solution with $\omega = 91.25$ days forms after a long transient.

The disease also persists (see Figure 3) for the proportion of infected humans when $R_0 > 1$ and after a long oscillating transient the infection approaches a positive $\omega-$periodic solution. When $R_0 < 1$, the proportions of infected water bugs population i_b turns to zero. The disease completely dies out, and similar patterns were observed for various initial conditions (result not shown), this provides some evidence that the disease free equilibrium is globally stable (see Figure 4a). When $R_0 > 1$, the disease persists after a long oscillating transient and the infection approaches a positive $\omega-$periodic solution (see Figure 4b).

The long-term behaviors when $R_0 > 1$ and the sub graph shows the global stability of

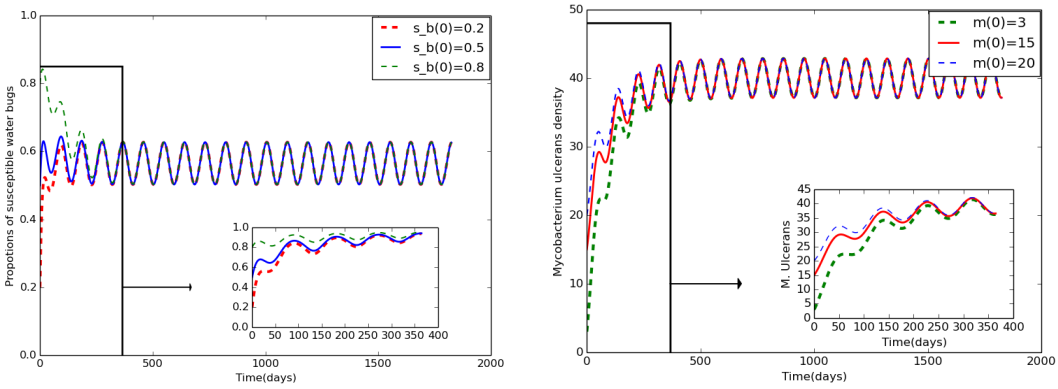

(a) Proportions of susceptible water bugs (b) *Mycobacterium ulcerans density*

Figure 5. Proportions of susceptible water bugs over a period of 1825 days for disease persistence in model 1. Different initial conditions; $s_b(0) = 0.2, 0.5, 0.8$ and with rest of the parameters as defined in Table 2 to be constant in Figure 6a. In Figure 6b gives the *Mycobacterium ulcerans* density over a period of 1825 days for disease persistence in model 1. Different initial conditions; $m(0) = 3, 15, 20$ and with rest of the parameters as defined in Table 2 to be constant. The inset plot shows proportions of susceptible water bugs and *Mycobacterium ulcerans* over a period of 365 days respectively.

the disease free equilibrium E^0 when $R_0 < 1$ for proportions of susceptible water bugs (see Figure 6a) and for *Mycobacterium ulcerans* density (see Figure 6b) respectively. Given different initial condition for the long-term behaviour and the disease free equilibrium, it exhibited the same patterns showing a long oscillating transient and infection approaches a positive $\omega-$solution respectively

7. Discussion

A model for the transmission of BU in periodic environments was presented. It incorporates periodic changes in the environments that results in periodicity in the disease transmission pathway and density of *Mycobacterium ulcerans* The model properties are summarized as the time-averaged reproduction number and the basic reproduction number in the presence of periodicity. Conditions for disease extinction and persistence are established. Numerical simulations are carried out for cases with the basic reproduction number below and above unit.

We found that the time-averaged basic reproduction number $[R_0]$ depends on the life spans of the water bugs and *Mycobacterium ulcerans* in the environments, shedding rate, and infection rates of the water bugs. We further found the basic reproduction number of the system (5i) by using the next infection operator introduced in [20] ($R_0 = \rho(L)$ where L is the next infection operator). We proved that the unique disease free equilibrium E^0 is globally asymptotically stable if $R_0 < 1$. However, when $R_0 > 1$ the disease uniformly persists implying there exists at least one positive periodic solution. Numerical simulations show that there is only one positive periodic solution which is globally asymptotically stable in the case of $R_0 > 1$ (see Figure 4). The basic reproduction numbers $[R_0]$ and R_0 were compared under various conditions by varying the baseline value $\hat{\beta}_3$ and the amplitude $\bar{\beta}_3$. It was clearly seen that the basic reproduction number R_0 is slightly less than the time-averaged reproduction number $[R_0]$ implying that the

time-averaged reproduction number overestimate the risk infection in BU transmission.

Our results on reproduction numbers, recapitulates that the management of BU depends mostly on the environmental management; that is, clearance of the bacteria from the environments and by reducing the shedding of the water bugs. This in turn will reduce the infection of the water bugs that transmit the infection to humans. The intricacy of modelling the BU lies in the fact that, apart from humans being victims, the transmission dynamics are subject to seasonal variations. Thus the construction of a realistic mathematical model lies in the consideration of ecological dynamics, climatic and environmental changes. The model presented in this paper echoes the attempts to model the BU with the incorporation of seasonal variations. The results have implications on designing interventions and policies geared towards the eradication of the BU in the presence of fluctuations.

Acknowledgements

This project is supported by the National Research Foundation (NRF; grants 81825 and 76912) and African Institute for Mathematical sciences (AIMS).

References

[1] W.H.O. *Buruli ulcer*, W.H.O., at http://www.who.int/buruli/en/.

[2] K. Asiedu and S. Etuaful, *Socio-economic implications of Buruli ulcer in Ghana: a three-year review*, Am. J. Trop. Med. Hyg. 59 (1998), pp. 1015-1022.

[3] H. R. Williamson, M. E. Benbow, L. P. Campbell et al.,*Detection of Mycobacterium ulcerans in the environment predicts prevalence of Buruli ulcer in Benin*, PLoS Negl. Trop. Dis. 6 (2012), pp. 1-9.

[4] G. E. Sopoh, Y. T. Barogui, R. C. Johnson et al. *Family relationship, water contact and occurrence of Buruli ulcer in Benin*, PLoS. Negl. Trop. Dis. 4 (2010), pp. 1-6.

[5] H. Darie, T. Le Guyadec, and J. E. Touze , *Epidemiological and clinical aspects of Buruli ulcer in Ivory Coast*, Bull. Soc. Pathol. Exot. 86 (1993), pp. 272-276.

[6] F. Portaels, *Epidemiology of ulcers due to Mycobacterium ulcerans*, Ann. Soc. Med. Trop. 69 (1989), pp. 91-103.

[7] K. Jacobsen and J. Padgett, *Risk factors for Mycobacterium ulcerans infection*, Int. J. Infect. Dis. 14 (2010), pp. 677-681.

[8] L. Marsollier, R. Robert, J. Aubry, et al. *Aquatic insects as a vector for Mycobacterium ulcerans*, Appl. Environ. Micro. 68 (2002), pp. 4623-4628.

[9] M.T. Silva, F. Portaels and J. Pedrosa, *Aquatic insects and Mycobacterium ulcerans: An association relevant to Buruli ulcer control*, PLoS Med. 4 (2007), pp 229-231.

[10] D. Walsh, F. Portaels, W. Meyers, *Buruli ulcer (Mycobacterium ulcerans infection*, Tran. Roy. Soc. Trop. Med. Hyg. 102 (2008), pp. 969-978.

[11] A. A. Duker, F. Portaels, M. Hale *Pathways of Mycobacterium ulcerans infection: A review*, Environ. Int. 32 (2006), pp. 567-573.

[12] A.Y. Aidoo, B. Osei, *Prevalence of aquatic insects and arsenic concentration determine the geographical distribution of Mycobacterium ulcerans infection*, Comput. Math. Methods. Med. 8 (2007), pp 235-244.

[13] *Buruli ulcer disease(Mycobacterium ulcerans infection) Fact Sheet Nnl99*, W.H.O., (2007) http://www.unicef.org, www.ghanainfo.org

[14] G-Q. Sun, Z. Bai, Z-K. Z, T. Zhou and Z. Jin *Positive Periodic Solutions of an Epidemic Model with seasonality*, The ScientificWorldJournal 2013(2013), pp. 1-10.

[15] E. Bonyah, I. Dontwi, and F. Nyabadza, *A theoretical model for the transmission dynamics of the Buruli ulcer with saturated treatment*, Comput. Math. Med. 2014 (2014), pp. 1-14.

[16] D. Posny, and J. Wang, *Modelling Cholera in periodic environments*, J. Biol. Dyn. 8 (2014), pp 1-19.

[17] M. J. Keeling, P. Rohani, and B. T. Grenfell, *Seasonally forced disease dynamics explored as switching between attractors*, Physica D. 148 (2001), pp. 665-679.

[18] J. L. Aron and I. B. Schwartz, *Seasonality and period-doubling bifurcations in an epidemic model* , J. Theor. Biol. 110 (1984), pp. 665-679.

[19] N. C. Grassly and C. Fraser, *Seasonal infectious disease epidemiology*, Proc. R. Soc. B. 273 (2006), pp 2541-2550.

[20] W. Wang and X-Q. Zhao, *Threshold dynamics for compartmental epidemic models in periodic environments*, J. Dyn. Differ. Equ. 20 (2008), pp 699-717.

[21] J. Ravensway, M. Benbow, A. Tsonis et al., *Climate and landscape factors associated with Buruli ulcer incidence in Victoria, Australia*, PLoS ONE, 7 (2012), pp. 1-12.

[22] W.H.O., *Buruli ulcer disease (Mycobacterium ulcerans infection)* W.H.O. Fact SheetNu199, WorldHealth Organization, (2007), http://www.who.int/mediacentre/fact-sheets/fs199/en/.

[23] R. W. Merritt, E. D. Walker, P. L. C. Small, J. Wallace, and P. Johnson, *Ecology and transmission of Buruli ulcer disease:A systematic review*, PLoS Neg. Trop. Dis., 4 (2010), pp. 1-12.

[24] M. Mcintosh, H. Williamson, M. E. Benbow et al. *Associations between Mycobacterium ulcerans and acquatic plant communuties of West Africa: Implications for Buruli ulcer disease*, EcoHealth. 11 (2014), pp. 184-196.

[25] P. Van den Driessche and J. Watmough, *Reproduction numbers and sub-threshold endemic equilibria for compartmental models of disease transmission*, Math. Biosci. 180 (2002), pp. 29-48.
[26] N. Bacaër, *Approximation of the basic reproduction number R_0 for vector-borne diseases with a periodic vector population"*, Bull. Math. Biol. 69 (2007), pp. 10671091.
[27] N. Bacaër and S. Guernaoui, *The epidemic threshold of vector-borne disease with seasonality*, J. Math. Biol. 53 (2006), pp. 421-436.
[28] D. Posny and J. Wang, *Computing the basic reproduction number for epidemiological models in periodic environments*, preprint, (2013).
[29] C. Rebelo, A.Margheri and N. Bacaër, *Persistence in seasonally forced epidemiological models*, J. Math. Biol. 64 (2012), pp. 933-949.
[30] Z. Bai and Y. Zhou, *Threshold dynamics of a baillary dysentery model with seasonal fluctuations*, Disc. Cont. Dyn. Sys. Ser. B 15 (2011), pp. 114.
[31] Z. Bai and Y. Zhou, *Global dynamics of an SEIRS epidemic model with periodic vaccination and seasonal contact rate*, Non. Anal.: RealWorld Appl. 13 (2012), pp. 10601068
[32] F. Zhang and X-Q. Zhao, *A periodic epidemic model in a patchy environment*, J. Math. Anal. Appl. 325 (2007), pp 496-516.
[33] X-Q. Zhao, *Uniform persistence in processes with application to non-autonomous competitive modes*, J. Math. Anal. Appl. 258 (2001), pp 87-101.
[34] N. Bacaër and R. Ouifki, Growth rate and basic reproduction number for population models with a simple periodic factor, Math. Biosci. 210 (2007), pp. 647658.
[35] A. Roche, B. Kamgang and R. Ossomba et al. *Mycobacterium ulcerans ecological dynamics and its association with freshwater ecosystems and aquatic communities: Results from a 12-month environmental survey in Cameroon*, PLoS. Negl. Trop. Dis. 8 (2014), pp. 1-11
[36] G. Rascalou, D. Potier, F. Menu, and S. Gourbiére, *Emergence and prevalence of human vector-borne disease in sink vector populations*, PLoS ONE 7 (2012), pp. 1-16.
[37] J. Wang and S. Liao, *A generalized cholera model and epidemic-endemic analysis*, J. Biol. Dyn. 6 (2012), pp. 568589.
[38] L. Luju, X-Q. Zhao, and Y. Zhou, *A tuberculosis model with seasonality*, Bull. Math. Biol. 72 (2010), pp. 931-952.
[39] Ghana statistical Service, (2014). http://www.statsghana.gov.gh/., G.S.S.
[40] Easy Track Ghana: Calendar, Weather and Climate (Accessed in 2015), http://easytrackghana.com/travel-information-ghanaunderscoreclimate-calendar.php.

Appendices

Evolution operator in section 3

The evolution operator can be easily be determined by solving the system of differential equations. $\frac{dy}{dt} = -V(t)y$. That is, for each $s \in \mathbb{R}$, the 2×2 matrix $Y(t,s)$ satisfies

$$\frac{d}{dt}Y(t,s) = -V(t)Y(t,s), \quad \forall t \geq s, Y(s,s) = I,$$

where I is the 2×2 identity matrix. $-V(t) = \begin{pmatrix} -\mu_b & 0 \\ \widetilde{\alpha}(t) & -\mu_m \end{pmatrix}$

$$\begin{pmatrix} \frac{dy_1}{dt} & \frac{dy_2}{dt} \\ \frac{dy_3}{dt} & \frac{dy_4}{dt} \end{pmatrix} = \begin{pmatrix} -\mu_b y_1 & -\mu_b y_2 \\ \widetilde{\alpha}(t)y_1 - \mu_m y_3 & \widetilde{\alpha}(t)y_2 - \mu_m y_4 \end{pmatrix}$$

Initial conditions $I_s = I_{2*2}$ such that $\begin{pmatrix} y_1(s) & y_2(s) \\ y_3(s) & y_4(s) \end{pmatrix} = \begin{pmatrix} 1 & 0 \\ 0 & 1 \end{pmatrix}$.
Solving for y_1, y_2, y_3 and y_4, we have

$$\frac{dy_1}{dt} = -\mu_b y_1 \Rightarrow y_1 = c_1 e^{-\mu_b t}, \quad c_1 = e^c.$$

Applying the initial conditions and solving for the constant c_1 we get $c_1 = e^{\mu_b s}$, Therefore $y_1(t) = e^{-\mu_b(t-s)}$. Similarly, $\frac{dy_2}{dt} = -\mu_b y_2 \Rightarrow y_2 = c_2 e^{-\mu_b t}, \quad c_2 = e^c$.

Applying the initial conditions and substituting for c_2 we get $c_2 = 0$. Hence $y_2(t) = 0$.

$$\frac{dy_4}{dt} = y_2\widetilde{\alpha}(t) - y_4\mu_m, \Rightarrow -y_4\mu_m \Rightarrow y_4 = c_4 e^{-\mu_m t}, \quad c_4 = e^c.$$

Applying the initial conditions and substituting for c_4 give $c_4 = e^{\mu_m s}$.
Hence $y_4(t) = e^{-\mu_m(t-s)}$. Similarly, $\frac{dy_3}{dt} + y_3\mu_m = e^{-\mu_b(t-s)}\widetilde{\alpha}(t)$.
Multiplying throughout by the integrating factor, $I = e^{\mu_m t}$, and simplifying we get

$$y_3 e^{\mu_m t - \mu_b s} = \int e^{(\mu_m - \mu_b)t}\widetilde{\alpha}(t)dt, \quad \text{and} \quad \widetilde{\alpha}(t) = \hat{\alpha}\left[1 + \bar{\alpha}\sin\left(\frac{2\pi t}{91.25}\right)\right] \tag{24}$$

$$\begin{aligned} y_3 e^{\mu_m t - \mu_b s} &= \hat{\alpha}\int e^{(\mu_m - \mu_b)t}dt + \hat{\alpha}\bar{\alpha}\int e^{(\mu_m - \mu_b)t}\sin\left(\frac{2\pi t}{91.25}\right)dt \\ &= \hat{\alpha}\frac{e^{(\mu_m - \mu_b)t}}{\mu_m - \mu_b} + \hat{\alpha}\bar{\alpha}\int \sin\left(\frac{2\pi t}{91.25}\right)e^{(\mu_m - \mu_b)t}dt. \end{aligned} \tag{25}$$

We solve $\int \sin\left(\frac{2\pi t}{91.25}\right) e^{(\mu_m-\mu_b)t}dt$ using integration by parts we obtain,

$$\int e^{(\mu_m-\mu_b)t}\sin\left(\frac{2\pi t}{91.25}\right)dt = \frac{1}{(\mu_m-\mu_t)}\sin\left(\frac{2\pi t}{91.25}\right)e^{(\mu_m-\mu_b)t}) - \frac{1}{\mu_m-\mu_t}\left(\frac{2\pi t}{91.25}\right)\int \cos\left(\frac{2\pi t}{91.25}\right)e^{(\mu_m-\mu_b)t}dt + C. \tag{26}$$

Also $$\int \cos\left(\frac{2\pi t}{91.25}\right)e^{(\mu_m-\mu_b)t}dt = \frac{1}{(\mu_m-\mu_b)}e^{(\mu_m-\mu_b)t}\cos\left(\frac{2\pi t}{91.25}\right)) + \frac{1}{(\mu_m-\mu_b)}\left(\frac{2\pi}{91.25}\right)\int \sin\left(\frac{2\pi t}{91.25}\right)e^{(\mu_m-\mu_b)t}dt + C \tag{27}$$

Substituting equation (7) into equation (26) and simplifying we get

$$\int \sin\left(\frac{2\pi t}{91.25}\right)e^{(\mu_m-\mu_b)t}dt = \frac{1}{(\mu_m-\mu_b)}\sin\left(\frac{2\pi t}{91.25}\right)e^{(\mu_m-\mu_b)t} - \frac{1}{\mu_m-\mu_b}\left(\frac{2\pi t}{91.25}\right) \times \left[\frac{1}{(\mu_m-\mu_b)}e^{(\mu_m-\mu_b)t}\cos\left(\frac{2\pi t}{91.25}\right)\right] + \left[\frac{1}{(\mu_m-\mu_b)}\left(\frac{2\pi}{91.25}\right)\int \sin\left(\frac{2\pi t}{91.25}\right)e^{(\mu_m-\mu_b)t}dt + C\right] \tag{28}$$

Substituting equation (28) into equation (7) and simplifying we get

$$y_3 e^{\mu_m t-\mu_b s} = e^{(\mu_m-\mu_b)t}\left[\frac{\hat{\alpha}}{(\mu_m-\mu_b)} + \frac{\hat{\alpha}\bar{\alpha}(\mu_m-\mu_b)}{(\mu_m-\mu_b)^2+\left(\frac{2\pi}{91.25}\right)^2}\sin\left(\frac{2\pi t}{91.25}\right)\right] - e^{(\mu_m-\mu_b)t}\left[\frac{\hat{\alpha}\bar{\alpha}(\mu_m-\mu_b)}{(\mu_m-\mu_b)^2+\left(\frac{2\pi}{91.25}\right)^2}\left(\frac{2\pi}{91.25}\right)\cos\left(\frac{2\pi t}{91.25}\right)\right] + C_1 \tag{29}$$

Dividing through by $e^{\mu_m t-\mu_b s}$ and applying the initial condition to solve for the constant C_1

$$C_1 = -e^{(\mu_m-\mu_b)s}\left[\frac{\hat{\alpha}}{(\mu_m-\mu_b)} + \frac{\hat{\alpha}\bar{\alpha}(\mu_m-\mu_b)}{(\mu_m-\mu_b)^2+\left(\frac{2\pi}{91.25}\right)^2}\sin\left(\frac{2\pi s}{91.25}\right)\right] e^{(\mu_m-\mu_b)s}\left[\frac{\hat{\alpha}\bar{\alpha}(\mu_m-\mu_b)}{(\mu_m-\mu_b)^2+\left(\frac{2\pi}{91.25}\right)^2}\left(\frac{2\pi}{91.25}\right)\cos\left(\frac{2\pi s}{91.25}\right)\right], \tag{30}$$

Substituting equation (30) into equation (7) to obtain

$$\widetilde{Y}(t,s) = \left[\frac{1}{\mu_m-\mu_b} + \frac{\bar{\alpha}}{\left(\frac{2\pi}{91.25}\right)^2+(\mu_m-\mu_b)^2}\left((\mu_m-\mu_b)\sin\left(\frac{2\pi t}{91.25}\right) - \left(\frac{2\pi}{91.25}\right)\cos\left(\frac{2\pi t}{91.25}\right)\right)\right] \times e^{-\mu_b(t-s)}\hat{\alpha} - e^{-\mu_m(t-s)}\hat{\alpha}\times \left[\frac{1}{\mu_m-\mu_b} + \frac{\bar{\alpha}}{\left(\frac{2\pi}{91.25}\right)^2+(\mu_m-\mu_b)^2}\left((\mu_m-\mu_b)\sin\left(\frac{2\pi s}{91.25}\right) - \left(\frac{2\pi}{91.25}\right)\cos\left(\frac{2\pi s}{91.25}\right)\right)\right].$$

To appear in the *Journal of Biological Dynamics*
Vol. 00, No. 00, Month 20XX, 1–21

A STELLA model for Buruli ulcer transmission with periodicity

Belthasara Assan[†*], Farai Nyabadza[†], Pietro Landi[†] and Cang Hui[†‡]

[†]*Department of Mathematical Sciences, University of Stellenbosch, Private Bag X1, Matieland, 7602, South Africa.*

[†‡]*African Institute for Mathematical Sciences (AIMS), Cape Town 7945, South Africa.*

(*v5.0 released March 2015*)

We propose a systems dynamic model for the transmission of Buruli ulcer dynamics in periodic environments using *STELLA* model. The model incorporates seasonal variation into the disease transmission pathways and the *Mycobacterium ulcerans* density. The model simulation confirms that when $R_0 < 1$ and $R_0 > 1$ the solutions converge to the disease free and endemic equilibrium respectively. It also confirms that if $R_0 > 1$ the infection is sustained seasonally. The *STELLA* model however, provided flexibility through its ability to accommodate more social dynamics without adding mathematical intractability. The model provides useful insights in the dynamics of Buruli ulcer and has significant implication to the management of disease.

Keywords: Buruli ulcer, *Mycobacterium ulcerans, STELLA*, basic reproduction number, periodicity.

1. Introduction

Buruli ulcer has been reported in 33 countries in Africa, the Americas, Asia and the Western Pacific. Most cases occur in tropical and subtropical regions except in Australia, China and Japan. BU is a neglected emerging disease that has recently been reported endemic in some part of West and Central Africa. Countries with most cases are Benin, Cameroon, Cote d'Ivoire, Democratic Republic of the Congo and Ghana. BU is a serious necrotizing cutaneous infection caused by *Mycobacterium ulcerans* [5, 6]. It is presently the third most common mycobacterial disease of humans, after tuberculosis and leprosy, and the least understood of the three [5, 6]. It is associated with rapid environmental changes to the landscapes, such as deforestation, construction, and mining [6–8, 10]. These factors affect the survival and transmissions of the pathogens in the environment. The disease is mainly found in rural areas located near wetlands (ponds, swamps, marshes, impoundments, backwaters) and slow-moving rivers, especially in areas prone to flooding. *Mycobacterium ulcerans* survives best under low oxygen tensions, such as in the mud or the bottom of swamps [5]. In 2014 [3], 12 countries reported nearly 2200 new cases, more than 50% reduction from 2009 when 5000 cases were reported. Except for a few countries, the number of cases has declined since 2010 although the exact cause of decline is still unknown. The worst affected age group is children aged between 4 and 15 years. The disease begins typically as a painless nodule under the skin at the site of a trauma. Infection leads to extensive destruction of skin and soft tissue with

*Corresponding author. Email: belthasara@aims.ac.za

the formation of large ulcers usually on the legs or arms. Patients who are not treated early enough often suffer from long-term functional disability such as difficulty of joint movement as well as the obvious cosmetic problem, scarring, contractual deformities and amputations [7, 35]. Early diagnosis and treatment are vital in preventing such disabilities. The disease is commonly referred to as the mysterious disease because the mode of transmission is poorly understood, although several hypotheses have been proposed. The common two modes of transmission are as follows; firstly, Portaels et al. [33] hypothesised that some water-filtering organisms could have concentrated *Mycobacterium ulcerans* and then be ingested by water-dwelling predators, which becomes a passive reservoir for *Mycobacterium ulcerans*. Bites of these insects may lead to the injection of *Mycobacterium ulcerans* into the skin. The second mode of transmission occurs through direct contacting with *Mycobacterium ulcerans* in the environments [9, 33, 34].

It is well known that many diseases exhibit seasonal fluctuations, such as whooping cough, measles, influenza, polio, chickenpox, mumps, etc. [21, 22, 25]. Seasonally effective contact rate [23, 27, 28], periodic changing in birth rate [26], vaccination program [24], disease transmission pathways and pathogen concentration [20] are often regarded as sources of periodicity. A series of epidemiological studies show seasonal variations in the appearance of BU cases due to environmental and climatic changes [3]. In this paper, we take periodic transmission rate into account based on the facts that the number of BU cases increases during dry periods or after inundations [29, 30]. These conditions are probably favourable for the development of *Mycobacterium ulcerans*, because of the density of possible vectors in areas that are frequently visited by humans. For example if we consider Ghana where BU is endemic, this country experience a typical tropical climate. Where in December to February is Harmattan (dry and dusty weather), March is the hottest month, through April to June they experience major rainfall, July to October there is small rains and in the month of November there is mild and dry weather [39]. Such field observations underline the limitation of all current BU models and imply that mathematical insights into BU seasonality has largely lagged behind. It is thus important for mathematical BU studies to incorporate these seasonal factors to gain deeper quantitative understanding of the short and long-term evolution of BU.

The purpose of this study is to develop a model for the transmission of BU in periodic environment, we aim to incorporates aspects that will make the BU model mathematically intractable using *STELLA*. *STELLA* which is the Structural Thinking Experimental Learning Labratory with Animation software, can be found from [32]. It is a user-friendly and commercial software package for building a dynamic modelling system. It uses an iconographic interface to facilitate construction of dynamic systems models. It includes a procedual programming language that are created as a result of manipulating the icons. The main features of *STELLA* are stocks, flows, convectors and connectors and we defined them as follows;

- Stocks, which are the state variables for accumulation. They collect whatever flows into and out of them.
- Flows, which are the exchange variables and which control the arrival or the exchanges of information between the state variables.
- Converters, which are the auxiliary variables. These variables can be represented by constant values or by values depending on other variables and functions of various categories.
- Connectors, which connect among modelling features, variables and elements.

Mathematically, the systems is geared towards formulating models as systems of ordinary differential equations and solving them numerically as difference equations. *STELLA* has

been widely used in environmental, biological, ecological, economic and epidemiologic sciences [13–18]. This paper is arranged as follows; in Section 2, we formulate the causal loop diagram, conceptual model, and the *STELLA* model in periodic environment. In Section 2 we estimate our parameters and show results of numerical simulations of the model. We expand the model by adding social dynamics to improve the model in Section 3 and the paper is concluded in Section 4.

2. Model construction

We present below the systems dynamic model for the transmission of BU in both fluctuating and non-fluctuating environments. The human population size NH, comprises of susceptible individuals SH, infectious individuals IH, those under treatment TH and the recovered RH. Thus, the population at any time t is

$$NH = SH + IH + TH + RH.$$

Similarly, the water bugs population size NWB, includes susceptible water bugs SWB and infectious water bugs IWB, so that, the population of water bugs at any time t is

$$NWB = SWB + IWB.$$

The compartment, MU represents *Mycobacterium ulcerans* in the environment whose carrying capacity is KM.

2.1. *Causal loop diagram for the transmission of BU*

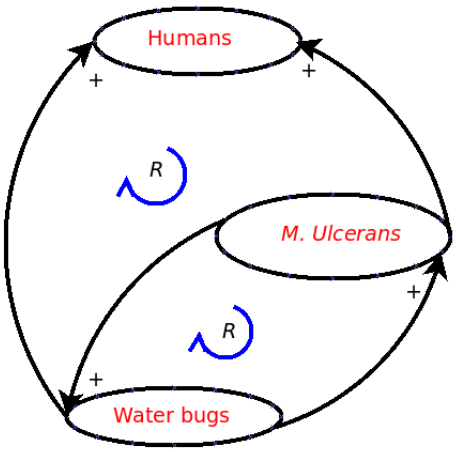

Figure 1. Causal loop diagram for the transmission of Buruli ulcer. The lines with arrow head moving from one variable to another with a positive sign on indicate the relationship between them. The curves with arrow head with the text R indicate reinforcing loop and the sign "+ " indicates the loops polarity.

Figure 1 represents the causal loop diagram for the transmission of BU. The causal diagram helps in picturing the different variables in the system that are interrelated. The nodes include the humans, *Mycobacterium ulcerans* and the water bugs as the variables, the edge with arrows are the link that represent connections. Figure 1 is a reinforcing loop because the effect of a variation in any variable propagates through the loop and returns to the variable reinforcing the initial deviation, meaning if a variable increases in a reinforcing loop the effect through the cycle will return an increase to the same variable and vice versa [1, 4, 13]. A link marked positive indicates a positive relation which means the two nodes change in the same direction. A closed cycle is either defined as a reinforcing or balancing loop. In Figure 1 humans with an open cut when have direct contact with *Mycobacterium ulcerans* in the environments result in BU infection, which indicates a positive relation. The *Mycobacterium ulcerans* and the water bugs have a positive relation since the water bugs shed back increasing the *Mycobacterium ulcerans* density in the environment. Similarly, water bugs bite the humans which in turns transmit the disease, indicating a positive relation.

2.2. *A conceptual model*

Conceptual model are generated before any field or laboratory studies have been conducted, and their main purpose is to examine what features are the most critical in determining system behaviour.

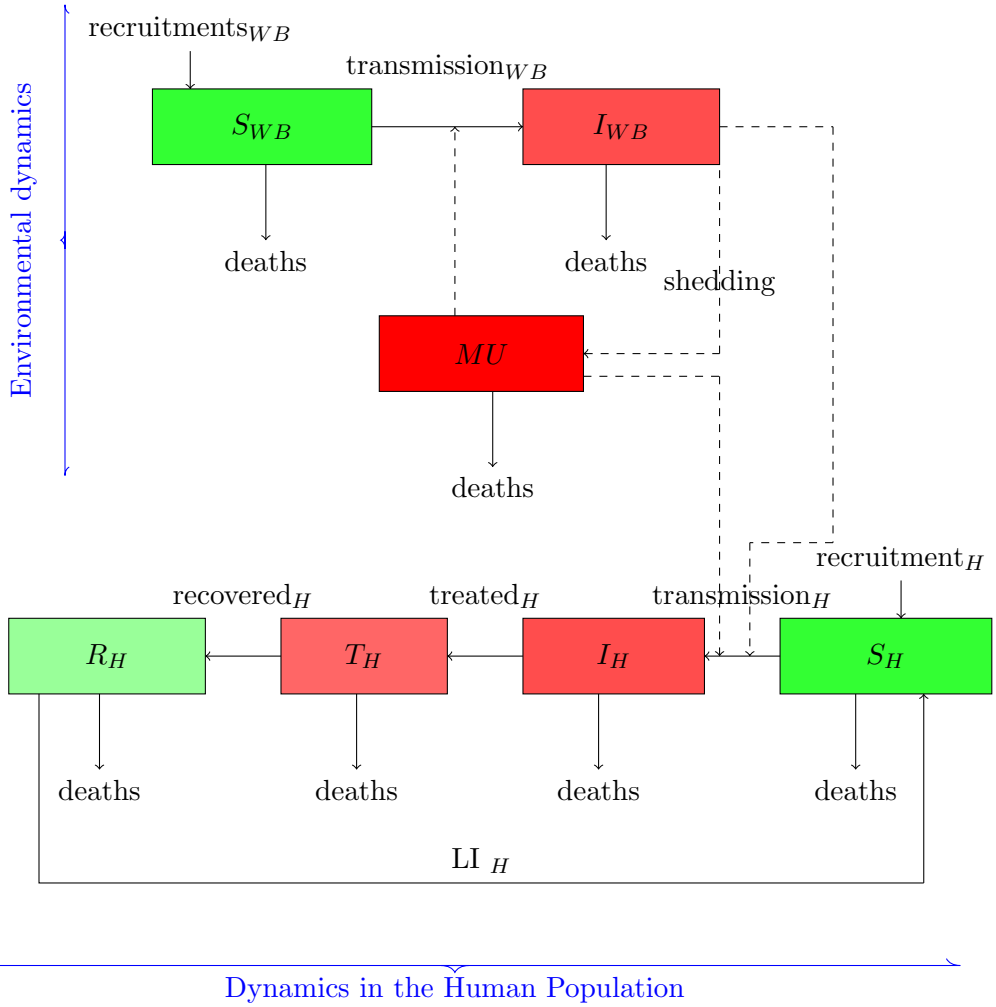

Figure 2. Conceptual model for Buruli ulcer transmission. The rectangles represent both the human and environmental population dynamics. We have in the human population susceptible human(S_H), infected humans(I_H), individuals in treatments(T_h) and the recovered humans(R_H). In the environmental population S_B is the susceptible water bugs, I_B is the infected water bugs and MU is the *Mycobacterium ulcerans* in the environment. We denote LI to be the loss of immunity, and the dashed lines with arrow head to indicates contact, solid lines with arrow head to indicates movement.

2.3. *Model structure in STELLA*

The first step in modelling processes was to develop a basic structure to capture the processes and procedures described above using *STELLA* see Figure 3.

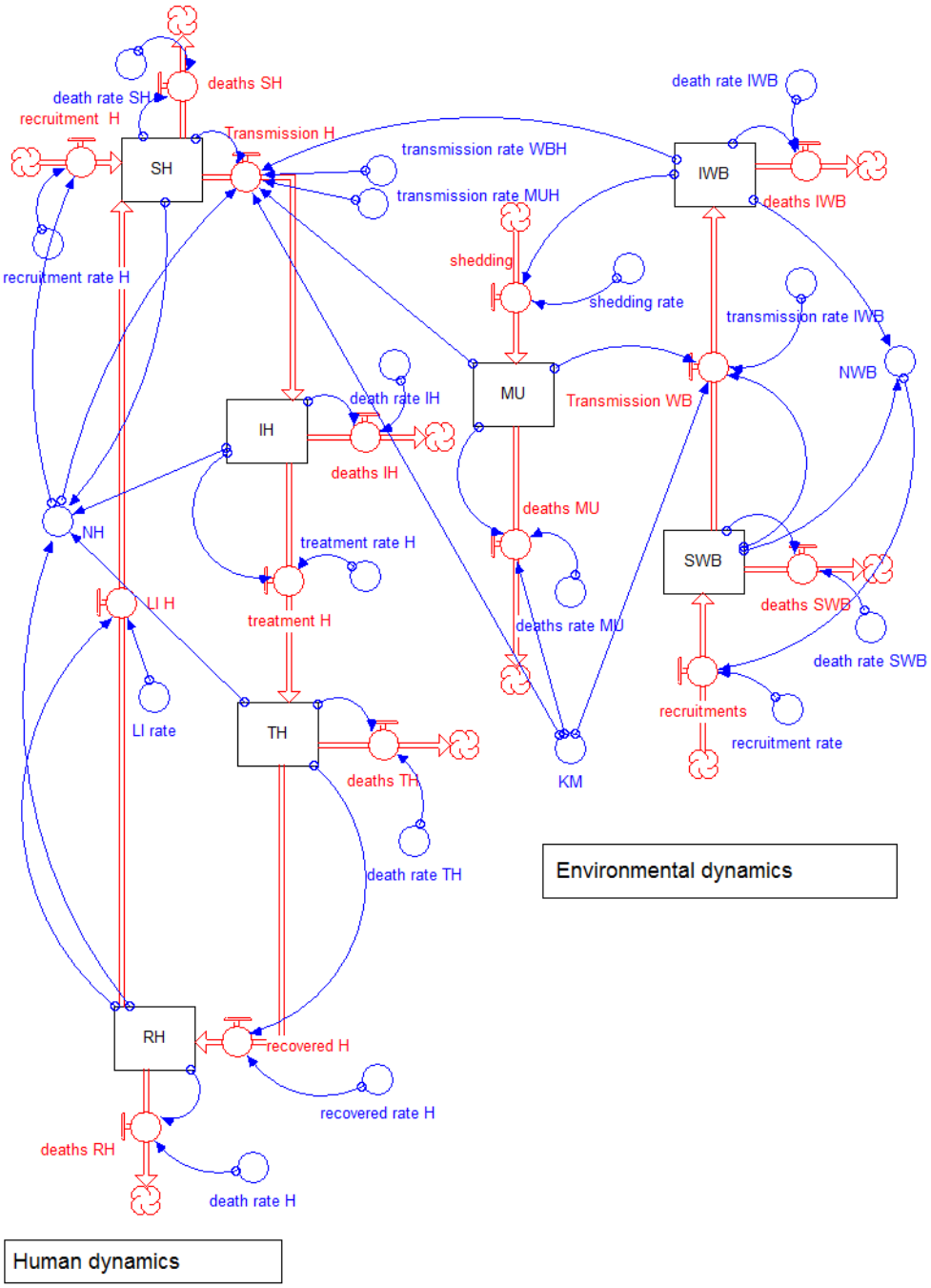

Figure 3. A *STELLA* model for the transmission of Buruli ulcer. The rectangles; SH, IH, TH, RH, SWB, IWB and MU represent stocks, the circles represent converters, the double lines with arrow represent flows and the single lines with arrow represent connectors connecting the flows and the stocks LI is the loss of immunity for the recovered individual, the flows indicates movement and the connectors indicate contact.

2.4. *System dynamic equations*

From the above *STELLA* model the following system dynamic are derived to describe the dynamics of the transmission of BU in both non fluctuating and fluctuating environments:

$$\left.\begin{aligned}
S_H(t) &= S_H(t-dt) + (recruitment_H + LI_H - Transmission_H - deaths_{SH}) * dt \\
I_H(t) &= I_H(t-dt) + (Transmission_H - deaths_{IH} - treatment_H) * dt, \\
T_H(t) &= T_H(t-dt) + (treatment_H - recovered_H - deaths_{TH}) * dt, \\
R_H(t) &= R_H(t-dt) + (recovered_H - LI_H - deaths_{RH}, \\
S_{WB}(t) &= S_{WB}(t-dt) + (recruitment_{WB} - Transmission_{WB} - deaths_{SWB}) * dt, \\
I_{WB}(t) &= I_{WB}(t-dt) + (Transmission_{WB} - deaths_{IWB} - treatment_H) * dt, \\
MU(t) &= MU(t-dt) + (shedding - deaths_{MU}) * dt
\end{aligned}\right\} \tag{1}$$

where disease transmission pathways for humans and water bugs in non fluctuating environments is defined below,

$$\text{Transmission}_H = \left(TR_{WBH} \times \left(\frac{IWB}{N_H}\right) + TR_{MUH} \times \left(\frac{MU}{(K_{50} + MU)}\right)\right). \tag{2}$$

The parameters TR_{WBH} and TR_{MUH} are the effective contact rates of susceptible humans with the water bugs and *Mycobacterium ulcerans* in the environments, respectively. Here TR_{WBH} is the product of the biting frequency of water bugs on humans, density of water bugs per human host, and the probability that a bite will result in an infection also TR_{MUH} is the product of density of *Mycobacterium ulcerans* per human host and the probability that a contact will result in an infection. The parameter K_{50} gives the concentration of *Mycobacterium ulcerans* in the environment that is assumed to yield 50% chance of infection with BU.

$$\text{Transmission}_{WB} = TR_{IWB} \times \left(\frac{MU}{K_{50}}\right), \tag{3}$$

$$\text{Shedding} = SR_{MUIWB} \times I_{WB}. \tag{4}$$

TR_{IWB} is infection rate of water bugs by *Mycobacterium ulcerans* and SR_{MUIWB} means the shedding rate of *Mycobacterium ulcerans* by water bugs in the environments.

2.5. *The basis reproduction number*

The basic reproduction number, denoted R_0, is the expected number of secondary cases produced, in a completely susceptible population, by a typical infective individual. If $R_0 < 1$, then on average, an infected individual produces less than one new infected individual over the course of its infectious period, and the infection cannot grow. Conversely, if $R_0 > 1$, then each infected individual produces, on average, more than one new infection, and the disease can invade the population [19, 36]. The concept of reproduction

number is fundamental to the study of epidemiology of infectious diseases. It is useful in predicting factors and parameters that enhance the growth of an epidemic or those that help reduce or stop the growth of the epidemic. Its value is very useful in prevention strategies and management plans in disease epidemics [40].

We defined our basic reproduction number R_0 in non fluctuating environments as derived in [31] below,

$$R_0 = \frac{TR_{IWB} \times SR_{MUIWB}}{\text{deaths rate MU} \times \text{deaths rate WB}}. \tag{5}$$

We interpreted our R_0 above to be the number of secondary cases of infected water bugs generated by the shedding rate of *Mycobacterium ulcerans* in the environments. The basic reproduction number R_0 is independent of the parameters of human population but only dependent on the life spans of the water bugs and *Mycobacterium ulcerans* in the environments, shedding rate, and infection rate of the water bugs. From this we can conclude that the infection of BU is driven by the water bug population and the density of the *Mycobacterium ulcerans* in the environments.

2.6. *Parameter estimation*

The Buruli ulcer is a vector borne disease and some of the model parameters were estimated based on literature on vector borne diseases and on the assumption of the disease because not much of the disease is understood [37]. For the mortality rate of human, we assume that life expectancy of human population in sub-Saharan Africans is 61 year, which is 4.5×10^{-5} days. Recovery rates of vector borne disease is from 1.6×10^{-5} to 0.5 per day [37]. The mortality rate for water bugs is not completely known, it is assumed to be 0.15 per day [9]. For vector borne disease the loss of immunity ranges between 0 and 1.1×10^{-2} per day [37] See Table 1 for details of model parameters and variables for our simulations. Simulations were done using *STELLA* software and we set our time in days.

Table 1. Model parameters and variables

Parameter/variables	Value(day^{-1})	Source
TR_{IWB}	0.09	[34]
TR_WBH	1×10^{-5}	[34]
TR_MUH	2×10^{-7}	[34]
death rate H	4.5×10^{-5}	[39]
death rate WB	0.8	[34]
deaths rate MU	0.15	[9]
SR_{MUIWB}	0.00615	[34]
LI	1.1×10^{-2} – 0	[37]
Recovery rate	1.6×10^{-5} – 0.5	[37]
Treatment rate	0.08 – 0.4	[34]

Table 1 gives model parameters, values and source used with the initial conditions for the proportions of human and environmental populations dynamics.

2.7. *Simulation for model without fluctuations*

Simulations are performed using the *STELLA* software and we set our time in days.

Plots of disease free equilibrium

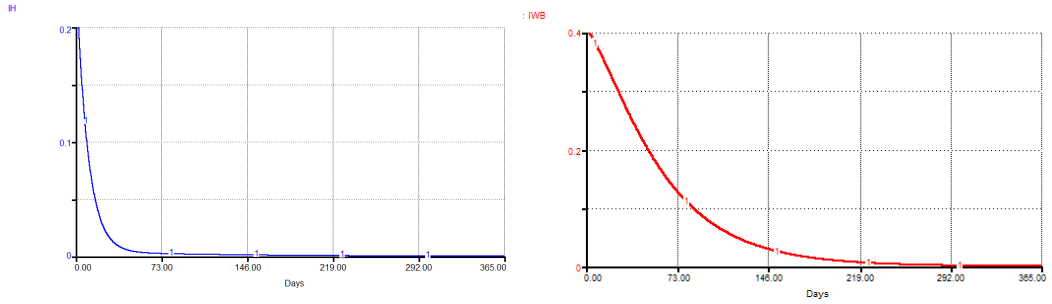

(a) Plot of proportions of infected humans when $R_0 < 1$.

(b) Plot of proportions of infected water bugs when $R_0 < 1$.

Figure 4. Plot of proportions of infected humans(I_H) and water bugs(I_{WB}) when $R_0 < 1$ respectively, in model 3 for a period of 365 days. Initial conditions; $I_H(0) = 0.2$, $I_{WB}(0) = 0.4$ and with other parameters as in Table 1 to be constant. The solution converges to the disease free equilibrium with $(I_H^0, I_{WB}^0) = (0, 0)$.

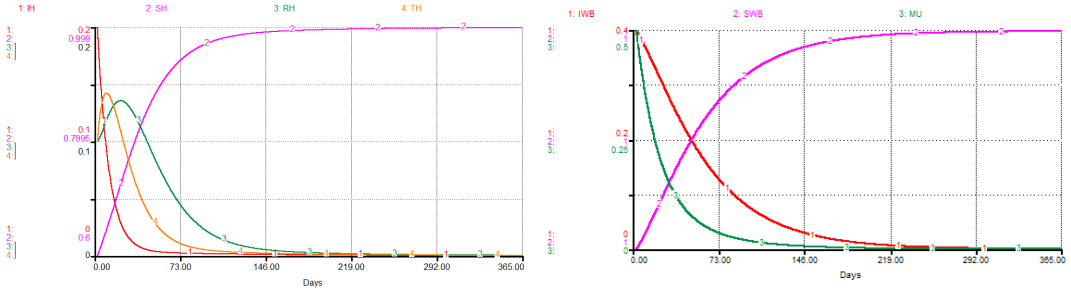

(a) Plot of proportions of humans population dynamics when $R_0 < 1$.

(b) Plot of the environmental daynamics when $R_0 < 1$.

Figure 5. Plot of proportions of humans and the environmental population dynamics when $R_0 < 1$ respectively, in model 3 for a period of 365 days. Initial conditions; $S_H(0) = 0.6$, $T_H(0) = 0.1$, $R_H(0) = 0.1$, $S_{WB}(0) = 0.6$, $MU(0) = 0.5$ and with other parameters as in Table 1 to be constant. The solution converges to the disease free equilibrium with $S_H^0 = 1$, $T_H^0 = 0$, $R_H^0 = 0$, $S_{WB}^0 = 1$, $MU^0 = 0$.

When $R_0 < 1$, the proportions of infected humans(I_H) and water bugs(I_{WB}) turns to zero respectively, showing that the disease completely dies out. In each Figure 5, the proportions of both the humans and environmental dynamics turns to its disease free equilibrium point respectively. This provides some evidence that the disease free equilibrium is globally asymptotically stable.

Plots of endemic equilibrium

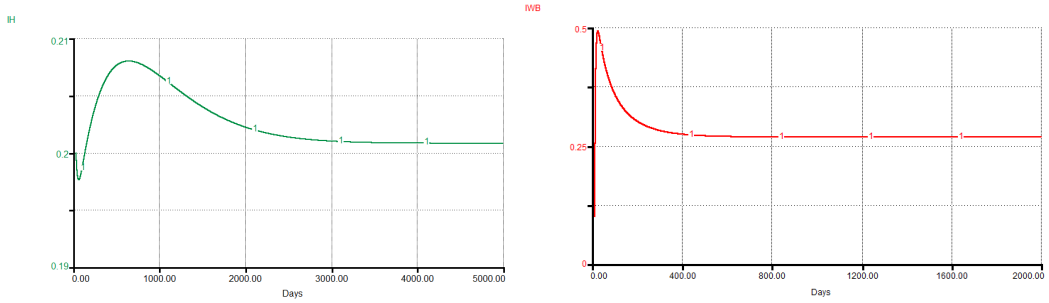

(a) Plot of proportions of infected humans when $R_0 > 1$.

(b) Plot of proportions of infected water bugs when $R_0 > 1$.

Figure 6. Plot of proportions of infected humans(I_H) and water bugs(I_{WB}) when $R_0 > 1$ respectively, in model 3. Initial conditions; $I_H(0) = 0.2$, $I_{WB}(0) = 0.1$ and with other parameters as in Table 1 to be constant. The disease persist even after 365 days and solution converges to the endemic equilibrium.

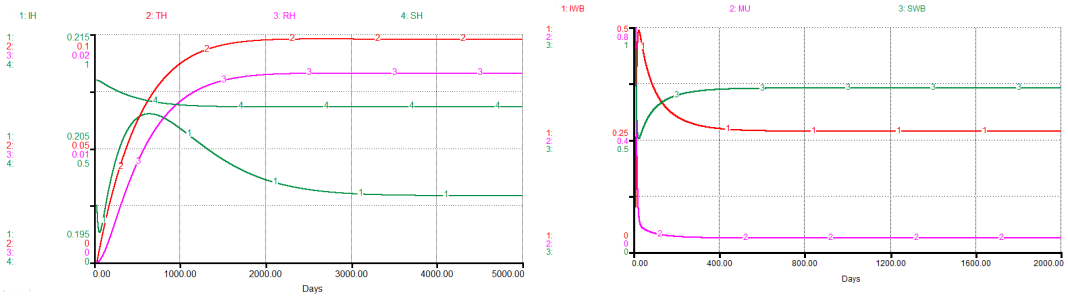

(a) Plot of proportions of humans population dynamics when $R_0 > 1$.

(b) Plot of proportions of infected water bugs when $R_0 > 1$.

Figure 7. Plot of proportions of humans and environmental population dynamics when $R_0 > 1$ respectively, in model 3. Initial conditions; $S_H(0) = 0.8$, $I_H(0) = 0.2$, $T_H(0) = 0$, $R_H(0) = 0$, $S_{WB}(0) = 0.9$, $I_{WB}(0) = 0.1$, $MU(0) = 0.8$ and with other parameters as in Table 1 to be constant. The disease persist even after 365 days and solution converges to the endemic equilibrium.

When $R_0 > 1$, the proportions of infected humans(I_H) and water bugs(I_{WB}) turns to it endemic equilibrium point. The proportions of humans and environmental population dynamics turns to their endemic equilibrium point respectively, after a long term the disease persist in Figure 6-7.

2.8. *Periodic environments*

In this subsection, based on the *STELLA* model we can incorporate periodicity in the disease transmission pathways (Transmission$_H(t)$, Transmission$_{WB}(t)$) and also in the *Mycobacterium ulcerans* density (Shedding(t)). These are both periodic functions of time with a common period, $\omega = \frac{365}{4}$ days. Periodic transmission is often assumed to be sinusoidal, from equation 1, we defined our new disease transmission for both humans

and water bugs population in fluctuating environments to be as follows:

$$\text{Transmission}_H(t) = \tag{6}$$
$$\left(TR_{WBH} \times SINWAVE(amplitude, period) \times \left(\frac{I_{WB}}{N_H}\right)\right)$$
$$+ \left(TR_{MUH} \times SINWAVE(amplitude, period) \times \left(\frac{MU}{(K_{50} + MU)}\right)\right), \tag{4.6.1}$$

$$\text{Transmission}_{WB}(t) = TR_{IWB} \times SINWAVE(amplitude, period) \times \left(\frac{MU}{K_{50}}\right), \tag{7}$$
$$\text{Shedding(t)} = SR_{MUIWB} \times SINWAVE(amplitude, period) \times I_{WB}. \tag{8}$$

SR_{MUIWB} means the shedding rate of *Mycobacterium ulcerans* by the water bugs in the environments. To ensure that both rates be positive, we require that $0 < amplitude < 1$ and the $period = \frac{365}{4}$. We defined basic reproduction number R_0 with periodicity as derived in [31] to be,

$$R_0 = \tag{9}$$
$$\frac{TR_{IWB}(SINWAVE(amplitude, period)) \times SR_{MUIWB}(SINWAVE(amplitude, period))}{\text{deaths rate MU} \times \text{deaths rate WB}}.$$

Plots of disease free equilibrium

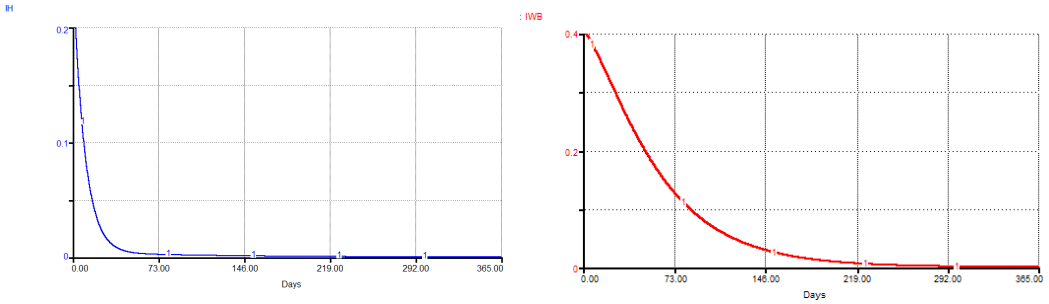

(a) An infection curve of humans when $R_0 < 1$. (b) An infection curve of water bugs when $R_0 < 1$.

Figure 8. Plot of proportions of infected humans(I_H) and water bugs(I_{WB}) when $R_0 < 1$ respectively, in model 3 for a period of 365 days. Initial conditions; $I_H(0) = 0.2$, $I_{WB}(0) = 0.4$ and with other parameters as in Table 1 to be constant. The solution converges to the disease free equilibrium with $(I_H^0, I_{WB}^0) = (0, 0)$.

Plots of endemic equilibrium

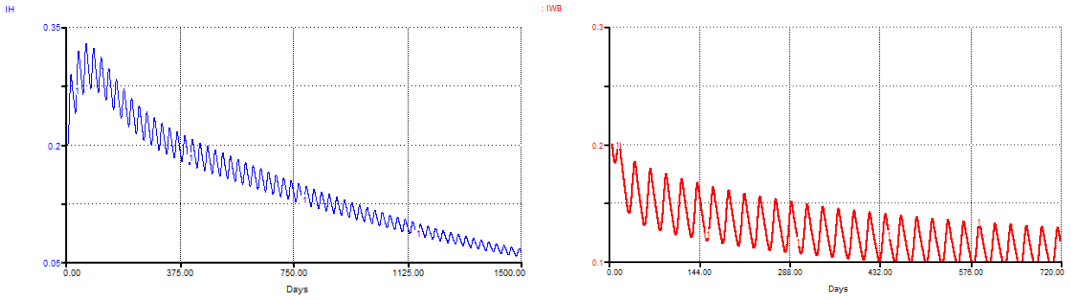

(a) An infection curve for the proportions of infected humans when $R_0 > 1$.

(b) An infection curve for the proportions of infected water bugs when $R_0 > 1$.

Figure 9. Plot of proportions of infected humans(I_H) and water bugs(I_{WB}) when $R_0 > 1$ respectively, in model 3. Initial conditions; $I_H(0) = 0.2$, $I_{WB}(0) = 0.2$ and with other parameters as in Table 1 to be constant. The disease persist and a periodic solution with $\omega = 91.25$ days forms after a long transient.

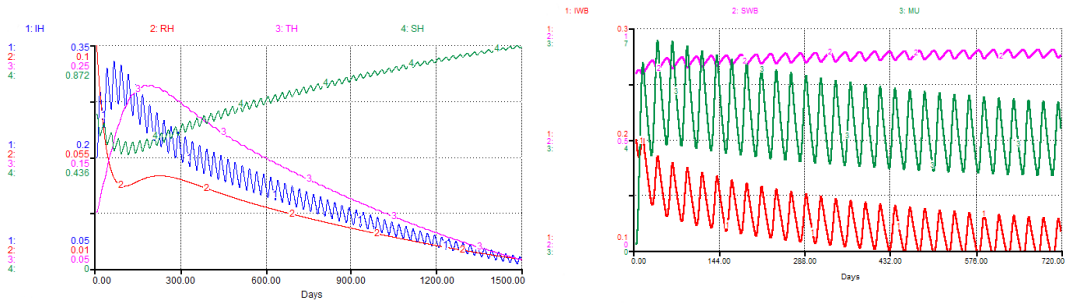

(a) Plot of proportions of human dynamics when $R_0 > 1$.

(b) Plot of proportions of environmental dynamics when $R_0 > 1$.

Figure 10. Plot of proportions of humans and environmental population dynamics when $R_0 > 1$ respectively, in model 3. Initial conditions; $S_H(0) = 0.6$, $I_H(0) = 0.2$, $T_H(0) = 0.1$, $R_H(0) = 0.1$, $S_{WB}(0) = 0.8$, $I_{WB}(0) = 0.2$, $MU(0) = 0$ and with other parameters as in Table 1 to be constant. The disease persist and a periodic solution with $\omega = 91.25$ days forms after a long transient.

When $R_0 < 1$, the proportions of infected humans(I_H) and infected water bugs population (I_{WB}) decreases to zero respectively, showing that the disease dies out. This gives an evidence that the disease free equilibrium is globally asymptotically stable (see Figure 8). In Figure 9-10 illustrates proportions of the human and environmental dynamics respectively, when $R_0 > 1$. In each case the disease persist after a long, oscillating transient the infection approaches a positive $\omega-$periodic solution.

3. *STELLA* model for the transmission of BU with social dynamics

In this section, we explore the effect of social dynamics in the transmission of BU disease such as; the effect of educational campaigns, treatment delays and logistic function to the *Mycobacterium ulcerans* density. We first treated them separately and then combined them to see it effectiveness on the disease endemic population.

3.1. *Eduction campaigns and delay treatments*

Studies to identify factors contributing to delayed presentation indicate that awareness of the disease is generally good in endemic regions, but wide variation exists in perceived cause of the disease and the role of sorcery in its transmission and treatment [38]. The use of traditional healers as first line therapy also contributes to delayed treatment, as do lack of awareness about the availability of effective treatment and financial concerns. Epidemiological data from existing BU control programs indicate that active educational campaigns are successful in increasing understanding and decreasing infection rate and disease progression [3, 38]. We add educational campaign to our *STELLA* model 11. We define our new human transmission as the force of the infection in the fluctuating environments already defined in equation (4.6.1) with the education function, we express this below

$$\text{New transmission}_H(t) = \text{Transmission}_H(t) \times education \tag{10}$$

where new transmission is due to the changes in the disease transmission pathway of the humans with the effect from the educational campaign. We express education as $(1-m)$ and m is the efficacy of it. In addition to the *STELLA* model in 11 we added a delay function. The delay function in *STELLA* helps us to monitor treatment delays, we define the delay function as follows:

$$\text{delay}_T = DELAY(input, \text{delay duration}[, initial]), \tag{11}$$

$$\text{treatment}_H = \text{treatment rate H} \times T_H \times \text{delay}_T.$$

Here we model the effect of treatment delays for 30 days and 60 days respectively.

3.2. *Environmental degradation through mining*

An aquatic environment is not the only factor that has been linked to the prevalence of *Mycobacterium ulcerans*. It has been observed that if, in addition, high levels of arsenic (As) concentration prevail in such environments, the occurrence of *Mycobacterium ulcerans* is enhanced. Duker et al. [9, 12] have advanced the hypothesis that As may play a significant role in the spatial distribution of BU [9, 11]. Concentration of As in surface and ground water in areas where BU is a serious health threat has been noted to be higher than average. Aidoo and Osei [9] asset that, in Ghana, West Africa, the Amansie West District which accounts for high BU cases coincides with the highest levels of As, possibly released into rivers and lakes and ground water by intensive gold mining activities [9, 11]. Furthermore, a convenient specification for the change in the *Mycobacterium ulcerans* density is the logistic function(LF). We again included LF into *STELLA* model 11 to monitor the density of the *Mycobacterium ulcerans* in the environment. We define LF below,

$$\triangle MU = R \times MU \times \left(1 - \frac{MU}{K_M(t)}\right) \tag{12}$$

where the constant R defines the growth rate and K_M is the carrying capacity. K_M is not constant over time because of the seasonal fluctuations in the environments. For

simplicity, we assume that these seasonal fluctuations occur along a sinewave around the carrying capacity. We define carrying capacity as

$$K_M(t) = K_M + SINWAVE(amplitude, period),$$

therefore our *Mycobacterium ulcerans* dynamics is given as

$$MU(t) = MU(t - dt) + (shedding + LF - deaths_{MU}) * dt. \tag{13}$$

We present below a *STELLA* model for the transmission of Buruli ulcer with social dynamics as described above.

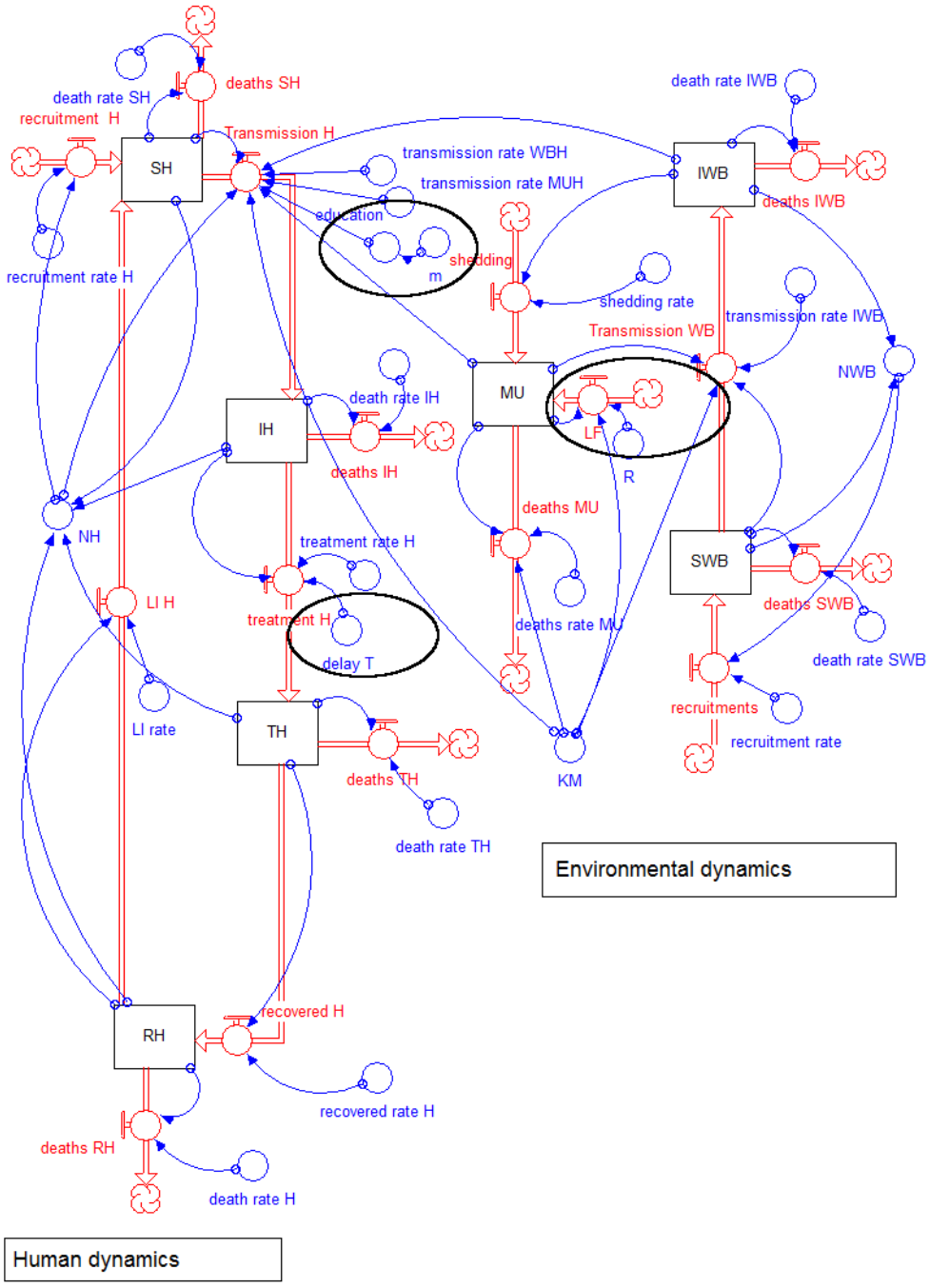

Figure 11. A *STELLA* model for the transmission of Buruli ulcer with social dynamics. Where the highlighted ellipse are the added social dynamics: education, treatment delays and LF. The rectangles; SH, IH, TH, RH, SWB, IWB and MU represent stocks, the circles represent converters, the double lines with arrow represent flows and the single lines with arrow represent connectors which connect the flows and the stocks. The flows indicates movement and the connectors indicates contact.

Effects of educational campaigns

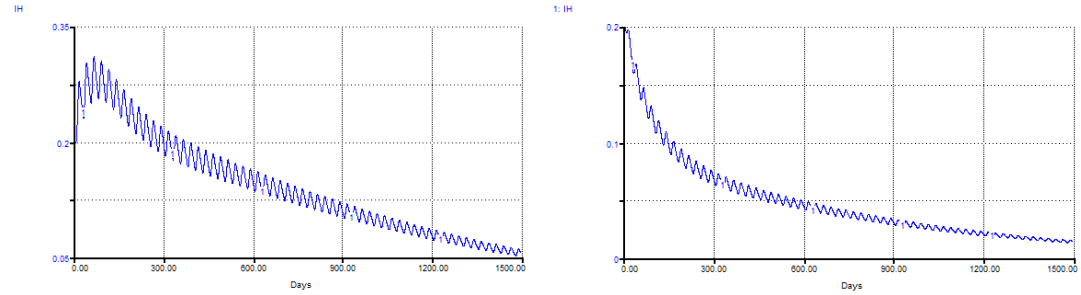

(a) Plot of proportions of infected humans with education efficacy of 0.1 or 10%.

(b) Plot of proportions of infected humans with education efficacy of 0.8 or 80%.

Figure 12. An infection curve for proportions of humans with education efficacy of 0.1 and 0.8 respectively, in model 11. With an initial condition $I_H(0) = 0.2$, and with rest of the parameters as defined in Table 1 to be constant. The disease persist and a periodic solution with $\omega = 91.25$ days forms after a long transient.

With the inclusion of educational campaign in the model 11, there is no much difference in the infection rate when the efficacy is less than 50% as seen in Figure 12(a). When the education efficacy is between $(50 - 80)\%$, or more it reduces the disease infection rate since individuals become aware of BU disease and its transmission mode as seen in Figure 12. In Figure 12 the disease persists after a long oscillating transient the infection approaches a positive $\omega-$periodic solution.

Effects of treatment delays

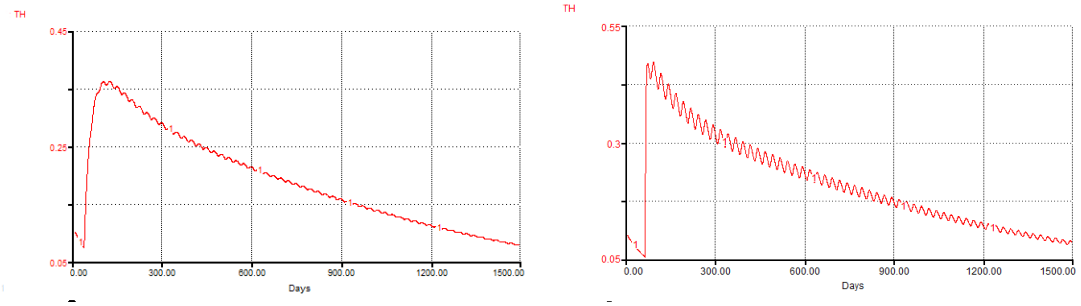

(a) Plot of treatment delays for 30 days.

(b) Plot of treatment delays for 60 days.

Figure 13. Treatment delays for 30 and 60 days respectively, in model 11, with an initial condition $T_H(0) = 0.1$. The rest of the parameters as defined in Table 1 o be constant, the disease persists and a periodic solution with $\omega = 91.25$ days forms after a long transient.

Considering Figure 13, we analyse the effect of inclusion of treatment delays without educational campaign. In Figure 13 when treatment delays for more than 30 days, it increases treatment rate and the disease persists even after long time and after a long oscillating transient the infection approaches a positive $\omega-$periodic solution.

Effect of environmental degradation through mining

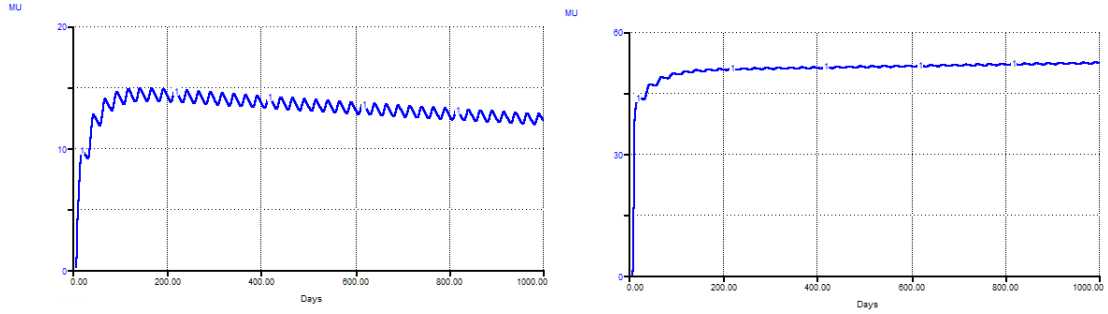

(a) Plot of *Mycobacterium ulcerans* density with low or no environmental degradation.

(b) Plot of *Mycobacterium ulcerans* density with environmental degradation through intensive mining

Figure 14. Plot of *Mycobacterium ulcerans* density with environmental degradation through intensive mining, with initial conditions; $MU(0) = 0, K_M(0) = 0.4$ and $K_M(0) = 40$ respectively. The rest of the parameters as defined in Table 1 to be constant, the disease persists and a periodic solution with $\omega = 91.25$ days forms after a long transient.

With the inclusion of Logistic function and exclusive of educational campaigns and treatment delays in the model 11, we noted that when the carrying capacity K_M is increased by environmental degradation through mining, the *Mycobacterium ulcerans* density in the environment increases. Figure 14 indicates that high levels of arsenic (As) concentration positively induces the growth and spread of *Mycobacterium ulcerans* in the environment. This cause the disease to persists and a periodic solution with $\omega = 91.25$ days forms after a long transient.

3.3. *All social dynamics*

Here we analyse all the social dynamics together, by plotting both the good and bad scenarios of *STELLA* model 11. In the good scenarios we considered high educational efficacy, no treatment delays and no or low environmental degradation through mining (see Figure 15) also in the bad scenarios we considered low educational efficacy, treatment delays and environmental degradation through mining (see Figure 16).

3.4. *Good scenarios*

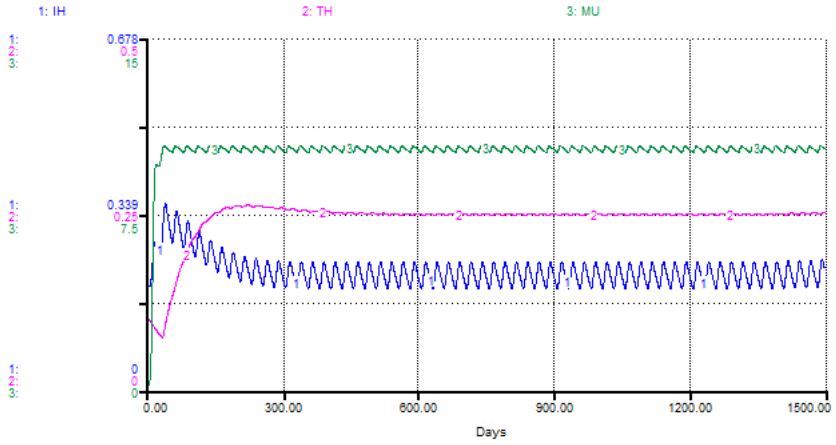

Figure 15. Plot of good social dynamics with initial conditions; $I_H(0) = 2, T_H = 0, MU(0) = 0$ and $K_M(0) = 0.4$. The rest of the parameters as defined in Table 1 to be constant, the disease persists and a periodic solution with $\omega = 91.25$ days forms after a long transient.

With the inclusion of all social dynamics into the *STELLA* model 11. We increased the education efficacy to 80%, gave no treatment delays and no environmental degradation through mining. In Figure 15 the infection rate decreases, treatment rate minimise and the *Mycobacterium ulcerans* density also decreases respectively. Our results implies that the BU disease can be reduce over time with the above social dynamics being considered.

3.5. *Worst scenarios*

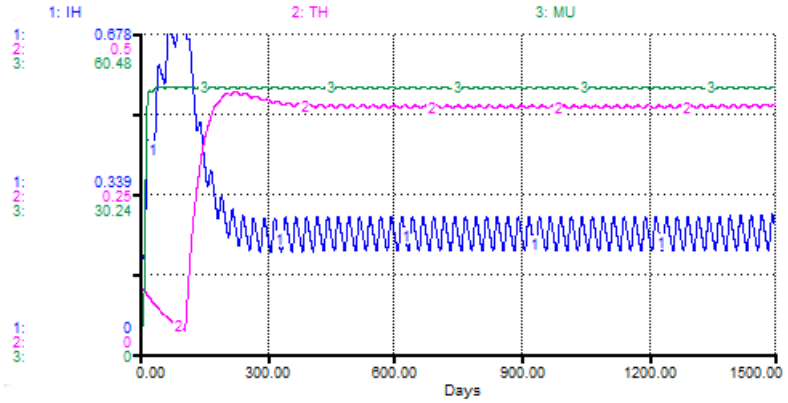

Figure 16. Plot of bad social dynamics with initial conditions; $I_H(0) = 2, T_H = 0, MU(0) = 0$ and $K_M(0) = 40$. The rest of the parameters as defined in Table 1 to be constant, the disease persists and a periodic solution with $\omega = 91.25$ days forms after a long transient.

We again in Figure 16 plotted the effect of educational campaign, treatment delays and a logistic function to the *Mycobacterium ulcerans* density (see model 11). We noted that when the efficacy of educational campaign is low such as less than 50%, treatment delays for more than 30 days and there are intensive mining activities in the environments this increases the carrying capacity K_M. Figure 16 indicates that the infection rate increases,

treatment rate increases and the *Mycobacterium ulcerans* density also increases. This causes BU disease to persist even for a very long time. Our results from model 16 indicates that not only shedding back of *Mycobacterium ulcerans* by water bugs increases the density of the *Mycobacterium ulcerans* in the environment but also through intensive mining activities.

3.6. *Summary*

We investigated the effect of educational campaigns, treatment delays and logistic function to the *Mycobacterium ulcerans* density, through environmental degradation such as mining. We treated them separately to see its effectiveness on the disease endemic population. We noticed that when educational campaigns have more than 50% efficacy it reduces the disease infection rate since individuals now becomes aware of the prevention strategies (by wearing protective apparel and boots) and early detection of the disease. With the use of the delay function in *STELLA* we detected that if treatment delays for more than 30 days it increases the treatment rates and causes the infection to persists. From our simulation results *Mycobacterium ulcerans* density can also be increased through environmental degradation and not water bugs shedding back only. Environmental degradation through mining causes the bacteria carry capacity K_M to increase.

However, our simulations again confirm that clearance of water bugs from the environments will decrease BU disease but this is not practically feasible. Research on malaria now looks at vector control, sterilisation, and genetic modification of the mosquito. Such an approach could be beneficial with regard to the control of water bugs. However, models presented in this project can be used to suggest the type of data that should be collected as research on the ulcer intensifies.

4. Conclusion

A system dynamic model for the transmission of BU in periodic environment using *STELLA* was presented. The main aim was to capture the two modes of transmission. It incorporates seasonal variation in the disease transmission pathways and the *Mycobacterium ulcerans* deansity. The *STELLA* modelling analysis was carried out using the basic reproduction number R_0 in [31]. Model parameters were estimated based on literature on vector borne diseases and some assumptions. This was because not much of the disease is understood. Our results have established R_0 as a sharp threshold for BU dynamics; i.e. disease completely dies out if $R_0 < 1$ and persists if $R_0 > 1$.

Our simulation results confirms that BU can be prevented through community health education, early detection and treatment of the disease. Patients should be made aware of the disturbing conditions in their surroundings (by wearing protective apparel and boots). Early detection of the major symptoms of the disease such as identification of any small lesions, nodules or plaques on one's body would help aid in early diagnosis and possible prevention of ulcers and disabilities.

The model presented in this paper echoes the attempts to model the BU with the incorporation of seasonal variations. The results have implications on designing more social interventions like poverty reduction, provision of social services and policies geared towards the eradication of the BU in the presence of fluctuations. The populations considered here are constant. It would be interesting also to investigate on how a non-constant population model will evolve. Moreover, the studies suggests that the model, developed with *STELLA*, has great potentials as a modelling tool for effective investigations of the

transmission dynamics of BU due to its simplicity and realism.

Acknowledgements

This project is supported by the National Research Foundation (NRF; grants 81825 and 76912) and African Institute for Mathematical Sciences (AIMS).

References

[1] Nathaniel Osgood, *A Glimpse of System Dynamics Models of Infectious Disease*, Accessed (2015), Institute for Systems Sciences and Health, pp. 1–45.
[2] Wikipedia , *Causal loop diagram*, Wikipedia Accessed (2015), Available at http://en.wikipedia.org/wiki/Causalloopdiagram.
[3] WHO *Buruli ulcer*, WHO, at http://www.who.int/mediacentre/factsheets/fs199/en/.
[4] Thwink.org, *Causal Loop Diagram (CLD)*, Accessed (2015), Available at http://www.thwink.org/sustain/glossary/CausalLoopDiagram.htm.
[5] F. Portaels, M T. Silva and W. M. Meyers, *Buruli ulcer.*, Clindermatol. 27 (2009), pp. 291–305.
[6] D. Walsh, F. Portaels, W. Meyers, *Buruli ulcer (Mycobacterium ulcerans infection)*, Transactions of the Roy. Soc. Trop. Med. Hyg. 102 (2009), pp. 969–978.
[7] R. W. Merritt, E. D. Walker, P. L. C. Small, J. Wallace, and P. Johnson, *Ecology and transmission of Buruli ulcer disease:A systematic review*, PLoS Neg. Trop. Dis., 4 (2010), pp. 1-12.
[8] A. A. Duker, F. Portaels, M. Hale *Pathways of Mycobacterium ulcerans infection: A review*, Environ. Int. 32 (2006), pp. 567–573.
[9] A.Y. Aidoo, B. Osei, *Prevalence of aquatic insects and arsenic concentration determine the geographical distribution of Mycobacterium ulcerans infection*, Comput. Math. Methods. Med. 8 (2007), pp 235–244.
[10] M. Wansbrough-Jones and R. Phillips, *Buruli ulcer: emerging from obscurity*, The Lancet 367 (2006), pp 1849–1858.
[11] A. A. Duker, M. E. J. Carranza and M. Hale *Spatial relation between arsenic in drinking water and Mycobacterium ulcerans infection in Amansie West District, Ghana, Mineralogical Magazine*, PLoS Neg. Trop. Dis. 69 (2005), pp 707–717.
[12] A. A. Duker, M. E. J. Carranza and M. Hale *Spatial dependency of buruli ulcer prevalence on arsenic-enriched domains in Amansie-West District, Ghana: implications for arsenic mediation in Mycobacterium ulcerans infection*, Int. J. H. Geo. 69 (2004), pp 1–19.
[13] O. Ying, E.Z. Jia and L. Dian, *A STALLA model for the estimation of atrazine runoff, leaching, adsorption, and degradation from an agricultural land*, J. Soils Sediments 10 (2010), pp 263–271.
[14] S. Aassine, M. C El Jai, *Vegetation dynamics modelling: a method for coupling local and space dynamics*, Ecol. Model. 154 (2002), pp 237–249.
[15] R.L. Bengtson,H.M. Selim,R. Ricaud, *Water quality from sugarcane production on alluvial soils*, Trans. ASAE. 41 (1998), pp 1331–1336.
[16] R. Costanza, A. Voinov, *Modeling ecological and economic systems with STELLA: Part III* , Ecol. Model. 143 (2001), pp 1–7.
[17] B. Hannon, M. Ruth, *Dynamic modeling* , Springer,New York (1994).
[18] J. Diamond, *STELLA Modeling of a Zombie Invasion* , Scribd. (2009), pp 1–6.
[19] O. Diekmann, J. A. P. Heesterbeek, J. A. J. Metz, *On the definition and the computation of the basic reproduction ratio R0 in models for infectious diseases in heterogeneous populations*, J. Math. Biol. 28 (1990), pp 365-382.

[20] D. Posny, and J. Wang, *Modelling Cholera in periodic environments*, J. Biol. Dyn. 8 (2014), pp 1-19.
[21] O. N. Bjornstad, B. F. Finkenstadt and B. T. Grenfell, *Dynamics of measles epidemics: Estimating scaling of transmission rates using a time series SIR model*, Ecol. Monogr. 72 (2002), pp 169–184.
[22] S. F. Dowell, *Seasonal variation in host susceptibility and cycles of certain infectious diseases*, Emerg. Infect. Dis. 7 (2001), pp 365-382.
[23] J. Dushoff, J. B. PlotkinF, S. A. Levin and D. J. D Earn *Dynamical resonance can account for seasonality of influenza epidemics*, Proc. Natl. Acad. Sci. USA, 101 (2004), pp 16915–16916.
[24] D. Earn, P. Rohani, B. Bolker and B. Grenfell, *A simple model for complex dynamical transitions in epidemics*, Science. 287 (2000), pp 667–670.
[25] W. London, J. A. Yorke, *Recurrent outbreaks of measles, chickenpox and mumps. i. Seasonal variation in contact rates*, Am. J. Epidemiol. 98 (1973), pp 453–468.
[26] J. Ma and Z. Ma, *Epidemic threshold conditions for seasonally forced SEIR models*, Math. Biosci. Eng., 3 (2006), pp 161-172.
[27] I. Schwartz and H. Smith, *Infinite subharmonic bifurcation in an SIER epidemic model*, J. Math. Biol. 18 (1983), pp 233–253.
[28] H. Smith, *Multiple stable subharmonics for a periodic epidemic model*, Math. Biol. 17 (1983), pp 179-190.
[29] F. Portaels, *Epidemiology of ulcers Mycobacterium ulcerans*, Ann. Soc. Med. Trop. 69 (1989), pp. 91-103.
[30] H. Darie, T. Le Guyadec, and J. E. Touze , *Epidemiological and clinical aspects of Buruli ulcer in Ivory Coast*, Bull. Soc. Pathol. Exot. 86 (1993), pp. 272-276.
[31] B. Assan, F. Nyabadza, P. Landi and C. Hui, *Modelling the transmission of Buruli ulcer in fluctuating environments*, J. Biol. Dyn. Review (2015), pp. 1-19.
[32] Isee Systems, *Technical document for the iThink and STELLA* software available at http://www.iseesystems.com.
[33] M.T. Silva, F. Portaels, J. Pedrosa, *Aquatic insects and Mycobacterium ulcerans: An association relevant to buruli ulcer control*, PLoS Med. 4 (2007), pp 229-231.
[34] E. Bonyah, I. Dontwi, and F. Nyabadza, *A theoretical model for the transmission dynamics of the Buruli ulcer with saturated treatment*, Comput. Math. Med. 2014 (2014), pp. 1-14.
[35] K. Asiedu and S. Etuaful, *Socio-economic implications of Buruli ulcer in Ghana: a three-year review*, Am. J. Trop. Med. Hyg. 59 (1998), pp. 1015-1022.
[36] R. M. Anderson and R. M. May, *Infectious diseases of humans*, Dyn. Ctrl. Oxford, (1991).
[37] G. Rascalou, D. Potier, F. Menu, and S. Gourbiére, *Emergence and prevalence of human vector-borne disease in sink vector populations*, PLoS ONE 7 (2012), pp. 1-16.
[38] B. J. Webb, F. R. Hauck, E. Houp, F. Portaels, *Buruli ulcer in West Africa: strategies for early detection and treatment in the antibiotic era.*, Pub Med. 6 (2009), pp. 144-147.
[39] Ghana statistical Service, (2014). http://www.statsghana.gov.gh/., G.S.S.
[40] P. Van den Driessche and J. Watmough, *Reproduction numbers and sub-threshold endemic equilibria for compartmental models of disease transmission.*, Math. Biosci. 180 (2002), pp. 29-48.